Dynamical Varieties

by

Danny Stoll

A dissertation submitted in partial fulfillment
of the requirements for the degree of
Doctor of Philosophy
(Mathematics)
in the University of Michigan
2024

Doctoral Committee:

       Professor Sarah Koch, Chair
       Professor Nikhil Bansal
       Professor John H. Hubbard, Cornell University
       Professor Ralf Spatzier
       Professor Giulio Tiozzo, University of Toronto

Due to formatting requirements, the chapters, sections, lists, figures, and pages in the present work are indexed starting from 1. The author would like to remark that this is incosistent with his philosophy that the ordinal number "first" should be identified with the cardinal number zero.

A zero-based indexing system eliminates a number of cointerintuitive properties in our notation for time, dates, birthdays, and musical intervals, to name a few, while also remaining more consistent with mathematical foundations and computer science.

If a system of notation consistently and losslessly simplifies the representation of a breadth of ideas, then that system brings us closer to a fundamental truth about the universe. The advent of Arabic numerals, Einstein tensor notation, Dirac notation for quantum states, and, indeed, mathematical notation as a whole, has shown us that we can often gain a deeper understanding of complex objects when we switch to a notation that minimizes cognitive boilerplate.

As the same is true for zero-based indexing by way of resolving the fencepost problem, the author sees no good reason to preserve a one-based convention.

Daniel C. Stoll

dastoll@umich.edu

ORCID iD: 0000-0003-1259-6262

DEDICATION

To

Pat Stoll

ACKNOWLEDGEMENTS

TABLE OF CONTENTS

LIST OF FIGURES

LIST OF TABLES

LIST OF APPENDICES

LIST OF NOTATION

- $\mathbb{D}$ denotes the open unit disk in $\mathbb{C}$, and $\mathbb{D}^* = \mathbb{D} \smallsetminus \{0\}$ the punctured disk.

- $\mathbb{N} = \{0, 1, 2, \dots\}$ denotes the natural numbers including zero, and $\mathbb{N}^* = \mathbb{N} \smallsetminus \{0\}$ denotes the positive integers.

- For $n \in \mathbb{N}$, $[n]$ denotes the set $\{0, \dots, n-1\}$.

- S^1 denotes the circle with coordinates given by $\mathbb{R}/\mathbb{Z}$, so that rational angles are represented by rational numbers.

- $\tau = 2\pi$ denotes the full circle constant.

- For a map f from a space to itself, the notation f^n denotes the nth iterate of f.

- For an angle $\theta \in S^1$, the notation (θ) denotes the orbit of θ under angle doubling, defined up to a cyclic permutation.

- We use the symbol $\infty\!\bigcirc\!\circ$ as a graphical indicator for the basilica map $f_{\infty\bigcirc\circ}(z) = z^2 - 1$ and related dynamical objects.

ABSTRACT

The locus of periodic cycles is of fundamental importance to any discrete time dynamical system. We introduce a family $\mathrm{Cyc}_p(\mathcal{F})$ of *marked cycle varieties* that parameterize the p-cycles of an algebraic family of dynamical systems. We describe a dynamically natural cell structure for marked cycle curves over the moduli space Per_1 of quadratic polynomials and over the moduli space Per_2 of quadratic rational maps with a 2-periodic critical point. We then analyze the combinatorics of the resulting cell structures, obtaining formulas for the number of cells of each dimension.

CHAPTER 1

Introduction

Starting with Isaac Newton's invention of his eponymous root-finding algorithm, the field of complex dynamics has grown in an effort to understand the behavior of iterated complex functions.

The iteration in question is a discrete process: unlike in the case of continuous-time dynamical systems, systems arising in complex dynamics generally do not act on the underlying space by homeomorphisms, instead posessing *critical points* near which the map is not invertible. Furthermore, points may enter cycles under forward iteration, even if the initial point did not belong to this cycle. Thus, a great deal can be learned about a complex dynamical system by understanding its critical points and periodic cycles.

When generalizing from a single dynamical system to a family $\mathcal{F}$ of holomorphic maps, a number of interesting questions arise.

- How do the periodic cycles change as we move around $\mathcal{F}$?

- To what extent is it possible to produce a consistent labeling of these cycles?

- When do cycles collide with one another or degenerate?

- What can we learn about the structure of $\mathcal{F}$ from the answers to the above?

The present work is devoted to understanding such questions. In Chapter 2, we provide a brief summary of some of the classical results in complex dynamics. In Chapter 3, we introduce three classes of branched covers over an algebraic dynamical family $\mathcal{F}$ — the *dynatomic variety*, the *marked cycle variety*, and the *Misiurewicz variety*, each of which adjoins extra certain dynamical data to elements of $\mathcal{F}$.

Chapters 4 and 5 are devoted to describing the structure of these dynamical varieties. In Chapter 4, we derive Algorithm 4.6.1 to compute the cell structure of the marked cycle varieties over the family Per_1 of quadratic polynomials. This algorithm is then extended

in Chapter 5 to also describe the marked cycle varieties over the family Per_2 of quadratic rational maps with a critical 2-cycle.

In Chapter 7, we study the combinatorics of dynamical varieties over Per_1 and Per_2. In Chapter 8, we conclude by suggesting some further directions of study, such as Misiurewicz curves and marked cycle curves over other families.

Finally, two appendices are provided with further details on how to replicate the examples produced here. Appendix A gives a more formal description of Algorithm 4.6.1 (a complete implementation in *Rust* is also available at [Sto23b]). Appendix B shows some of the computations used to explicitly parameterize some of the dynamical varieties shown graphically throughout this work. The exact code used to produce these pictures (and many more) may be found at [Sto23a].

CHAPTER 2

Background

2.1 Dynamics

We are interested in studying the behavior of meromorphic functions, in particular rational maps, under forward iteration.

We begin with an extremely general definition that applies to any discrete-time dynamical system.

Definition 2.1.1. Let f be a self-map of a set X, and let $x \in X$. We say that x has *preperiod k* and *period p* under f if

$$f^k(x) = f^{k+p}(x),$$

where k and p are minimal subject to the above.

Definition 2.1.2. A *p-cycle* of a self-map f of a set X is a set of distinct points $x_0, \ldots, x_{p-1}$ such that $f(x_i) = x_{i+1}$, where addition is done mod p, unordered but for the circular order induced by f.

We now restrict our attention to holomorphic self-maps f of a Riemann surface S.

Definition 2.1.3. The *multiplier* of a p-cycle of f is the derivative of the pth iterate of f at any point in the cycle. Equivalently, the multiplier is given by the product

$$\lambda = \prod_{i=0}^{p-1} f'(z_i).$$

The multiplier is of great importance in understanding the dynamics of f near a p-cycle. We have the following classification:

Definition 2.1.4. A p-cycle of a holomorphic map f with multiplier λ is

- *superattracting* if $\lambda = 0$,

- *attracting* if $0 < |\lambda| < 1$,

- *indifferent* if $|\lambda| = 1$, or

- *repelling* if $|\lambda| > 1$.

An indifferent cycle is *parabolic* if λ is a root of unity and no iterate of f is the identity.

Examples 2.1.5.

- Any polynomial of degree $d \geq 2$ has a superattracting fixed point at ∞.

- The periodic points of $f(z) = z^2$ are the superattracting fixed points 0 and ∞, together with all points of the form $\exp\left(\frac{m}{2^p-1}\tau i\right)$ (recall $\tau \overset{\text{def}}{=} 2\pi$) for $p \in \mathbb{N}^*$, $0 \leq m < 2^p - 1$, which belong to repelling cycles of periods dividing p.

Definition 2.1.6. The *basin* $\mathcal{A}$ of a cycle ξ is the set of all $z \in \hat{\mathbb{C}}$ whose forward iterates under f converge toward ξ. $\mathcal{A}$ is an open subset of $\hat{\mathbb{C}}$, often having infinitely many connected components. The *immediate basin* $\mathcal{A}_0$ of f is the union of the components of $\mathcal{A}$ that are not disjoint from ξ.

The following classical result underscores the significance of the critical points of a map f in understanding its dynamics.

Theorem 2.1.7 (Fatou, Julia). *If f is a rational map of degree $d \geq 2$, then the immediate basin of every attracting and every parabolic cycle of f contains at least one critical point.*

In particular, since the basins of distinct cycles are disjoint, the number of attracting or parabolic cycles is bounded by the number of critical points. For instance, a rational map of degree d has $2d - 2$ critical points, so it has at most $2d - 2$ attracting or parabolic cycles.

Definition 2.1.8. The *Fatou set* of a rational map f is the set of all $z \in \hat{\mathbb{C}}$ such that for some neighborhood U of z, the set $\{f^n|_U : n \in \mathbb{N}\}$ of forward iterates of f on U forms a normal family.

The Fatou set contains the basins of all attracting and parabolic cycles of f. In certain cases, the Fatou set may also contain rotation domains known as Siegel disks (resp. Herman rings), in which f is conjugate to an irrational rotation on a disk (resp. annulus).

Definition 2.1.9. The *Julia set* $\mathcal{J}(f)$ of f is the complement of the Fatou set. Equivalently, the Julia set is the closure of the set of repelling cycles of f.

When f is a polynomial, we define the *filled Julia set* $\mathcal{K}(f)$ to be the set of all $z \in \mathbb{C}$ whose forward orbit under f is bounded. For such maps, the Julia set coincides with the boundary of the filled Julia set (c.f. [Mil06], Lemma 9.4).

Definition 2.1.10. A map $f : S \to S$ on a Riemann surface S is *hyperbolic* if the forward orbit of every critical point of f converges towards an attracting or superattracting cycle.

Hyperbolic maps are of interest because attracting cycles are easy to understand. The following classical theorems provide a complete description of the dynamics of holomorphic maps near attracting and superattracting cycles, respectively.

Theorem 2.1.11 (Kœnigs, c.f. [Mil06] Theorem 8.2)**.** *Let f be a holomorphic self-map of a Riemann surface S, and suppose that z_0 is an attracting fixed point of f with multiplier $\lambda \in \mathbb{D}^*$. Then f is locally conjugate to multiplication by λ. Formally, there is a neighborhood U of z_0 and a conformal isomorphism $\psi : U \to \mathbb{D}$, unique up to a rotation, such that $\psi \circ f \circ \psi^{-1}(z) = \lambda z$ for all $z \in U$.*

Theorem 2.1.12 (Böttcher, c.f. [Mil06] Theorem 9.1)**.** *Let f be a holomorphic self-map of a Riemann surface S, and suppose that z_0 is a superattracting fixed point of f with local degree $n \geq 2$. Then f is locally conjugate to the nth power map on the disk.*

More strongly, there exists $r \in (0,1]$, a neighborhood U of z_0, and a conformal isomorphism $\psi : U \to \mathbb{D}_r$, such that $\psi \circ f \circ \psi^{-1}(z) = z^n$ for all $z \in U$. If $r = r_*$ is chosen to be maximal, then either $r_* = 1$, or ∂U necessarily contains a critical point of f.

Corollary 2.1.13. *The map φ defined above extends uniquely to a holomorphic map $\varphi : \mathcal{A}_{z_0}$*

Analogous results for cycles of higher period follow by applying the above results to iterates of f.

Example 2.1.14. The polynomial $f_c(z) = z^2 + c$ has a superattracting fixed point at ∞. Thus, by Böttcher's theorem, f_c is conjugate in a neighborhood U of ∞ to the map $z \mapsto z^2$.

Choose the maximal radius $r_* = r_*(c)$. If $r_* < 1$, the Böttcher map extends until its domain touches the finite critical point of f. If, on the other hand, $r_* = 1$, then the boundary of the domain U coincides with the Julia set of f.

The map $c \mapsto -\log r_*(c)$ turns out to be equivalent to the Green's function on the complement of the Mandelbrot set.

2.2 Dynamical Families and Moduli Spaces

We are often interested not only in a single dynamical system, but rather in how the dynamics change as we modify the map.

Definition 2.2.1. A (complex) *dynamical family* on a complex manifold X is a complex orbifold $\mathcal{F}$ consisting of self-maps of X, such that the evaluation map $e(f, x) = f(x)$ is holomorphic from $\mathcal{F} \times X$ to X. We refer to X as the *mapping space* of $\mathcal{F}$.

If $\phi \in \mathrm{Aut}(X)$ is a conformal automorphism of X, then the dynamics of $T_\phi(f) = \phi \circ f \circ \phi^{-1}$ are equivalent to the dynamics of f. Thus, two maps which at first appear distinct may end up having identical dynamics. For instance, taking $X = \hat{\mathbb{C}}$, the maps $g_0(z) = z^2 + \lambda z$, $g_1(z) = z^2 + (2 - \lambda)z$, and $g_2(z) = z^2 + (\lambda(2 - \lambda))/4$ are all conjugate to one another. It is therefore useful to study dynamical families from a viewpoint that removes such redundant copies.

Definition 2.2.2. The *dynamical moduli space* $\mathrm{Mod}(\mathcal{F})$ associated to a dynamical family $\mathcal{F}$ on X is the collection of $\mathrm{Aut}(X)$-conjugacy classes of elements of $\mathcal{F}$.

The space $\mathrm{Mod}(\mathcal{F})$ is endowed with a natural orbifold structure, obtained by pulling back the complex structure on $\mathcal{F}$.

Remark 2.2.3. Studying dynamical moduli spaces, instead of arbitrary families of maps, allows us to isolate properties of dynamical systems that are intrinsic to the dynamics themselves, rather than artifacts of the coordinate system being used. For instance, the filled Julia set of a polynomial f is defined as the set of z with bounded forward orbit under f. This definition suffices if we view f as a map on $\mathbb{C}$, whose automorphism group is the set of affine maps. However, if we are viewing f as a map on $\hat{\mathbb{C}}$, then this definition becomes incompatible with the dynamical moduli space, since the property of boundedness is not Möbius invariant.

Two properties are of fundamental importance to a dynamical system: the critical points (and by extension the postcritical set), and the periodic cycles (together with their multipliers). The critical points, postcritical set, and periodic cycles are all covariant under conjugation, while the multipliers of cycles are invariant.

Remark 2.2.4. Moduli spaces have a tendency to resemble the spaces they parameterize. While this statement in general is too vague to be formalized, it might nevertheless be thought of as the *fundamental analogy of moduli spaces*. As a first example, the moduli space of triangles in the plane up to similarity is itself a filled triangle. A more fruitful

Dynamical system	Moduli space
Julia set	bifurcation locus
Fatou component	J-stable component
(pre)-attracting Fatou component	hyperbolic component
repelling periodic point	Misiurewicz point
attracting (pre)-periodic point	component center
Böttcher map	Douady-Hubbard map

Table 2.1: Correspondence between dynamical systems and their moduli spaces

example is projective space (and similarly the Grassmanian), which parameterizes lines in an affine space, and which inherits many of the same geometric properties of affine space.

In complex dynamics, the most prominent instance of this analogy is given by the tendency for the geometry of the Mandelbrot set near a point f to resemble that of the Julia set of f. This was proven by Tan Lei in [Lei90] when f is a Misiurewicz point (i.e. when the critical orbit of f is strictly preperiodic). Further instances of this analogy are given in Remark 2.2.4.

2.2.1 Examples of Dynamical Families

For the purpose of this thesis, we are interested in the case where $S = \hat{\mathbb{C}}$ is the Riemann sphere. In this case, the holomorphic self-maps of $\hat{\mathbb{C}}$ are precisely the rational maps, and $\mathrm{Aut}(S)$ is the family of Möbius transformations.

The space of all rational maps is not itself a dynamical family (being infinite dimensional), but it can be expressed as a countable union of dynamical families. Formally, for $n \in \mathbb{N}$, we define Rat_n to be the dynamical family consisting of all rational maps of degree n. We denote the corresponding moduli space by $\mathcal{M}_n = \mathrm{Mod}(\mathrm{Rat}_n)$.

- The case $n = 0$ is uninteresting, as $\mathrm{Rat}_0 \cong \hat{\mathbb{C}}$ consists only of constant functions, and $\mathcal{M}_0$ is just a point.

- $\mathrm{Rat}_1 \cong \mathrm{PSL}(2, \mathbb{C})$ consists of the Möbius transformations, whose dynamics are characterized by the multipliers of their two fixed points. By conjugating by a Möbius transformation to move place the fixed points at 0 and ∞, we may take f to have the form $f_\lambda(z) = \lambda z$. By possibly conjugating by $z \mapsto \frac{1}{z}$, we may take λ to belong to $\overline{\mathbb{D}} \smallsetminus 0$. Thus, $\mathcal{M}_1$ is a punctured sphere, since the upper half of $\partial \mathbb{D}$ is identified with the lower half via the conjugacy $z \mapsto \frac{1}{z}$, which takes $\lambda \in \partial \mathbb{D}$ to $\frac{1}{\lambda} = \bar{\lambda}$. In all cases, the dynamics are uninteresting: if $|\lambda| = 1$, then $\mathcal{J}(f_\lambda)$ is empty; otherwise, $\mathcal{J}(f_\lambda) = \{\infty\}$ consists

only of the repelling fixed point.

- The case Rat_2 is already highly nontrivial, and many questions remain open about its structure. A wonderful analysis of the structure of $\mathcal{M}_2$ may be found in [Mil93]. For our purposes, the relevant properties are summarized as follows:

  - As an algebraic variety, $\mathcal{M}_2$ is canonically isomorphic to $\mathbb{C}^2$. Explicit coordinates for a conjugacy class $f \in \mathcal{M}_2$ are given by evaluating the elementary symmetric polynomials e_1 and e_2 on the multipliers of the three fixed points of f.

  - The natural orbifold structure on $\mathcal{M}_2$ is distinct from that of $\mathbb{C}^2$. The singular locus consists of all maps conjugate to a map of the form $f(z) = k(z + 1/z)$. Such maps have an automorphism group of order 2, except for the case $k = -1/2$, for which the automorphism group is of order 6. A common representative for the $k = -1/2$ class is the map $f(z) = 1/z^2$, which commutes with $z \mapsto 1/z$ and $z \mapsto \omega z$, where ω is a cube root of unity.

- The cases Rat_d, $d \geq 3$, are even more complicated. An easy computation shows that Rat_d has complex dimension $2d+1$. Since $\mathrm{PSL}(2, \mathbb{C})$ has complex dimension 3 and acts freely by conjugation on a nonempty Zariski open subset of Rat_d, the moduli space $\mathcal{M}_d$ has complex dimension $2d - 2$, equal to the number of critical points.

  Segal in [Seg79] analyzes the topology of Rat_d, showing for instance that Rat_d has fundamental group $\mathbb{Z}/2d\mathbb{Z}$. Little is known about the structure of $\mathcal{M}_d$, or the dynamics therein, which are more complicated than in Rat_2. For example, there exist maps in Rat_d, $d \geq 3$, with Fatou components that are topological annuli known as Herman rings.

For $n \in \mathbb{N}^*$, $\lambda \in \mathbb{C}$, the *Milnor curve* $\mathrm{Per}_n(\lambda) \subset \mathcal{M}_2$ is defined to be the set of all conjugacy classes of maps $f \in \mathrm{Rat}_2$ with an n-cycle of multiplier λ. The degree of the curve $\mathrm{Per}_n(\lambda)$ in $\mathcal{M}_2$ is equal to the number $\mathrm{Hyp}_1(n)$ of hyperbolic components of period n in the Mandelbrot set.

Another natural subspace of $\mathcal{M}_n$ is the moduli space $\mathcal{P}_n$ of polynomials of degree n. The simplest nontrivial case is again when $n = 2$, giving rise to the quadratic family, which will be discussed in the following section. For $n \geq 3$, many questions remain open due to the presence of multiple free critical points. The family $\mathcal{P}_3$ of cubic polynomials shares many similarities with $\mathcal{M}_2$; in particular, both families have complex dimension 2, with two free critical points and three "free" fixed points multipliers (in both cases, the latter are subject to a codimension 1 restriction given by the holomorphic index formula).

Many properties known or conjectured to be true in $\mathcal{P}_2$ are known not to hold in $\mathcal{P}_n$ for $n > 2$. For instance, Lavaurs showed in [Lav89] that the bifurcation locus in $\mathcal{P}_3$ is locally disconnected.

A more manageable subfamily of $\mathcal{P}_n$ is the *unicritical family* $\mathcal{U}_n$, consisting of all conjugacy classes of polynomials with a single (finite) critical point. The simplest and most commonly used coordinates for this family are the coordinates $f_c(z) = z^n + c$, but the relation $f_{\zeta c}(z) = \zeta f_c(\zeta^{-1} z)$, where ζ is a primitive $(n-1)^{\text{nd}}$ root of unity, implies that for $n \geq 3$, these coordinates describe a branched cover of moduli space. A true parameterization of moduli space is given by the coordinates $f_c(z) = c\left(1 + \frac{z}{n}\right)^n$, which have critical point $-n$ and critical value 0.

Unlike with the broader case of $\mathcal{P}_n$, much that is known about $\mathcal{P}_2 = \mathcal{U}_2$ extends naturally to $\mathcal{U}_n$. In particular, unless otherwise specified, every result in Section 2.3 has an analogue for $\mathcal{U}_n$, often with a similar or identical proof.

2.2.2 Hyperbolic components and stability

Recall that a map f on a Riemann surface S is hyperbolic if all critical points of f converge toward attracting or superattracting cycles. As hyperbolicity is an open condition, the set of hyperbolic maps in a given dynamical family or moduli space is a disjoint union of connected open sets, known as *hyperbolic components*.

Within a hyperbolic component, dynamics are "stable" in a number of ways.

Definition 2.2.5. A dynamical family $\mathcal{F}$ is *structurally stable* at $f \in \mathcal{F}$ if all maps in neighborhood of f are topologically conjugate to f.

Definition 2.2.6. A dynamical family $\mathcal{F}$ is *J-stable* at $f \in \mathcal{F}$ if the Julia set of g changes continuously (in the Hausdorff topology) for g in a neighborhood of f.

Since both structural stability and J-stability are well-defined up to conjugacy, they can equivalently be applied to dynamical moduli spaces. Evidently, structural stability implies J-stability, since $\mathcal{J}(\phi \circ f \circ \phi^{-1}) = \phi(\mathcal{J}(f))$. The following result is simple to show by perturbing the multipliers of the attracting cycles:

Proposition 2.2.7. *If $f \in \mathcal{F}$ is hyperbolic and does not have any superattracting cycles, then $\mathcal{F}$ is structurally stable at f.*

The following result is also classically known, see e.g. Theorem 3.4 of[McM95].

Proposition 2.2.8. *J-stability holds for all hyperbolic maps $f \in \mathcal{F}$.*

9
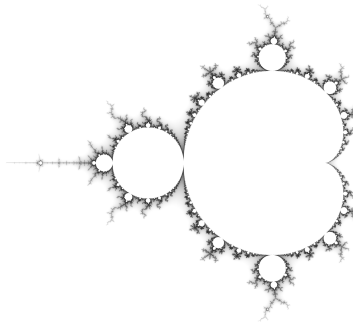
Figure 2.1: Moduli space $\mathcal{P}_2$ of quadratic polynomials. The black region accumulates on the bifurcation locus $B(\mathcal{P}_2)$, while the white regions are hyperbolic components. It is conjectured that the latter regions are dense in $\mathbb{C}$.

Both J-stability and structural stability are known to be generic in the families of rational maps, polynomials, and unicritical polynomials.

Theorem 2.2.9 (Mañé, Sad, Sullivan [MSS83])**.** *For $n \geq 2$, J-stable maps are dense in $\mathcal{U}_n$, in $\mathcal{P}_n$, and in $\mathfrak{M}_n$.*

Theorem 2.2.10 (Eremenko, Lyubich [EL92])**.** *For $n \geq 2$, structurally stable maps are dense in $\mathcal{U}_n$, in $\mathcal{P}_n$, and in $\mathfrak{M}_n$.*

It is conjectured that hyperbolicity similarly generic in the families of rational maps and unicritical polynomials. Indeed, all known J-stable maps in these families are hyperbolic. However, this conjecture remains open even in the simplest nontrivial case $\mathcal{P}_2 = \mathcal{U}_2$ of quadratic polynomials. It is widely considered to be one of the deepest open problems in complex dynamics.

Conjecture 2.2.11 (Density of Hyperbolicity)**.** *For all $n \geq 2$, hyperbolic maps are dense in $\mathcal{U}_n$, in $\mathcal{P}_n$, and in $\mathfrak{M}_n$.*

The complement of the set of J-stable parameters in a dynamical family $\mathcal{F}$ is known as the *bifurcation locus $B(\mathcal{F})$*. The bifurcation locus may be thought of as the analogue of the Julia set in parameter space.

2.3   Particulars of the Quadratic Family

Of basic interest is the dynamical moduli space $\mathcal{P}_2 = \mathcal{U}_2$ of quadratic polynomials. We present in this section a brief overview of the classical results on this family, most of which were proven by Adrien Douady, John H. Hubbard, and Tan Lei in [DH84]. A more modern

treatment may be found in Chapter 10 of [Hub16].

As every quadratic polynomial is affine conjugate to a unique polynomial of the form $f_c(z) = z^2 + c$, $\mathcal{P}_2$ is naturally identified with $\mathbb{C}$, parameterized by the critical value c.

The *Mandelbrot set* $\mathcal{M}$ is defined to be the set of parameters $c \in \mathbb{C}$ for which the critical orbit

$$\{f_c^n(0) : n \in \mathbb{N}\}$$

is bounded. The boundary of $\mathcal{M}$ is the bifurcation locus $B(\mathcal{P}_2)$, and all known components of the interior of $\mathcal{M}$ are hyperbolic components.

2.3.1 External rays

The following proposition follows from Böttcher's Theorem 2.1.12 by considering the super-attracting fixed point at ∞:

Proposition 2.3.1. *For $c \in \mathcal{M}$, the filled Julia set $\mathcal{K}(f_c)$ is connected. The complement $\mathbb{C} \smallsetminus \mathcal{K}(f_c)$ is conformally isomorphic to $\mathbb{C} \smallsetminus \overline{\mathbb{D}}$ via the map*

$$\phi_c(z) = \lim_{n \to \infty} f_c^n(c)^{2^{-n}},$$

where the 2^n-th roots may be chosen in such a way that $\lim_{z \to \infty} \frac{\phi_c(z)}{z} = 1$. Furthermore, the map $(c, z) \mapsto \phi_c(z)$ is holomorphic on its domain.

The final claim follows from the fact that ϕ_c is defined as a limit of functions depending uniformly on z and c, where the convergence is uniform on compacta.

By construction, ϕ_c conjugates f_c to the squaring map. We denote by $\psi_c : \mathbb{C} \smallsetminus \overline{\mathbb{D}} \longrightarrow \mathbb{C} \smallsetminus \mathcal{K}(f_c)$ the inverse map.

Remark 2.3.2. The map ϕ_c clearly need not extend to the boundary $\mathcal{J}(f_c)$, since the Julia set of f_c need not be a circle. More interestingly, the inverse map ψ_c also need not extend continuously to the boundary $\partial\mathbb{D}$ of its domain. Indeed, Caratheodory's theorem on conformal mappings implies that ψ_c extends continuously to $\partial\mathbb{D}$ if and only if $\mathcal{J}(f_c)$ is simply connected. This is not always the case; for instance, if $c = \lambda(2 - \lambda)/4$, where $\lambda = \exp(\tau i\theta)$ and θ is a non-Brjuno number, then $c \in \mathcal{M}$ and $\mathcal{J}(f_c)$ is locally disconnected.

By Böttcher's theorem, the map $\psi_c = \phi_c^{-1}$ can still be defined for $c \notin \mathcal{M}$, but its domain is now only $\mathbb{C} \smallsetminus \overline{\mathbb{D}_r}$ for some $r_c > 1$, such that the critical point of f lies on the boundary of the range $\psi_c(\mathbb{C} \smallsetminus \mathbb{D}_{r_c})$. However, we can still extend ϕ_c if we only remember its absolute

value. To this end, we introduce the Green's function

$$G_c(z) = \lim_{n \to \infty} \frac{1}{2^n} \log |f_c^n(z)|.$$

By construction, $G_c(z) = \log |\phi_c(z)|$ wherever $\phi_c(z)$ is defined.

Proposition 2.3.3. *The Green's function satisfies the functional equation*

$$G_c(f_c(z)) = 2G_c(z). \tag{2.1}$$

Its gradient satisfies the functional equation

$$\nabla G_c(f_c(z))z = \nabla G_c(z), \tag{2.2}$$

where z is regarded as a linear map on $\mathbb{R}^2$.

Proof. Equation (2.1) is immediate from the definition of G_c. Equation (2.2) then follows by differentiating (2.1). $\square$

Proposition 2.3.4 (c.f. Proposition 8.1 and 8.2 of [DH84])**.** *The Green's function G_c is harmonic on $\mathbb{C} \smallsetminus \mathcal{K}(f_c)$, and has critical points precisely at the iterated preimages of the critical point of f_c, including the critical point itself.*

In particular, $G_c(z) > 0$ for all $z \in \mathbb{C} \smallsetminus \mathcal{K}(f_c)$. For $c \in \mathbb{C} \smallsetminus \mathcal{M}$, if $G_c(z) > G_c(0)$, then $\phi_c(z)$ is well-defined. Thus, since

$$G_{\mathcal{M}}(c) \overset{\text{def}}{=} G_c(c) = G_c(f_c(0)) = 2G_c(0) > G_c(0),$$

the value $\phi_c(c)$ is always well-defined for $c \in \mathbb{C} \smallsetminus \mathcal{M}$.

Theorem 2.3.5 (Douady, Hubbard, c.f. [DH84])**.** *The map*

$$\phi_{\mathcal{M}}(c) = \phi_c(c) = \lim_{n \to \infty} f_c^n(c)^{2^{-n}}$$

is analytic, proper, and injective on $\mathbb{C} \smallsetminus \mathcal{M}$, and thus induces a conformal isomorphism $\mathbb{C} \smallsetminus \mathcal{M} \to \mathbb{C} \smallsetminus \overline{\mathbb{D}}$. In particular, the Mandelbrot set is connected.

The following famous conjecture is important in part because it implies Conjecture 2.2.11 for quadratic polynomials.

Conjecture 2.3.6 (MLC)**.** *The Mandelbrot set is locally connected.*
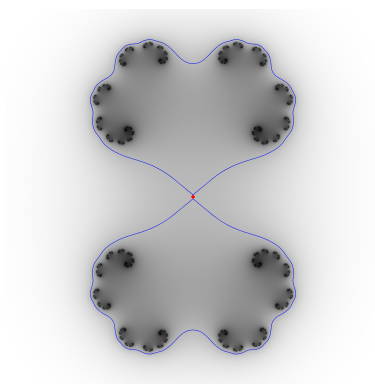
Figure 2.2: Dynamical plane for $f_c(z) = z^2 + \frac{1}{2}$, shaded according to the value of $G_c(z)$, with brighter areas corresponding to larger values of G_c. The Julia set if the collection of black points, where $G_c(z) = 0$. The blue curve is the critical equipotential $\{z : G_c(z) = G_c(0)\}$. The domain of ϕ_c is the unbounded component outside the blue curve.

While the above has been proven for particular subsets of $\mathcal{M}$, the problem in general remains open.

Definition 2.3.7. The *parameter ray* $\mathcal{R}(\theta)$ to $\mathcal{M}$ at angle $\theta \in S^1$ is the curve

$$\gamma(t) = \phi_{\mathcal{M}}^{-1}(\exp(t + \theta\tau i)),$$

defined for all $t > 0$, which satisfies $G_{\mathcal{M}}(\gamma(t)) = t$ and $\lim_{t \to \infty} \arg \gamma(t) = \theta\tau$.

Definition 2.3.8. The *dynamical ray* $\mathcal{R}_c(\theta)$ at angle $\theta \in S^1$ for f_c is the unique solution to the differential equation

$$\gamma'(t) = \frac{(\nabla G_c)^T}{\|\nabla G_c\|^2}(\gamma(t)), \tag{2.3}$$

defined on a maximal domain (t_0, ∞), such that

$$\lim_{t \to \infty} \arg \gamma(t) = \theta\tau,$$

and such that

$$G_c(\gamma(t)) = t$$

for some (and hence all) $t > t_0$.

The following proposition is, for parameter rays, a consequence of ϕ_M being bijective, and for dynamical rays, a consequence of existence and uniqueness for smooth initial value problems.

Proposition 2.3.9. *For any $c \in \mathbb{C} \setminus \mathcal{M}$, there exists a unique $\theta \in S^1$ such that c lies on $\mathcal{R}(\theta)$. For any $c \in \mathbb{C}$ and $z \in \mathbb{C} \setminus \mathcal{K}(f_c)$, there exists a unique $\theta \in S^1$ such that z lies on*

13

$\mathcal{R}_c(\theta)$.

This allows for another definition:

Definition 2.3.10. For $c \in \mathbb{C} \setminus \mathcal{M}$, the *external argument* of c is $\arg_{\mathcal{M}}(z) = \arg(\phi_{\mathcal{M}}(c)) = \theta\tau$, where $\theta \in S^1$ is the angle of the unique parameter ray through c.

For $c \in \mathbb{C}$ and $z \in \mathbb{C} \setminus \mathcal{K}(f_c)$, if z lies on a dynamical ray $\mathcal{R}_c(\theta)$, we say the *dynamical argument* of z relative to f_c is $\arg_c(z) = \theta\tau$.

The following proposition relates dynamical rays to the Böttcher map, justifying our definition for $\mathcal{R}_c(\theta)$.

Proposition 2.3.11. *For any $c \in \mathbb{C}$, let $U = \mathbb{C} \setminus \overline{\mathbb{D}}_{r_c}$ denote the domain of the inverse Böttcher map ψ_c, and for $\theta \in S^1$, let $R = \exp\left(\theta\tau i\right)\mathbb{R}_{>r_c}$ denote the straight ray at angle θ in U. Then*

$$\psi_c(R) = \mathcal{R}_c(\theta) \cap \psi_c(U).$$

Proof. Let $\gamma(t) = \psi_c(\exp\left(t + \theta\tau i\right))$ for $t > t_0 = \log r_c$. Since $\lim_{z\to\infty} \phi_c(z)/z = 1$, we know that $\lim_{t\to\infty} \arg(\gamma(t)) = \theta\tau$. Thus, by existence and uniqueness, it suffices to show that γ satisfies (2.3). Indeed,

$$G_c(\gamma(t)) = \log\left|\exp\left(t + \theta\tau i\right)\right| = t$$

for all $t > t_0$. Differentiating the above then gives

$$\nabla G_c(\gamma(t))\gamma'(t) = 1,$$

which is precisely $\nabla G_c(\gamma(t))$ multiplied by (2.3). Since ϕ_c^{-1} is conformal and maps circles centered at 0 to level curves of G_c, we also know that the component of $\gamma'(t)$ orthogonal to $\nabla G_c(\gamma(t))$ is zero. The result then follows. $\qquad\square$

Corollary 2.3.12. *If $c \in \mathbb{C} \setminus \mathcal{M}$ has external argument $\theta\tau$, then the dynamical ray $\mathcal{R}_c(\theta)$ passes through the critical value c of f_c.*

Proof. This is immediate from Proposition 2.3.11 together with the definition of $\phi_{\mathcal{M}}$. $\qquad\square$

Proposition 2.3.13. *For any $c \in \mathbb{C}$ and $\theta \in S^1$, $f_c(\mathcal{R}_c(\theta)) = \mathcal{R}_c(2\theta)$.*

Proof. Let $\gamma(t)$ parameterize the dynamical ray $\mathcal{R}_c(\theta)$. By definition, we know that

$$\lim_{t \to \infty} \arg(\gamma(t)) = \theta\tau.$$

Since f_c is monic of degree 2, and since $\gamma(t)$ tends to infinity as t tends to infinity, it follows that

$$\lim_{t \to \infty} \arg(f_c(\gamma(t))) = 2\theta\tau.$$

Moreover, using equation (2.2), we have

$$\begin{aligned}
\frac{\mathrm{d}}{\mathrm{d}t} f_c(\gamma(t)) &= f_c'(\gamma(t))\gamma'(t) \\
&= 2\gamma(t)\frac{(\nabla G_c)^T}{\|\nabla G_c\|^2}(\gamma(t)) \\
&= 2\gamma(t)\frac{(\nabla G_c(f_c(\gamma(t)))\gamma(t))^T}{\|\nabla G_c(f_c(\gamma(t)))\gamma(t)\|^2} \\
&= 2\frac{\gamma(t)\overline{\gamma(t)}}{|\gamma(t)|^2}\frac{(\nabla G_c)^T}{\|\nabla G_c\|^2}(f_c(\gamma(t))) \\
&= 2\frac{(\nabla G_c)^T}{\|\nabla G\|^2}(f_c(\gamma(t))).
\end{aligned}$$

Thus, after the reparameterization $t \leftarrow t/2$, we see that $f_c(\mathcal{R}(\theta))$ satisfies (2.3) and hence is equal to $\mathcal{R}(2\theta)$. $\qquad\square$

When considering the backward limit of a parameter ray $\gamma = \mathcal{R}(\theta)$, there are two possibilities:

(a) If $\lim_{t \searrow 0} \gamma(t)$ is a well-defined point $z_0 \in \partial\mathcal{K}(f_c) = \mathcal{J}(f_c)$, we say that $\mathcal{R}(\theta)$ *lands* at z_0.

(b) If $\lim_{t \searrow 0} \gamma(t)$ does not exist, we say that $\mathcal{R}(\theta)$ *oscillates*. By Caratheodory's theorem on conformal mappings, $\mathcal{M}$ is locally disconnected at every point in the ω-limit set of γ.

Thus, Conjecture 2.3.6 implies that (a) is only case that actually occurs.

When considering the backward limit of a dynamical ray $\gamma = \mathcal{R}_c(\theta)$, an additional possibility arises:

(a) If $\lim_{t \searrow 0} \gamma(t)$ is a well-defined point $z_0 \in \partial\mathcal{K}(f_c) = \mathcal{J}(f_c)$, we say that $\mathcal{R}_c(\theta)$ *lands* at z_0.

(b) If $\lim_{t \searrow 0} \gamma(t)$ does not exist, then $\mathcal{R}_c(\theta)$ *oscillates*, and $\mathcal{J}(f_c)$ is locally disconnected

15

at every point in the ω-limit set of γ.

(c) If γ is only defined for $t > t_0$ for some fixed $t_0 > 0$, then $\lim_{t \searrow t_0} \gamma(t)$ is necessarily a critical point of G_c in $\mathbb{C} \smallsetminus \mathcal{K}(f_c)$. In this case, we say that $\mathcal{R}_c(\theta)$ *bifurcates*.

Proposition 2.3.14. *If $c \in \mathbb{C} \smallsetminus \mathcal{M}$, then every dynamical ray $\mathcal{R}_c(\theta)$ either bifurcates or lands.*

Proof. Let $\varepsilon > 0$ be given. For $t > 0$, let $A(t) = \{z : G_c(z) < t\}$. Since

$$\mathcal{K}(f_c) = \bigcap_{t > 0} A(t)$$

is totally disconnected, there exists $\delta > 0$ such that every component of $A(\delta)$ has diameter less than ε.

Let γ parameterize $\mathcal{R}_c(\theta)$ as in (2.3). Assume that $\mathcal{R}_c(\theta)$ does not bifurcate, so $\gamma(t)$ is defined for all $t > 0$. Then for all $0 < t < \delta$, we have

$$G_c(\gamma(t)) = t < \delta,$$

so that $\gamma(t) \in A(\delta)$. Thus, the set $\{\gamma(t) : 0 < t < \delta\}$ has diameter less than ε. It follows that $\gamma(t)$ is Cauchy as $t \searrow 0$. $\square$

The following elementary fact is left as an exercise.

Exercise 2.3.15. An angle $\theta \in S^1$ has finite orbit under angle doubling if and only if θ is rational. Moreover, θ is periodic if and only if its denominator is odd; otherwise, it is strictly preperiodic.

Provided that θ is rational, the conclusion to Proposition 2.3.14 holds for all $c \in \mathbb{C}$:

Theorem 2.3.16 (Douady, Hubbard, c.f. [DH84], Proposition 8.4)**.** *Let $\theta \in \mathbb{Q}/\mathbb{Z}$ be rational. Then for any $c \in \mathbb{C}$, the dynamical ray $\mathcal{R}_c(\theta)$ either bifurcates or lands at some point $\gamma_c(\theta) \in \mathcal{J}(f_c)$. Moreover, the landing point $\gamma_c(\theta)$ is periodic if and only if θ is periodic under angle doubling; otherwise, it is strictly preperiodic.*

Proposition 2.3.17. *If $c \in \mathbb{C} \smallsetminus \mathcal{M}$ has external argument $\theta\tau$, $\theta \in S^1$, then the dynamical ray of f_c at angle $\theta' \in S^1$ bifurcates if and only if $2^k \theta' = \theta$ for some $k \in \mathbb{N}^*$. If this is the case, then the point at which $\mathcal{R}_c(\theta')$ bifurcates is an element of $f_c^{-k}(c) = f^{1-k}(0)$.*

Proof. Proposition 2.3.4 implies that the dynamical ray at angle θ' bifurcates if and only if

16

it passes through an iterated preimage of the critical point 0 of f. By Proposition 2.3.13, this occurs if and only if $\mathcal{R}_c(2^k\theta')$ passes through the critical value c of f_c for some $k \in \mathbb{N}^*$. By Corollary 2.3.12 (together with Proposition 2.3.9), $\mathcal{R}_c(2^k\theta')$ passes through c if and only if $2^k\theta' = \arg_{\mathcal{M}}(c) = \theta$. $\qquad\qquad\square$

Remark 2.3.18. In particular, this implies that the two rays at angles $\theta/2$ and $(\theta+1)/2$ land together at the critical point 0. Since f_c is even, $\mathcal{J}(f_c)$ is symmetric about 0, so these two rays partition the Julia set of f into two isometric components.

The following claim is another consequence of Proposition 2.3.13.

Proposition 2.3.19. *Suppose that θ is p-periodic under angle doubling, and that the dynamical ray $\mathcal{R}_c(\theta)$ lands at a point $z \in \mathcal{J}(f_c)$. Then the period q of z under f_c is a divisor of p. The number of angles in the orbit of θ which land at z is equal to $\frac{p}{q}$.*

2.3.2   Laminations

Definition 2.3.20. A *lamination* is a closed equivalence relation $\mathcal{L}$ on S^1. The *quotient* of a lamination $\mathcal{L}$ is the usual topological quotient $S^1/\mathcal{L}$.

Definition 2.3.21. The *filling* of a lamination $\mathcal{L}$ is the closed equivalence relation $\sim$ on $\overline{\mathbb{D}}$ obtained by setting $a \sim b$ whenever there exists an ideal triangle T, whose vertices are all equivalent with respect to $\mathcal{L}$, such that a and b both belong to $\overline{T}$.

The *filled quotient* of a lamination $\mathcal{L}$ is the quotient of $\overline{\mathbb{D}}$ by the filling of $\mathcal{L}$.

For a quadratic polynomial f_c, we obtain a lamination $\mathcal{L}(f_c)$ by identifying two angles $\alpha, \beta \in S^1$ if the dynamical rays $\mathcal{R}_c(\alpha)$ and $\mathcal{R}_c(\beta)$ land at the same point. By Proposition 2.3.13, the equivalence relation $\mathcal{L}(f_c)$ is invariant under angle doubling.

Proposition 2.3.22. *If $\mathcal{J}(f_c)$ is locally connected, then the quotient of $\mathcal{L}(f_c)$ is homeomorphic to $\mathcal{J}(f_c)$, and the filled quotient of $\mathcal{L}(f_c)$ is homeomorphic to $\mathcal{K}(f_c)$.*

Similarly, one may obtain a lamination for $\mathcal{M}$ by identifying two angles $\alpha, \beta \in S^1$ if the parameter rays $\mathcal{R}(\alpha)$ and $\mathcal{R}(\beta)$ land together. This is known as the *quadratic minor lamination* QML. If Conjecture 2.3.6 holds, then the quotient of QML is homeomorphic to $\partial\mathcal{M}$, and the filled quotient of QML is homeomorphic to $\mathcal{M}$.

A simpler equivalence relation QML_0 can be obtained by including only the ray pairings coming from angles that are periodic under doubling. The closure of QML_0 is equal to QML. The leaves of QML_0 may be generated using Lavaurs' algorithm [Lav89].

17
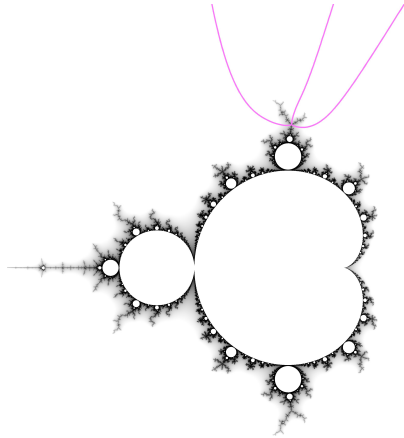
(a) The parameter rays at angles $\theta_0 = 9/56$, $\theta_1 = 11/56$, and $\theta_2 = 15/56$, which all have preperiod 3 and period 3, land together on $\partial\mathcal{M}$ at a Misiurewicz point c. The critical value of f_c has preperiod 3 and period 1.
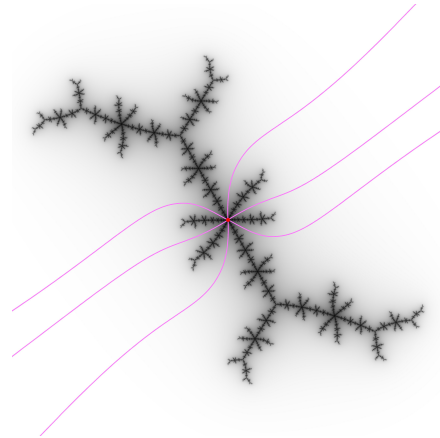
(b) For $i = 0, 1, 2$, the dynamical rays at angles $\theta_i/2$ and $(\theta_i + 1)/2$ land together at the critical point.
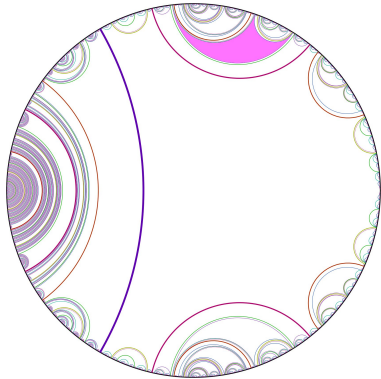
(c) Periodic arcs in QML up to period 10, with the ideal triangle $(\theta_0, \theta_1, \theta_2)$ highlighted. Refer to Table C.1 for the color scheme.
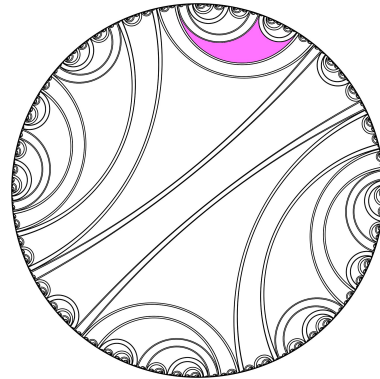
(d) The dynamical lamination $\mathcal{L}(f_c)$, with the ideal triangle $(\theta_0, \theta_1, \theta_2)$ highlighted.

2.3.3 Matings

Consider two laminations, L_0 and L_1, that are invariant under the angle doubling map. Denote by K_0 and K_1 the filled quotients of L_0 and L_1. One may then construct a topological space

$$L_0 \amalg L_1 = (K_0 \sqcup K_1)/ \sim,$$

where $\sim$ is the equivalence relation on the boundary $S^1 \sqcup S^1$ given by $(z, 0) \sim (1/z, 1)$ for all $z \in S^1$.

The space $L_0 \amalg L_1$ is known as the *mating* of the laminations L_0 and L_1. If $L_0 = \mathcal{L}(f_c)$ and $L_1 = \mathcal{L}(f_{c'})$ are the laminations of two quadratic polynomials with locally connected Julia sets, it follows from Proposition 2.3.13 that the disjoint union $f_c \sqcup f_{c'}$ projects to a well-defined map $f_c \amalg f_{c'}$ on $L_0 \amalg L_1$, whose Julia set is the image of S^1 in $L_0 \amalg L_1$. This map is known as the *mating* of f_c with $f_{c'}$.

The following fundamental criterion was conjectured by Adrien Douady and proved by Tan Lei, making use of Thurston's characterization of rational maps.

Theorem 2.3.23 (c.f. [Lei92]). *For two postcritically finite quadratic polynomials f_c and $f_{c'}$, the mating $\mathcal{L}(f_c) \amalg \mathcal{L}(f_{c'})$ is homeomorphic to $\hat{\mathbb{C}}$ if and only if c and c' do not belong to conjugate limbs of the Mandelbrot set.*

If this is the case, then the map $f_c \amalg f_{c'}$ is topologically conjugate to a postcritically finite quadratic rational map, which is unique up to Möbius conjugacy.

The mating construction can be generalized beyond the postcritically finite case. For instance, if f and g are hyperbolic quadratic polynomials whose attracting cycles have multipliers μ_f and μ_g, then there exist unique postcritically finite quadratic polynomials f_0 and g_0 that are topologically conjugate to f and g respectively. The mating $f_0 \amalg g_0$ is then topologically conjugate to a unique quadratic rational map whose attracting cycles for the images of the critical points of f and g have multipliers μ_f and μ_g respectively.

2.3.4 Hyperbolic components in $\mathcal{M}$

Let $U \subset \mathcal{M}$ be a bounded component of the quadratic family $\mathcal{P}_2$ of some period $p \in \mathbb{N}^*$. There is a natural holomorphic map $\mu : U \to \mathbb{D}$ given by taking the multiplier of the attracting p-cycle of f_c for $c \in U$.

Proposition 2.3.24 (c.f. [DH84], Theorem 14.6 or [Mil00], Theorem 6.5). *The multiplier map μ is injective on U, and thus provides a holomorphic coordinate for points in U. The*

inverse map $\mu^{-1} : \mathbb{D} \to U$ *extends continuously to* $\overline{\mathbb{D}}$.

Definition 2.3.25. The *center* of U is the point $\mu^{-1}(0)$, whose associated map has a super-attracting p-cycle. The *root* of U is the point $\mu^{-1}(1) \in \partial U$.

Definition 2.3.26. A *Misiurewicz point* in $\mathcal{M}$ is a parameter c for which the bounded critical orbit is strictly preperiodic. If k and p are respectively the preperiod and period of 0 under f_c, then we refer to c as a Misiurewicz point of preperiod k and period p.

Together, the centers of bounded hyperbolic components and the Misiurewicz points comprise the *postcritically finite* (pcf) maps in $\mathcal{P}_2$, i.e. the maps for which all critical orbits are finite sets.

The following important theorem of Douady and Hubbard provides an analogue of Theorem 2.3.16 for parameter space.

Theorem 2.3.27 (Douady, Hubbard, c.f. [DH84], Theorem 13.1)**.** *Let* $\theta \in \mathbb{Q}/\mathbb{Z}$ *be rational. Denote by* k *and* n *respectively the preperiod and period of* θ *under angle doubling.*

- *If* $k = 0$ *(equivalently, the denominator of* θ *is odd), then the parameter* $\mathcal{R}(\theta)$ *lands at the root of a hyperbolic component of period* p.

- *Otherwise, if* $k > 0$, *then* $\mathcal{R}(\theta)$ *lands at a Misiurewicz point of preperiod* $k + 1$ *and period dividing* p.

Proposition 2.3.28 (c.f. [DH84], Proposition 14.5)**.** *If* c *is the root of a hyperbolic component of period* $p > 1$, *then there are exactly two angles* $\theta_0, \theta_1 \in \mathbb{Q}/\mathbb{Z}$ *such that the parameter ray* $\mathcal{R}(\theta_i)$ *lands at* c. *Both values of* θ_i *have exact period* p *under angle doubling. Furthermore, the dynamical rays* $\mathcal{R}_c(\theta_i)$ *land together at a point* z_0 *on the boundary of the Fatou component of* $\mathcal{K}(f_c)$ *containing the critical value. The point* z_0 *necessarily belongs to a parabolic cycle of multiplier a* p^{th} *root of unity, not necessarily primitive.*

Definition 2.3.29. If two distinct parameter rays θ_0 and θ_1 land together at the root of a hyperbolic component U, the *wake* $\mathcal{W}(U) = \mathcal{W}(\theta_0, \theta_1)$ of U is the component of $\mathbb{C} \smallsetminus \left(\overline{\mathcal{R}(\theta_0)} \cup \overline{\mathcal{R}(\theta_1)} \right)$ not containing the positive real axis.

Since $\mathcal{R}(0)$ is the only parameter ray that intersects the positive real axis, and $\mathcal{R}(0)$ does not land together with any other rays, the above definition is justified.

Remark 2.3.30. There is a sense in which Proposition 2.3.28 also holds in period 1. If we regard the angles $\theta_0 = 0$ and $\theta_1 = 1$ as distinct, then both parameter rays land at the root $c = 1/4$ of the main cardioid. In this model, all of $\mathbb{C} \smallsetminus [1/4, \infty)$ would belong to the wake

$\mathcal{W}(\theta_0, \theta_1)$, which in light of Corollary 4.1.5 is consistent with the fact that one of the two fixed points is never accessible by a period 1 ray.

Suppose c is the root of a hyperbolic component U of some period p. Let $\xi : \overline{U} \to \mathbb{C}^p/(\mathbb{Z}/p\mathbb{Z})$ parameterize the attracting p-cycle throughout U, extended continuously to the boundary of U. Since $\xi(c)$ has multiplier 1, the polynomial

$$f_c^p(z) - z$$

has a double root for any z belonging to $\xi(c)$. There are thus two possibilities:

(a) There exists another p-cycle $\eta : \overline{U} \to \mathbb{C}^p/(\mathbb{Z}/p\mathbb{Z})$ which collides with ξ at c, i.e. $\eta(c) = \xi(c)$. In this case, we say that the hyperbolic component U is *primitive*.

(b) The p-cycle ξ collides with itself at c, degenerating to a cycle of some period d properly dividing p, whose multiplier is thus a $(p/d)^{\text{th}}$ root of unity. In this case, we say that the hyperbolic component U is *primitive*.

Theorem 2.3.31 (c.f. [Mil00], lemmas 6.1 and 6.2). *Let U be a hyperbolic component of period $p > 1$, and let θ_0 and θ_1 be the angles of the two parameter rays landing at the root of U. If θ_0 and θ_1 share a cycle under angle doubling, then U is satellite; otherwise, U is primitive.*

Finally, we state a result of Milnor and Thurston that has interesting implications regarding the structure of marked cycle curves.

Proposition 2.3.32 (c.f. [MT88]). *If θ_0 is periodic of period p, let θ_* be the unique (except possibly up to negation) angle in the orbit of θ_0 under doubling which is of minimal distance from $1/2$. Then the external ray $\mathcal{R}(\theta)$ lands on a hyperbolic component on the real axis.*

2.3.4.1 Veins

In general, path-connectedness for the Mandelbrot set has not been established; it would follow from Conjecture 2.3.6. However, an important subset of $\mathcal{M}$ *is* known to be path-connected.

Theorem 2.3.33 (Douady, Hubbard, c.f. [DH84] sections 20-22). *There exists a unique subset $T_{\mathcal{M}}$ of $\mathcal{M}$ satisfying the following points:*

1. *$T_{\mathcal{M}}$ contains the root and the center of every hyperbolic component in $\mathcal{M}$,*

2. *$T_{\mathcal{M}}$ contains every Misiurewicz point in $\mathcal{M}$,*

3. $T_{\mathcal{M}}$ *is a topological tree; in particular, it is path-connected,*

4. $T_{\mathcal{M}}$ *branches off only at the Misiurewicz points and the centers of hyperbolic components, and*

5. *if U is a hyperbolic component with center c_0, then every injective arc into $T_{\mathcal{M}} \cap (U \smallsetminus \{c_0\})$ is a geodesic ray with respect to the multiplier map on U.*

Definition 2.3.34. If $c \in \mathcal{M}$ is a Misiurewicz point or a root or center of a hyperbolic component, the *vein* to c in $\mathcal{M}$ is the unique path in $T_{\mathcal{M}}$ starting at 0 and ending at c.

CHAPTER 3

Marked Cycles

3.1 Cycle monodromy

Of fundamental importance to any discrete-time dynamical system is the set of periodic points. In light of this, we wish to study how cycles vary as we move around parameter space. Monodromy provides a combinatorial model for this behavior.

Definition 3.1.1. For a topological space Y and a positive integer $n \in \mathbb{N}^*$, recall that the nth symmetric power of Y is the quotient

$$\text{Sym}^n(Y) = Y^n/S_n,$$

where the symmetric group S_n acts on Y^n by permuting the coordinates.

Definition 3.1.2. For a topological space X, let $\rho : X \to \text{Sym}^n(Y)$ be a continuous map, let X_0 denote the subset of X where ρ takes values with all distinct coordinates, and let $x_0 \in X_0$ be a base point. The *monodromy* of ρ is the map

$$\text{mon}_\rho : \pi_1(X_0, x_0) \to \text{Aut}(\rho(x_0)),$$

where $\text{Aut}(\eta)$ denotes the set of all permutations of η.

Note that the codomain of mon_ρ is isomorphic to the symmetric group S_n, but not canonically so.

Example 3.1.3. If sqrt : $\mathbb{C}^* \to \text{UConf}_2(\mathbb{C})$ denotes the map sending a point z to the two solutions w to the equation $w^2 = z$, then for $\gamma \in \pi_1(\mathbb{C}^*, 1)$, the monodromy is given by

$$\text{mon}_{\text{sqrt}}(\gamma) = \sigma^k,$$

where σ is the permutation swapping the two elements of $\{-1, 1\}$, and where k is the winding

number of γ around 0.

Definition 3.1.4. If $g : Y \to X$ is a degree d branched cover with ramification locus $B \subset X$, then the map $g^{-1} : X \smallsetminus B \to \mathrm{UConf}_d(Y)$ is well-defined and continuous. For a base point $x_0 \in X$, we say the *preimage monodromy of g* is the map

$$\mathrm{mon}^g : \pi_1(X \smallsetminus B, x_0) \longrightarrow \mathrm{Aut}(g^{-1}(x_0))$$

given by $\mathrm{mon}^g = \mathrm{mon}_{g^{-1}}$.

For a dynamical family $\mathcal{F}$ on a complex manifold X, we have three natural families of maps from $\mathcal{F}$ to various symmetric powers:

- The dynatomic map
  $$\mathrm{dyn}_p : \mathcal{F} \longrightarrow \mathrm{Sym}^k(X)$$
  associates a map $f \in \mathcal{F}$ to the set of p-periodic points of f, where k is the number of p-periodic points for a generic $f \in \mathcal{F}$.

- The marked cycle map
  $$\mathrm{cyc}_p : \mathcal{F} \longrightarrow \mathrm{Sym}^k(\mathrm{Sym}^p(X))$$
  takes a map $f \in \mathcal{F}$ to the set of p-cycles of f, where k is the number of p-cycles for a generic $f \in \mathcal{F}$.

- The Misiurewicz map
  $$\mathrm{mis}_{k,p} : \mathcal{F} \longrightarrow \mathrm{Sym}^k(X)$$
  takes a map $f \in \mathcal{F}$ to the set of points $x \in X$ of preperiod k and period p under f, where k is the number of such points for a generic $f \in \mathcal{F}$.

The purpose of this thesis is to develop a theory describing the monodromy of these three classes of dynamical data. We will associate to each such class a branched cover over $\mathcal{F}$, which parameterizes maps in $\mathcal{F}$ together with the corresponding dynamical data.

Remark 3.1.5. In some cases, such as when $\mathcal{F}$ is a transcendental family, a generic $f \in \mathcal{F}$ has infinitely many p-periodic points. While the definitions provided above generalize naturally to infinite sets, this thesis is focused on algebraic families on Riemann surfaces, for which the set of p-periodic points is always Zariski closed (and so, in nontrivial cases, finite).

3.2 Dynamical Varieties

Definition 3.2.1. A dynamical family or moduli space $\mathcal{F}$ on a complex manifold X is *algebraic* if both X and $\mathcal{F}$ are quasi-projective varieties, and if the evaluation map $e : \mathcal{F} \times X \to X$ is a morphism of algebraic varieties.

Example 3.2.2. The families Rat_n, $\mathcal{M}_n$, Per_m, $\mathcal{P}_n$, and $\mathcal{U}_n$ defined in Section 2.2.1 are all algebraic.

The exponential family $\mathcal{E} = \{z \mapsto \lambda \exp(z) : \lambda \in \mathbb{C}\}$ is a dynamical family on $\mathbb{C}$, and both $\mathcal{E}$ and its mapping space $\mathbb{C}$ are algebraic varieties. However, the family $\mathcal{E}$ is not algebraic, since the maps $f \in \mathcal{E}$ are not all algebraic endomorphisms of $\mathbb{C}$.

Definition 3.2.3. For an algebraic dynamical family $\mathcal{F}$ on a Riemann surface S, the *dynatomic variety* $\mathrm{Dyn}_p(\mathcal{F})$ of period p is the Zariski closure of the quasi-projective variety

$$V_p(\mathcal{F}) = \{(f, z) : f \in \mathcal{F} \text{ and } z \in S \text{ has period } p \text{ under } f\}.$$

If $\mathcal{F}$ consists only of polynomials, then Dyn_p is the vanishing locus of the *dynatomic polynomial*

$$\varphi_p(f, z) = \prod_{d|p} (f^p(z) - z)^{\mu(p/d)},$$

where μ is the Möbius function.

Remark 3.2.4. The set V_p defined above is Zariski open in Dyn_p, but it is missing some points. For instance, consider the map $f(z) = z^2 - \frac{3}{4}$ in the quadratic family $\mathcal{P}_2$. While f has no 2-cycles, it has a degenerate 2-cycle at $z = -1/2$. If we perturb c away from $-3/4$, then this degenerate 2-cycle will split into a true 2-cycle near $-1/2$ (together with a nearby fixed point). Thus, $(f, -1/2)$ belongs to $\mathrm{Dyn}_2(\mathcal{P}_2)$, despite not belonging to $V_2(\mathcal{P}_2)$.

Theorem 3.2.5 (Bousch [Bou92], Schleicher [Sch94]). *For any period p, taking $\mathcal{F}$ to be the quadratic family $\mathcal{P}_2$, with $f_c = z^2 + c$, the dynatomic polynomial $\varphi_p(f_c, z)$ is irreducible. Thus, the dynatomic curve $\mathrm{Dyn}_p(\mathcal{P}_2)$ is irreducible.*

The curves Dyn_p admit a $\mathbb{Z}/p\mathbb{Z}$ action sending (f, z) to $(f, f(z))$. This action is faithful except on the exceptional locus Δ_p. Taking the quotient by this action, we obtain a curve parameterizing the period p cycles throughout $\mathcal{F}$:

Definition 3.2.6. For an algebraic dynamical family $\mathcal{F}$ on a Riemann surface S, the *marked*

cycle variety $\mathrm{Cyc}_p(\mathcal{F})$ of period p is the Zariski closure of the quasi-projective variety

$$C_p(\mathcal{F}) = \{(f, \zeta) : f \in \mathcal{F} \text{ and } \zeta \subset S \text{ is a } p\text{-cycle of } f\}.$$

In the case where $\mathcal{F}$ is a one-parameter family (i.e. an algebraic curve), we refer to $\mathrm{Dyn}_p(\mathcal{F})$ and $\mathrm{Cyc}_p(\mathcal{F})$ as the *dynatomic curve* and *marked cycle curve*, respectively, of period p over $\mathcal{F}$.

Let $\alpha : \mathrm{Dyn}_p(\mathcal{F}) \to \mathrm{Cyc}_p(\mathcal{F})$ denote the quotient map under the $\mathbb{Z}/p\mathbb{Z}$ action discussed above. Let $\pi : \mathrm{Cyc}_p(\mathcal{F}) \to \overline{\mathcal{F}}$ denote the natural projection to the Zariski closure of $\mathcal{F}$, and let $\mu : \mathrm{Cyc}_p(\mathcal{F}) \to \mathbb{C}$ denote the map that returns the multiplier of the marked cycle. In summary, we have the following maps:

$$\mathrm{Dyn}_p(\mathcal{F}) \xrightarrow{\ \alpha\ } \mathrm{Cyc}_p(\mathcal{F}) \xrightarrow{\ \pi\ } \overline{\mathcal{F}}$$
$$\Big\downarrow{\scriptstyle\mu}$$
$$\mathbb{C}$$

The map α is a p-fold branched cover, ramified over the exceptional locus Δ_p. The map π is an n_p-fold branched cover, where n_p is the number of p-cycles for a generic map in $\mathcal{F}$. This map ramifies over the points in $\mathcal{F}$ where multiple p-cycles coincide.

Finally, the multiplier map μ is well-defined on $\mathrm{Cyc}_p(\mathcal{F})$ and, together with $f \in \mathcal{F}$, may be used as a coordinate for $\mathrm{Cyc}_p(\mathcal{F})$.

Remark 3.2.7. The marked cycle curve Cyc_p provides the most natural domain on which the multiplier map is well-defined. The properties of the multiplier map for the quadratic family have been studied by T. Firsova, A. Belova and I. Gorbovickis. For instance, the image in $\mathcal{P}_2$ of the branch locus of μ is known as the set of *critical points of the multiplier*. Some of these points belong to $\mathcal{M}^\circ$, while others lie outside $\mathcal{M}$. Belova and Gorbovickis conjecture in [BG22] that the count measure on this set converges to a measure supported on $\partial\mathcal{M}$ as p tends to ∞. Firsova and Gorbovickis show in [FG20] that the accumulation set of the critical points contains the Mandelbrot set $\mathcal{M}$ along with a region outside $\mathcal{M}$ with nonempty interior.
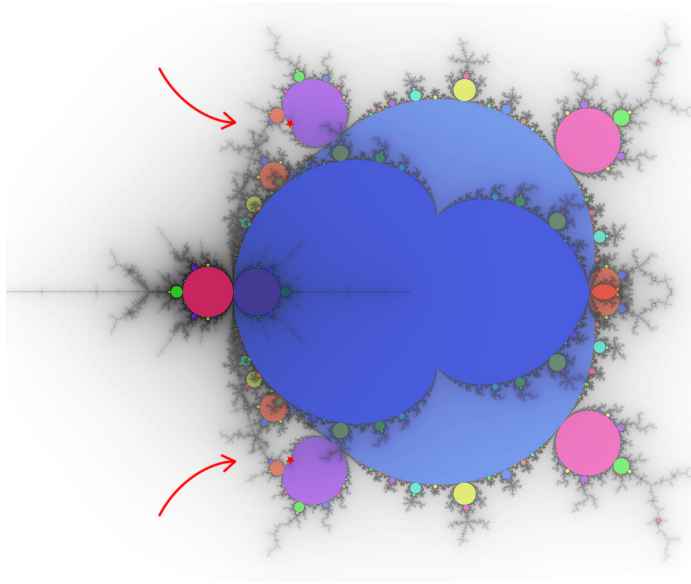
Figure 3.1: Forward image of $\mathrm{Cyc}_3(\mathcal{P}_2)$ in $\mathbb{C}$ under the multiplier map μ. The image is centered at $\lambda = -8$, and the prominent magenta component on the left is the unit disk. The multiplier map μ is a 3-fold branched cover, branched at two conjugate points (c_+, ξ_+) and (c_-, ξ_-). The ramification points $\mu(\xi_+)$ and $\mu(\xi_-)$ are marked by red stars. The parameters c_+ and c_- lie just outside $\mathcal{M}$.
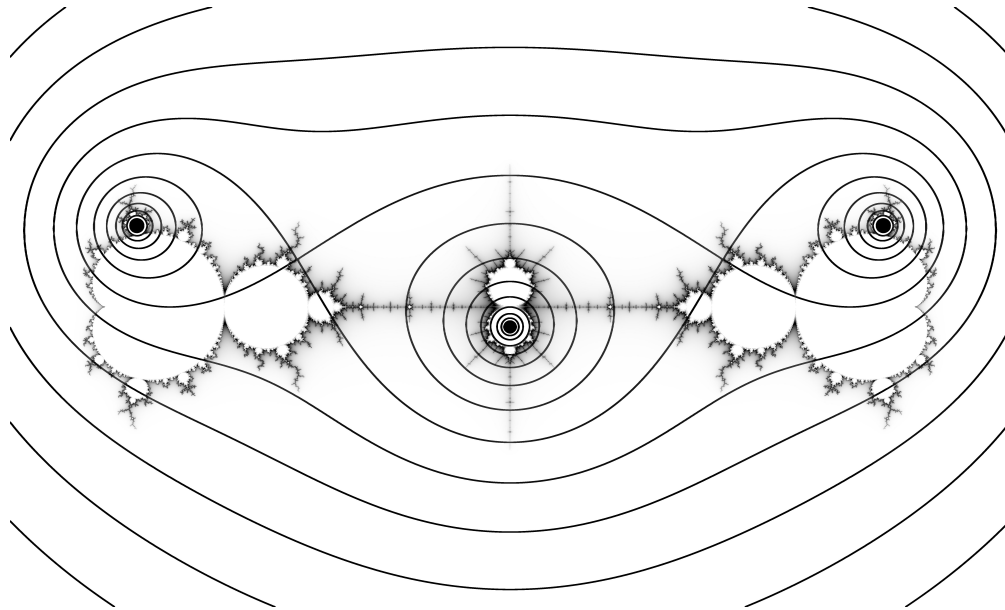
Figure 3.2: Contour plot of the multiplier map on $\mathrm{Cyc}_3(\mathcal{P}_2)$.

3.3 Examples of Dynamical Varieties

3.3.1 Quadratic polynomials

The most-studied family of dynamical systems on $\hat{\mathbb{C}}$ is the family of quadratic polynomials $\mathcal{P}_2 = \{f_c(z) = z^2 + c : c \in \mathbb{C}\}$. We can explicitly compute the dynatomic and marked cycle curves over $\mathcal{P}_2$ for small period.

In period 1, solving for $z = f_c(z)$, we obtain the relation $z^2 - z + c = 0$. Thus, $\mathrm{Cyc}_1(\mathcal{P}_2) = \mathrm{Dyn}_1(\mathcal{P}_2)$ is a rational plane curve of degree 2. The branched cover $\mathrm{Cyc}_1(\mathcal{P}_2) \longrightarrow \hat{\mathbb{C}}$ given by projection to c is ramified at $c = \infty$ and at $c = \frac{1}{4}$, where the two fixed points of f_c collide.
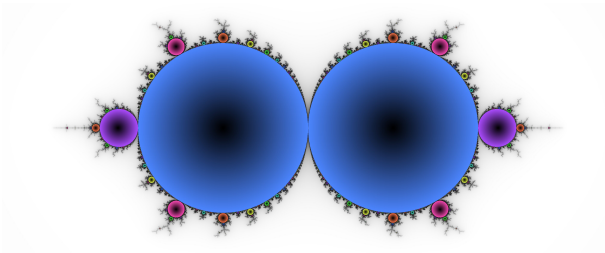
Figure 3.3: Quadratic polynomials with a marked fixed point, colored by period and multiplier of critical orbit (see Table C.1 for further details).

In period 2, we have

$$\varphi_2(c, z) = \frac{f_c^2(z) - z}{f_c(z) - z} = z^2 + c + z + 1.$$

Thus, $\mathrm{Dyn}_2(\mathcal{P}_2)$ is again a rational plane curve of degree 2. On the other hand, since a quadratic polynomial (other than $z^2 - \frac{3}{4}$) has a unique 2-cycle, the curve $\mathrm{Cyc}_2(\mathcal{P}_2)$ is just (the Zariski closure of) $\mathcal{P}_2$ itself.
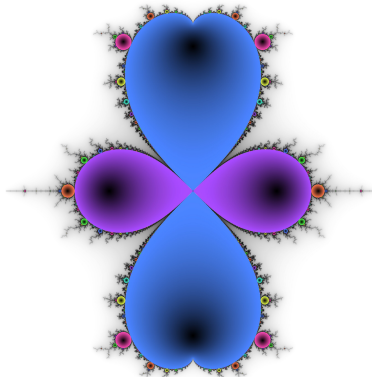
Figure 3.4: Quadratic polynomials with a marked point of period 2.

In period 3, things become more interesting. The dynatomic polynomial is now given by

$$\varphi_3(c, z) = z^6 + 3cz^4 + z^5 + 3c^2 z^2 + 2cz^3 + z^4 + c^3 + c^2 z$$
$$+ 3cz^2 + z^3 + 2c^2 + 2cz + z^2 + c + z + 1.$$

It follows that $\mathrm{Dyn}_3(\mathcal{P}_2)$ is a plane curve of degree 6. This curve turns out to still be rational, with a singular point at $c = \infty$. The projection to c ramifies at the roots of the period 3 components of the Mandelbrot set.
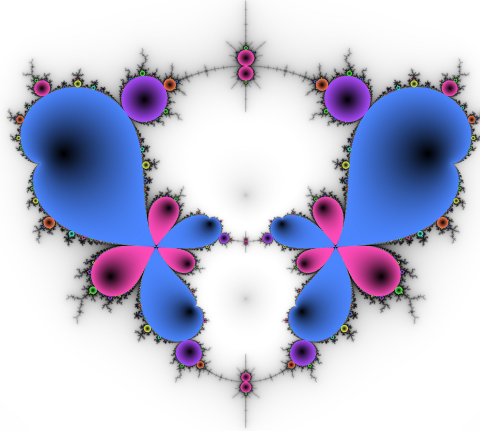
Figure 3.5: Quadratic polynomials with a marked point of period 3.

To describe the marked cycle curve of period 3, we may take the resultant of $\varphi_3(c, z)$ with $h - t$, where $h(c, z)$ is any nonconstant polynomial that is invariant along 3-cycles. Using $h(c, z) = z + f_c(z) + f_c^2(z)$, we obtain

$$\mathrm{Res}_z(\varphi_3, h - t) = \left(t^2 + c + t + 2\right)^3, \tag{3.1}$$

yielding a rational plane curve of degree 2. Unlike with $\mathrm{Dyn}_3(\mathcal{P}_2)$, the projection $\pi :$ $\mathrm{Cyc}_3(\mathcal{P}_2) \to Q$ is ramified only at $c = \infty$ and $c = -7/4$, the latter of which is the root of the "airplane" component, i.e. the unique primitive hyperbolic component of period 3 in the Mandelbrot set.

Remark 3.3.1. The third power appearing on the right-hand side of Equation (3.1) is rather spurious and is always equal to the period. Since computing resultants of high degree polynomials is computationally expensive, it would be interesting to know of a way to obtain a formula for $\mathrm{Cyc}_p(\mathcal{F})$ directly, instead of first passing through an nth power.
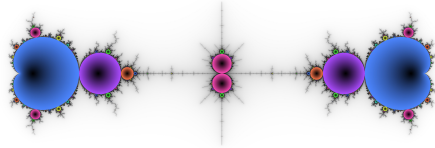
Figure 3.6: Quadratic polynomials with a marked 3-cycle.

In period 4, the dynatomic curve is no longer rational, having genus 2. The marked cycle curve, however, is rational of degree 3.

(a) $\mathrm{Cyc}_4(\mathcal{P}_2)$

(b) Contours of the multiplier map.
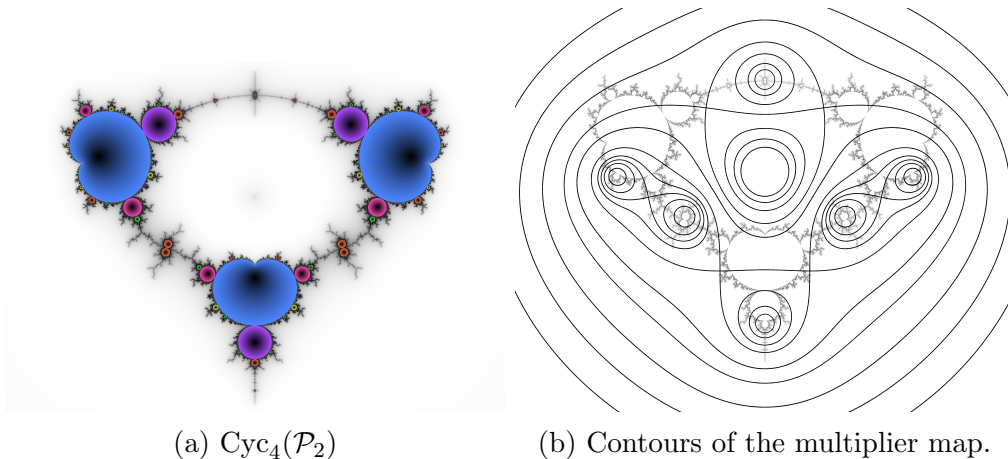
Figure 3.7: Quadratic polynomials with a marked 4-cycle.

Note the two escape regions in the image above. The unbounded escape region maps to the complement of the Mandelbrot set with degree 2. The bounded escape region, however, only maps with degree 1. As we shall see, this is due to the fact that among the three 4-cycles of the angle doubling map on the circle, one of them is invariant under complex conjugation, while the other two map to each other.

3.3.2   Quadratic Rational Maps

The quadratic family may be characterized as the subspace $\mathrm{Per}_1(0) \subset \mathcal{M}_2$ of quadratic rational maps with a superattracting fixed point (in the usual coordinates, ∞). A natural next step, then, is to study the family $\mathrm{Per}_2 \subset \mathcal{M}_2$ of quadratic rational maps with a superattracting 2-cycle. Recall that $\mathrm{Per}_2(0)$ is defined by

$$\mathrm{Per}_2(0) = \left\{ f : \hat{\mathbb{C}} \to \hat{\mathbb{C}} \text{ rational of degree 2 with a critical 2-cycle} \right\} / \sim,$$

where $f \sim g$ if $f \circ \varphi = \varphi \circ g$ for some Möbius transformation φ. For brevity, we will refer to $\mathrm{Per}_2(0)$ simply as Per_2.

A natural set of coordinates on Per_2 is given by $f_a(z) = \frac{z^2+a}{1-z^2}$, with superattracting 2-cycle $\infty \leftrightarrow -1$, free critical point 0, and free critical value a. The structure of Per_2 will be discussed in detail in Section 5.1; for now, we simply remark that Per_2 has a puncture at $a = -1$, where the family degenerates.
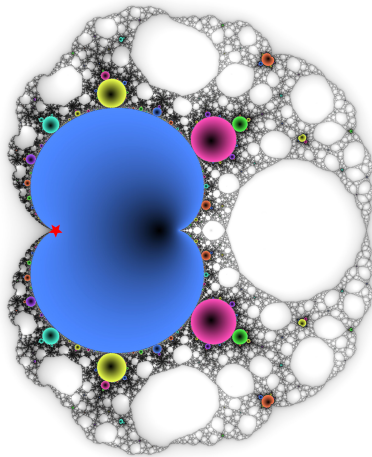
Figure 3.8: Parameter plane for Per_2, colored by period and multiplier of the free critical orbit. The red star denotes the puncture $a = -1$, where the associated map is degenerate.

The Milnor curve Per_2 may be used as a base for additional dynamical curves. As in the case of the quadratic family $\mathcal{P}_2 = \mathrm{Per}_1$, marking a fixed point produces a degree 2 branched cover of Per_2, ramified over the map $f(z) = \frac{z^2+5/27}{1-z^2}$ and over the puncture $a = -1$.
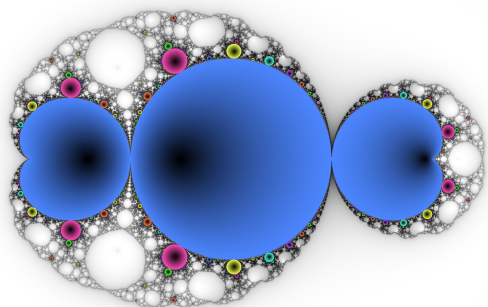
Figure 3.9: Quadratic rational maps in Per_2 with a marked fixed point.

The dynatomic and marked cycle curves in period 2 are trivial, since the unique 2-cycle

is the already-specified critical 2-cycle. In period 3, something interesting occurs. Setting $f_a^3(z) = z$ produces the relation

$$\psi_3(a, z) = z^6 - az^3 + z^4 + 3az^2 - z^3 + a^2 + az - 2z^2 - a + z + 1$$
$$= (z^3 + (\omega - \overline{\omega})z^2 + \omega a - z + \overline{\omega})(z^3 + (\overline{\omega} - \omega)z^2 + \overline{\omega}a - z + \omega)$$

where ω is a primitive cube root of unity. Thus, the curve $\mathrm{Dyn}_3(\mathrm{Per}_2)$ is not irreducible; indeed, $\mathrm{Dyn}_3(\mathrm{Per}_2)$ is the disjoint union of two 3-fold branched covers of Per_2.
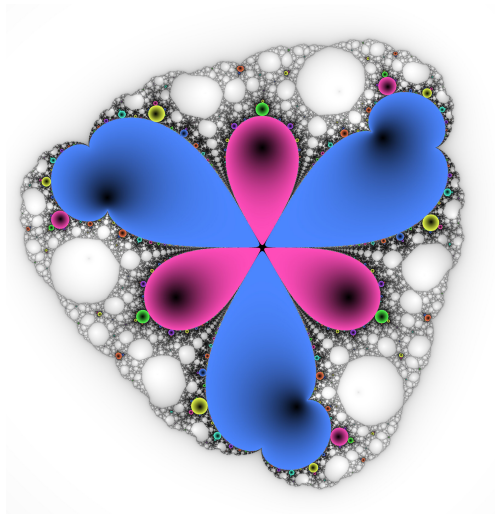
Figure 3.10: One of the two sheets of $\mathrm{Dyn}_3(\mathrm{Per}_2)$. The other sheet is the complex conjugate of this one.

The marked cycle curve, $\mathrm{Cyc}_3(\mathrm{Per}_2)$, is also disconnected, having two irreducible components, each isomorphic to Per_2 itself. This has the surprising consequence that it is possible to consistently label the two 3-cycles f_a as f_a moves throughout all of Per_2.

As we shall see, the disconnectedness of $\mathrm{Cyc}_3(\mathrm{Per}_2)$ (and hence $\mathrm{Dyn}_3(\mathrm{Per}_2)$) arises from the fact that the unique ramification point of $\mathrm{Cyc}_3(\mathrm{Per}_1)$, namely $z \mapsto z^2 - 7/4$, cannot be mated with the basilica map $f_{\circ\!\circ}(z) = z^2 - 1$.

Of course, we may continue to compute the dynatomic and marked cycle curves over Per_2 for higher periods. In period 4, both $\mathrm{Dyn}_4(\mathrm{Per}_2)$ and $\mathrm{Cyc}_4(\mathrm{Per}_2)$ are rational, so we may draw their parameter planes graphically.

32
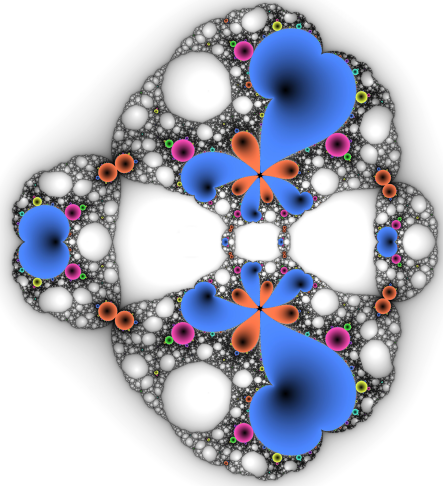
(a) Maps in Per_2 with a marked point of period 4.
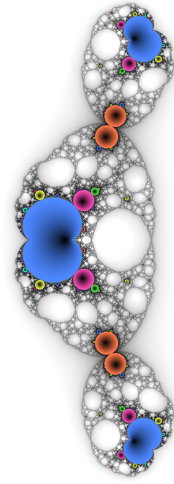
(b) Maps in Per_2 with a marked 4-cycle.

In period 5, $\mathrm{Dyn}_5(\mathrm{Per}_2)$ has genus 4 (and so cannot be easily parameterized), but $\mathrm{Cyc}_5(\mathrm{Per}_2)$ is rational.
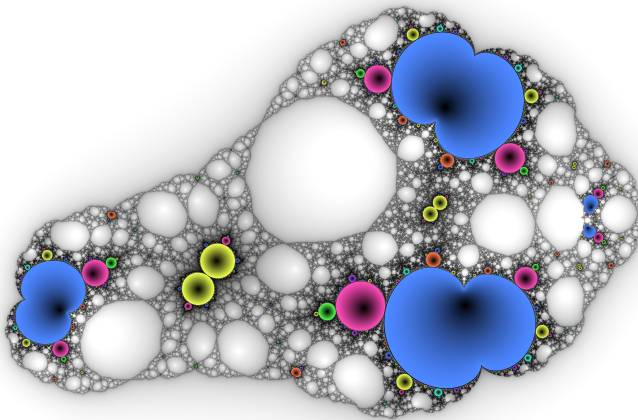
(a) The moduli space $\mathrm{Cyc}_5(\mathrm{Per}_2)$. In total, there are 6 period 1 components, corresponding to the 6 different 5-cycles. There are also 6 branch points (appearing as pairs of tangent yellow disks), corresponding to the 6 different primitive hyperbolic components in the Mandelbrot set outside the $\frac{1}{2}$-limb.
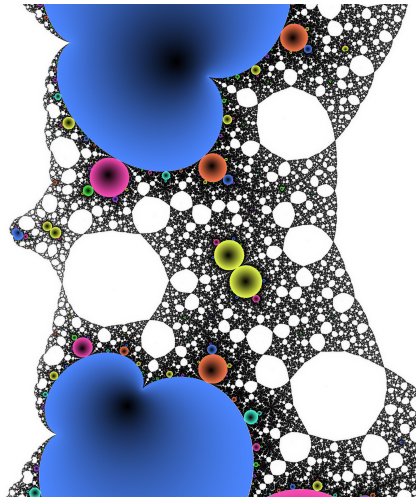
(b) Detail view of the region on the right-hand side. Note the small period 1 (blue) component on the left, which is too small to see in the zoomed-out image.

Figure 3.12: Maps in Per_2 with a marked 5-cycle.

CHAPTER 4

Marked Cycle Curves over Per_1

In light of the above examples, one would hope for a general description of the structure of $\mathrm{Dyn}_p(\mathrm{Per}_m)$ and $\mathrm{Cyc}_p(\mathrm{Per}_m)$. The general problem appears quite hard, partially due to the existence of non-mating components in Per_3 and higher. However, in the cases $m = 1$ and $m = 2$, we can obtain a canonical cell structure for the marked cycle curves of any period over Per_m. In the present chapter, we present an algorithm describing this procedure for the family $\mathrm{Per}_1 = \mathcal{P}_2$ of quadratic polynomials.

4.1 Additional properties of the quadratic family

We begin by extending the results of Section 2.3 by showing additional properties of the family of quadratic polynomials that are of particular relevance to cycle monodromy. The results presented in this section generally fall into the realm of "folklore", in the sense that largely equivalent statements may be found in the literature, but with different combinatorial models. For instance, Eike Lau and Dierk Schleicher in [Sch94] develop a similar theory using kneading sequences, while Milnor in [Mil00] develops a similar theory using orbit portraits. In the present treatment, we use external arguments to derive the needed monodromy results.

Definition 4.1.1. A wake $W = \mathcal{W}(\alpha, \beta)$ is *active* at $\theta \in \mathbb{Q}/\mathbb{Z}$ if the orbit of θ under angle doubling contains either α or β.

For a rational angle θ, denote by $\mathcal{O}_\theta$ the union of the closures of all external rays in the orbit of θ under angle doubling. In other words,

$$\mathcal{O}_\theta \stackrel{\text{def}}{=} \bigcup_{\alpha \in (\theta)} \overline{\mathcal{R}(\alpha)}.$$

For $c \in \mathbb{C} \smallsetminus \mathcal{O}_\theta$, it follows from Proposition 2.3.17 and Theorem 2.3.16 that $\mathcal{R}_c(\theta)$ lands at a point $\gamma_c(\theta) \in \mathcal{J}(f_c)$.
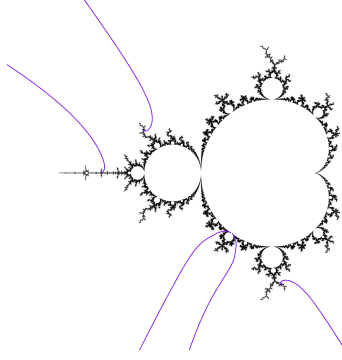
Figure 4.1: The set $\mathcal{O}_\theta$ for $\theta = 11/31$.

Lemma 4.1.2. *For $\theta \in \mathbb{Q}/\mathbb{Z}$ fixed, the map $g_\theta(c) = \gamma_c(\theta)$ is holomorphic on $\mathbb{C} \setminus \mathcal{O}_\theta$.*

Proof. Fix $\theta \in \mathbb{Q}/\mathbb{Z}$, and let $V = \mathbb{C} \setminus \mathcal{O}_\theta$. For $c \in V$, let $\gamma_c(\theta, t)$ parameterize the dynamical ray $\mathcal{R}_c(\theta)$ as in Definition 2.3.8. For $\varepsilon > 0$, define a map

$$g_\varepsilon : V \longrightarrow \mathbb{C}$$

by

$$g_\varepsilon(c) = \gamma_c(\theta, \varepsilon) \in \mathbb{C} \setminus \mathcal{K}(f_c).$$

Note that g_ε is continuous, since by Proposition 2.3.17, $\mathcal{R}_c(\theta)$ does not bifurcate for $c \in V$.

We claim that g_ε is holomorphic. To see this, fix some $c_0 \in V$, and choose a neighborhood U of c whose closure $\overline{U}$ is compact and contained in V. Since the Green's function $G_{\mathcal{M}}$ is bounded on the compact set $\overline{U}$ (where we put $G_{\mathcal{M}}(c) = 0$ for $c \in \mathcal{M}$), we may find $N \in \mathbb{N}$ sufficiently large such that

$$2^N \varepsilon > G_{\mathcal{M}}(c)$$

for all $c \in U$. It follows that

$$G_c(f^N(g_\varepsilon(c))) = 2^N G_c(g_\varepsilon(c)) = 2^N \varepsilon > G_{\mathcal{M}}(c) = G_c(c)$$

for all $c \in U$. Thus, ϕ_c is well-defined at $f^N(g_\varepsilon(c))$. Also, since $g_\varepsilon(c)$ is not an iterated preimage of a critical point of f_c (otherwise by Proposition 2.3.17, c would lie on the boundary of an active wake), the inverse function theorem implies that the holomorphic function

$$F(z, c) = (f_c^N(z), c)$$

35

has a holomorphic inverse F^{-1} defined on some neighborhood of $F(g_\varepsilon(c_0), c_0)$. Since

$$F(g_\varepsilon(c), c) = \phi_c^{-1}(\exp(\tau i\theta + 2^N \varepsilon))$$

depends holomorphically on c, we have that $g_\varepsilon(c)$ also depends holomorphically on c in a neighborhood of c_0. This proves that g_ε is holomorphic on V.

Now note that $g_\varepsilon(c)$ is nonzero on V. Since also $g_\varepsilon(c)/c \neq 1$ on $V \smallsetminus \{0\}$, Montel's theorem implies the maps $\{g_\varepsilon : \varepsilon > 0\}$ form a normal family on $\mathbb{C} \smallsetminus \{0\}$. Thus, the limit $g_\theta = \lim_{\varepsilon \to 0} g_\varepsilon$ exists and is holomorphic on $V \smallsetminus \{0\}$. Since g_θ is holomorphic and bounded in a neighborhood of 0, it follows from classification of singularities that g extends analytically through 0. Thus, g_θ is holomorphic on all of V. By construction, $g_\theta(c) = \gamma_c(\theta)$. $\qquad \square$

Lemma 4.1.3. *Suppose $\theta \in \mathbb{Q}/\mathbb{Z}$ has period p under angle doubling, and let g_θ be as above. The period of $g_\theta(c)$ under f_c is locally constant on $\mathbb{C} \smallsetminus \mathcal{O}_\theta$. Furthermore, for any periodic angle $\theta' \in \mathbb{Q}/\mathbb{Z}$ distinct from θ, the values of g_θ and $g_{\theta'}$ are either everywhere equal or nowhere equal on each component of $\mathbb{C} \smallsetminus (\mathcal{O}_\theta \cup \mathcal{O}_{\theta'})$.*

Proof. Denote by $A(c) \subset \mathcal{K}(f_c)$ the set of points of period dividing p under f_c. Thus, $A(c)$ is the set of roots of $f_c^p(z) - z$. Since f_c changes continuously with p and has constant degree, $A(c)$ is continuous with respect to the Hausdorff topology. By Proposition 2.3.19, $g_\theta(c)$ and $g_{\theta'}(c)$ belong to $A(c)$ wherever they are defined.

Define a map

$$\mu_\theta(c) \overset{\text{def}}{=} \frac{\mathrm{d}z}{\mathrm{d}f}_c(z) \bigg|_{z = g_\theta(c)}, \qquad (4.1)$$

which is holomorphic since g_θ is holomorphic. If $g_\theta(c)$ has period d under f_c, then $\mu(c)$ is the $(p/d)^{\text{th}}$ power of the multiplier of $g_\theta(c)$.

If $|\mu_\theta(c)| > 1$, then $z = g_\theta(c)$ belongs to repelling cycle of period $\pi(c)$. By Kœnigs linearization theorem, there is a value $\rho = \rho(c) > 0$ such that f_c^{-p} is well-defined from $\mathbb{D}_\rho(z)$ to itself and locally conjugate to multiplication by $1/\lambda$. In particular, f_c^{-p} has no fixed points other than $z = g_\theta(c)$. In other words,

$$A(c) \cap \mathbb{D}_{\rho(c)} = \{g_\theta(z)\}.$$

It follows from the proof of Kœnigs' theorem that the linearizing radius $\rho(c)$ depends continuously on c so long as the multiplier remains bounded away from 1.

Thus, as long as $|\mu_\theta(c)| > 1$, no other points of period dividing p collide with $g_\theta(c)$; hence,

36

the period of $g_\theta(c)$ is locally constant, and if $g'_\theta(c)$ is defined, then $g_\theta(c)$ is locally either everywhere or nowhere equal to $g'_\theta(c)$ (as their distance is either 0 or bounded below by $\rho(c)$).

All that remains is to show that $|\mu_\theta| > 1$ on $V = \mathbb{C} \smallsetminus \mathcal{O}_\theta$. Since $g_\theta(c)$ takes values in $\mathcal{J}(f_c)$, it can never belong to an attracting cycle. Thus, $|\mu_\theta| \geq 1$ on V. It follows from the open mapping theorem that in fact $|\mu_\theta| > 1$ on V, which completes the proof. $\qquad\square$

Corollary 4.1.4. *Suppose $\theta \in \mathbb{Q}/\mathbb{Z}$ has period p under angle doubling, and let g_θ be as in Lemma 4.1.2. For $c \in \mathbb{C} \smallsetminus \mathcal{O}_\theta$, $g_\theta(c)$ has period less than p under f_c if and only if c belongs to a satellite wake that is active at θ.*

Proof. Suppose first that $g_\theta(c)$ has period less than p under f_c. Since $g_\theta(0) = \exp(\theta\tau i)$ has exact period p, c cannot belong to the same component of $\mathbb{C} \smallsetminus \mathcal{O}_\theta$ as the origin. Thus, there must be some arc $\overline{\mathcal{R}(\alpha) \cup \mathcal{R}(\beta)}$ separating c from 0, which presently defines a satellite wake.

Conversely, suppose that c belongs to a satellite wake $W = \mathcal{W}(\alpha, \beta)$ which is active at θ, so that both α and β share an orbit with θ. Let c_0 be the root of W, which lies on the boundary of a satellite hyperbolic component U. By Proposition 2.3.28, the dynamical rays $\mathcal{R}_\alpha$ and $\mathcal{R}_\beta$ land together at a point $z_0 \in J(f_c)$ belonging to a parabolic cycle ξ.

By definition of a satellite component, the period d of ξ properly divides p, and ξ arises from the collision of a p-cycle with a d-cycle. If we perturb the parameter away from c_0 towards the center of U, then the p-cycle becomes attracting. Thus, since $g_\alpha(c)$ and $g_\beta(c)$ both have periods dividing p and both belong to $\mathcal{J}(f_c)$, they must land at points of ξ. By Lemma 4.1.3, it follows that $g_\alpha(c)$ and $g_\beta(c)$ have period $d < p$ for all $c \in W$. $\qquad\square$

Corollary 4.1.5. *Suppose $\theta, \theta' \in \mathbb{Q}/\mathbb{Z}$ are distinct with period p under angle doubling, and let g_θ, g'_θ be as above. Suppose further that θ and θ' do not share an orbit. For any $c \in \mathbb{C} \smallsetminus (\mathcal{O}_\theta \cup \mathcal{O}_{\theta'})$, we have that $g_\theta(c)$ and $g_{\theta'}(c)$ share an orbit if and only if c belongs to a primitive wake that is active at θ and θ'.*

Proof. Write $V = \mathbb{C} \smallsetminus (\mathcal{O}_\theta \cup \mathcal{O}_{\theta'})$, and let V_c be the component of V containing c.

Suppose first that $g_\theta(c)$ and $g_{\theta'}(c)$ share an orbit; wlog say $g_\theta(c) = g_{\theta'}(c)$. Since $g_\theta(0) = \exp(\theta\tau i)$ is distinct from $g_{\theta'}(0) = \exp(\theta'\tau i)$, c must be separated from the origin by an arc $A = \overline{\mathcal{R}(\alpha) \cup \mathcal{R}(\beta)}$, both of whose defining angles belong to $(\theta) \cup (\theta')$. Without loss of generality, assume that A is the innermost such arc, so that $A \subset \partial V_c$.

If A is a primitive arc, then we have shown the forward implication. Otherwise, up to relabeling θ and θ', we may assume that neither α nor β belongs to the orbit of θ.

Then g_θ extends analytically past A, so in particular, the pseudo-multiplier μ_θ defined in eq. (4.1) satisfies $|\mu_\theta(c_0)| > 1$, where c_0 is the landing point of the rays in A. On the other hand, we also know that $|\mu_{\theta'}(c_0)| = 1$, since $g_{\theta'}(c_0)$ belongs to a parabolic cycle. Thus, $g_\theta \neq g_{\theta'}$ in a neighborhood U of c_0. Since $A \in \partial V_c$, we have that U intersects V_c nontrivially, so by Lemma 4.1.3 in fact $g_\theta \neq g'_\theta$ throughout all of V_c. This contradicts the assumption that $g_\theta(c) = g_{\theta'}(c)$, proving the forward implication.

Conversely, suppose that c belongs to a primitive wake $W = \mathcal{W}(\alpha, \beta)$ which is active at θ, so that exactly one of $\{\alpha, \beta\}$ shares an orbit with θ. Without loss of generality, assume $\theta \in (\alpha)$. Let c_0 be the root of W, which lies on the boundary of a primitive hyperbolic component U.

By Proposition 2.3.28, the dynamical rays $\mathcal{R}_{c_0}(\alpha)$ and $\mathcal{R}_{c_0}(\beta)$ land together at a parabolic point $z_0 \in \mathcal{J}(f_{c_0})$. Since U is primitive, this point z_0 has exact period p and bifurcates into two distinct p-cycles, ξ and η, when the parameter varies away from c_0. If we perturb the parameter into U, one of these p-cycles, say ξ, becomes attracting.

Thus, since $g_\alpha(c)$ and $g_\beta(c)$ both belong to $J(f_c)$, we see that they both belong to the η when $c \in U$. Since $g_\alpha(c_0) = g_\beta(c_0)$, and since the elements of η are bounded away from one another in a neighborhood N of c_0, it follows that $g_\alpha(c) = g_\beta(c)$ in $U \cap N$. Hence, by Lemma 4.1.3, in fact $g_\alpha(c) = g_\beta(c)$ throughout all of W. $\qquad\square$

Corollaries 4.1.4 and 4.1.5 have the following direct consequence:

Corollary 4.1.6. *For a p-periodic angle θ, if c does not belong to the closure of any wake active at θ, then $\gamma_c(\theta)$ has exact period p, and $\theta\tau$ is its unique external argument.*

Proposition 4.1.7 (c.f. [Mil93], Lemma 2.6 and Theorem 3.1). *If $W = \mathcal{W}(\alpha, \beta)$ is a p-periodic wake, and if $\delta_k = \mathrm{dist}_{S^1}\left(2^k\alpha, 2^k\beta\right)$, then $\delta_0 < \delta_k$ for all $1 \leq k < p$.*

Corollary 4.1.8 (No nested active wakes). *If $W = \mathcal{W}(\alpha, \beta)$ is a p-periodic wake, and if $\alpha < \theta < \beta$, then $\theta \notin (\alpha) \cup (\beta)$.*[1]

Proof. Let c be the root of W, and let k be arbitrary such that $1 \leq k < p$. By Proposition 2.3.28, the dynamical rays $\mathcal{R}_c(\alpha)$ and $\mathcal{R}_c(\beta)$ land together in $\mathcal{J}(f_c)$. Thus, for any $k \in [p]$, the dynamical rays $\mathcal{R}_c(2^k\alpha)$ and $\mathcal{R}_c(2^k\beta)$ also land together. By Proposition 4.1.7 we know that

$$\mathrm{dist}_{S^1}(2^k\alpha, 2^k\beta) > \mathrm{dist}_{S^1}(\alpha, \beta),$$

---

[1]Recall that (α) denotes the orbit of α under angle doubling.

so it cannot be the case that $2^k\alpha$ and $2^k\beta$ both belong to the arc $(\alpha, \beta)^2$. Since dynamical rays cannot cross, it follows that neither $2^k\alpha$ nor $2^k\beta$ belongs to (α, β). Since k was chosen to be arbitrary, the result then follows.

$\square$

Corollary 4.1.9. *For any $\theta \in \mathbb{Q}/\mathbb{Z}$, there is a unique hyperbolic component on the real axis which is the landing point of an angle in the orbit of θ.*

Proof. Existence is given by Proposition 2.3.32. Uniqueness follows from Corollary 4.1.8 and the fact that any two real wakes are nested. $\square$

4.2   Cycle Monodromy for Quadratic Polynomials

Thanks to the theory developed above, the monodromy of cycles in the family $\mathrm{Per}_1 = \mathcal{P}_2$ of quadratic polynomials can be classified in terms of the roots of the primitive hyperbolic components in $\mathcal{M}$.

4.2.1   Primitive case

We begin with the following key lemma, which locally describes the monodromy for marked cycle curves.

Lemma 4.2.1 (Compare [Sch94] Lemma 3.5, [BT11] Lemma 4.2)**.** *Suppose that U is a primitive hyperbolic component of period $p > 1$, and let $\theta_0, \theta_1 \in \mathbb{Q}/\mathbb{Z}$ be the two rational angles whose parameter rays land at the root of U, with $\theta_0 < \theta_1$. Then for any $c \in \mathcal{W}(\theta_0, \theta_1)$, the dynamical rays $\mathcal{R}_c(\theta_0)$ and $\mathcal{R}_c(\theta_1)$ land together at a point $z_1 \in \mathcal{J}(f_c)$ of period p.*

Proof. With notation as in the previous section, let $V_0 = \mathbb{C} \smallsetminus \mathcal{O}_{\theta_0}$, and let $V_1 = \mathbb{C} \smallsetminus \mathcal{O}_{\theta_1}$. Since θ_0 and θ_1 do not share an orbit, the arc $\overline{\mathcal{R}(\theta_0) \cup \mathcal{R}(\theta_1)}$ is not fully contained in either $\mathcal{O}_{\theta_0}$ or $\mathcal{O}_{\theta_1}$. Thus, by Corollary 4.1.8, c lies in the same component of V_0 as the origin, and likewise for V_1. By Lemma 4.1.3, then, the points $g_{\theta_0}(c)$ and $g_{\theta_1}(c)$ both have period p.

Suppose for the sake of contradiction that $g_{\theta_0}(c) \neq g_{\theta_1}(c)$. By Corollary 4.1.5, we know that there exist $\alpha \in (\theta_0)$ and $\beta \in (\theta_1)$ such that $g_\alpha(c) = g_{\theta_1}(c)$ and $g_\beta(c) = g_{\theta_0}(c)$.

---

[2]We note that $\beta - \alpha$ cannot exceed $\frac{1}{3}$; for instance, it can be shown explicitly that an angle θ belongs to $(0, \frac{1}{3})$ (resp. $(\frac{2}{3}, 1)$) if and only if $\mathcal{R}_\mathcal{M}(\theta)$ lands at a point c in the upper (resp. lower) half plane with $\mathrm{Re}(c) > -3/4$.
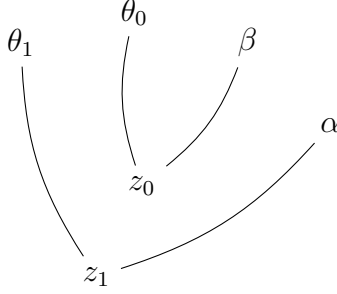
Figure 4.2: Schematic depicting the situation in the proof of Lemma 4.2.1.

Since dynamical rays cannot cross, the pairs $\{\theta_1, \alpha\}$ and $\{\theta_0, \beta\}$ must be unlinked in S^1. Since θ_0 and β land together, they must then be adjacent in S_1, and likewise for θ_1 and α. Also, by Corollary 4.1.8, neither α nor β may belong to (θ_0, θ_1). Lastly, since the critical value $c \in \mathcal{W}(\theta_0, \theta_1)$ is separated from 0 by $\mathcal{O}_{\theta_0} \cup \mathcal{O}_{\theta_1}$, it cannot be the case that $\beta < \theta_0 < \theta_1 < \alpha$. Thus, the only possibilities are $0 < \alpha < \beta < \theta_0 < \theta_1 < 1$ and $0 < \theta_0 < \theta_1 < \alpha < \beta < 1$.

Without loss of generality, assume the former set of inequalities holds. Write $z_0 = g_{\theta_0}(c) = g_\beta(c)$ and $z_1 = g_{\theta_1}(c) = g_\alpha(c)$. Since θ_0 and α share an orbit, we have that $\alpha = 2^k \theta_0 \pmod 1$ for some k. It follows that also $z_1 = f_c^k(z_0) \pmod 1$ and $\theta_1 = 2^k \beta \pmod 1$.

Since the angle doubling map is orientation preserving and $(0, \beta, \theta_0)$ are in positive circular order, it follows that

$$(0, 2^k \beta, 2^k \theta_0) = (0, \theta_1, \alpha)$$

is also in positive circular order, contradicting that $0 < \alpha < \theta_1 < 1$.

The contradiction in the other case $0 < \theta_0 < \theta_1 < \alpha < \beta < 1$ may be derived equivalently.

□

Lemma 4.2.1 provides a description of the local monodromy of cycles in a neighborhood of the root of a primitive hyperbolic component. Informally, it implies that if c is the root of a primitive hyperbolic component with external arguments θ_0 and θ_1, and if c_0 is a point near c outside the wake $\mathcal{W}(\theta_0, \theta_1)$, then following a following small loop γ based at c_0 with winding number 1 around c has the effect of swapping a point in $\mathcal{J}(f_{c_0})$ of external argument $2^k \theta_0$ with a point of external argument $2^k \theta_1$.

4.2.2 Satellite case

The monodromy around roots of satellite is slightly different. In fact, it follows from Corollary 4.1.4 and Corollary 4.1.8 that there is *no* cycle monodromy about such points, because

only a single cycle degenerates at the root of a satellite component. Thus, satellite roots have no meaningful effect on the structure of marked cycle curves.

4.3   Abstract binary cycles

To encode the cell structure for $\mathrm{Cyc}_p(\mathrm{Per}_1)$, it is useful to have a combinatorial description for any p-cycle ξ of a quadratic polynomial. Broadly speaking, this is done by representing the dynamical arguments of the elements of ξ using the first p digits of their binary expansions.

Definition 4.3.1. Let $\Sigma_p = \{0, 1\}^p$, and define the *shift map* $\sigma : \Sigma_p \to \Sigma_p$ by

$$\sigma(a_0, \ldots, a_{p-1}) = (a_1, \ldots, a_{p-1}, a_0).$$

Two elements $\xi, \eta \in \Sigma_p$ are said to be *shift-equivalent* if $\sigma^k(\xi) = \eta$ for some $k \in \mathbb{N}$.

Definition 4.3.2. An element $\xi \in \Sigma_p$ is *of exact period p* if for all k not a multiple of p, $\sigma^k(\xi) \neq \xi$.

Evidently, having exact period p is a shift-invariant property.

Definition 4.3.3. For $p \in \mathbb{N}^*$, an *abstract binary point* (ABP) of period p is an element of Σ_p of exact period p.

Definition 4.3.4. For $p \in \mathbb{N}^*$, an *abstract binary cycle* (ABC) of period p is a shift equivalence class of ABPs of period p. We will denote such equivalence classes using parentheses, analogously to our notation for angle orbits. For instance, $(011) = \{011, 110, 101\}$.

Example 4.3.5. There are 9 abstract binary cycles of period 6:

$$\begin{array}{lll}
(000001), & (000011), & (000101), \\
(000111), & (001011), & (001101), \\
(001111), & (010111), & (011111).
\end{array}$$

Lemma 4.3.6. *For any $c \geq 0$ real, and $p \geq 2$, the p-cycles of $f_c(z) = z^2 + c$ are in natural bijection with the ABCs of period p. Furthermore, two p-cycles are complex conjugates if and only if the associated ABCs differ by a bit-flip.*

Proof. Let $c \geq 0$. Since c is real and positive, it does not belong to any p-periodic wake. Thus, by Corollaries 4.1.4 and 4.1.5, every p-periodic point z of f_c is the landing point of a unique dynamical ray, whose angle $\theta(z)$ has period p. Taking the base 2 expansion of $\theta(z)$

41

produces a binary sequence of exact period p. By Proposition 2.3.13, $\theta(f_c(z)) = \sigma(\theta(z))$. Thus, the map sending the orbit (z) of z to the ABC $(\theta(z))$ is well-defined.

Conversely, since every p-periodic angle θ lands at a p-periodic point by Corollary 4.1.4, the map $(z) \mapsto (\theta(z))$ has an inverse, so it is a bijection.

Since $(\theta(\bar{z})) = (-\theta(z)) = \eta((\theta(z)))$, complex conjugation on p-cycles is equivalent to bit-flip on ABCs. □

The 2-symbol shift admits a unique nontrivial automorphism, namely the "bit-flip" involution η induced by exchanging 0s and 1s.

Definition 4.3.7. An *abstract binary point class* (ABP class) is an orbit of an ABP under η. We will denote ABP classes using square brackets, e.g. $[011] = \{011, 100\}$.

Since η commutes with the shift, it descends to a well-defined map (η) on the set of ABCs of period p. An *abstract binary cycle class* (ABC class) is an orbit of an ABC under η. We will denote cycle classes using angle brackets, e.g. $\langle 011 \rangle = \{(011), (001)\}$.

While every ABP class contains exactly two ABPs (as η has no fixed points), an ABC class may contain either one or two ABCs. We refer to an ABC class as *reflexive* if it contains only one ABC.

Example 4.3.8. There are five ABC classes of period 6, namely $\langle 000001 \rangle$, $\langle 000011 \rangle$, $\langle 000101 \rangle$, $\langle 000111 \rangle$, and $\langle 001011 \rangle$. Among these, only $\langle 000111 \rangle$ is reflexive.

Remark 4.3.9. Abstract binary cycles have many other combinatorial interpretations. For instance, ABCs of period p are in canonical bijection with irreducible polynomials of degree p in $\mathbb{F}_2[x]$. As we shall see, ABC classes also count a number of interesting dynamical objects.

4.4 Itineraries

Suppose f is a self-map of some topological space X. Let $\mathcal{U} = (U_0, \dots, U_{k-1})$ be a collection of disjoint open sets in X.

Definition 4.4.1. The *itinerary* $I_{\mathcal{U}}(x)$ of a point $x \in X$ relative to $\mathcal{U}$ is the unique sequence

$$(\varepsilon_0, \varepsilon_1, \dots) \in ([k] \cup \{*\})^{\mathbb{N}}$$

such that

$$f^i(x) \in U_{\varepsilon_i},$$

whenever $f^i(x)$ belongs to $\bigcup \mathcal{U}$, and such that $\varepsilon_i = *$ for all other $i \in \mathbb{N}$.

Definition 4.4.2. The *itinerary orbit* $\overline{I}_{\mathcal{U}}(x)$ of a point $x \in X$ relative to $\mathcal{U}$ is the orbit of $I_{\mathcal{U}}(x)$ under the left shift $\sigma(\varepsilon_0, \varepsilon_1, \dots) = (\varepsilon_1, \varepsilon_2, \dots)$.

If x and x' belong to the same p-cycle, then they have the same itinerary orbit. Thus, for a p-cycle ξ of f, the itinerary orbit $I_{\mathcal{U}}(\xi)$ is well-defined. The group $S_k \times (\mathbb{Z}/p\mathbb{Z})$ acts naturally on $I_{\mathcal{U}}(\xi)$. For $\sigma \in S_k, j \in \mathbb{Z}/p\mathbb{Z}$, and $(\varepsilon_0, \dots, \varepsilon_{p-1}) \in I_{\mathcal{U}}(\xi)$, we set

$$(\sigma, j) \cdot (\varepsilon_0, \dots, \varepsilon_{p-1}) = (\sigma(\varepsilon_j), \sigma(\varepsilon_{j+1}) \dots, \sigma(\varepsilon_{j-1})),$$

where addition in indices is done modulo p.

Proposition 4.4.3. *The action defined above is transitive.*

Proof. In the definition of labeled itinerary, only two choices were made: a choice of shift, corresponding to an element of $\mathbb{Z}/p\mathbb{Z}$, and a choice of labeling on $\mathcal{U}$, corresponding to an element of S_k. Two labeled itineraries for the same cycle ξ can therefore differ only up to these two actions. $\square$

Of particular importance in complex dynamics is the following type of partition and its associated itineraries:

Definition 4.4.4. For $\theta \in S^1$ and $p \in \mathbb{N}^*$, the *canonical partition* of degree p for θ is the partition

$$P^{(n)}(\theta) = \left\{ \left(\frac{\theta}{n}, \frac{\theta+1}{n} \right), \left(\frac{\theta+1}{n}, \frac{\theta+2}{n} \right), \dots, \left(\frac{\theta+n-1}{n}, \frac{\theta}{n} \right) \right\},$$

where intervals on S^1 are understood to wrap around mod 1, so that, for instance,

$$\left(\frac{5}{6}, \frac{1}{6} \right) = \left(\frac{5}{6}, 1 \right] \cup \left[0, \frac{1}{6} \right).$$

Definition 4.4.5. The *canonical itinerary* $\mathcal{I}_\theta^{(n)}(\alpha)$ of degree n for $\alpha \in S^1$ relative to $\theta \in S^1$ is the itinerary of α relative to $P^{(n)}(\theta)$.

Remark 4.4.6. For quadratic polynomials f_c, $c \notin \mathcal{M}$, the canonical itinerary of z relative to $\arg_{\mathcal{M}}(c)$ and the dynamical argument of z provide distinct ways to label points $z \in \mathcal{J}(f_c)$. These two sequences are equal when $\arg_{\mathcal{M}}(c) = 0$. In general, however, the relationship

between the canonical itinerary and the dynamical argument (where the latter is uniquely defined) is quite complicated.

In the present work, we use the dynamical argument to label periodic points in $\mathcal{J}(f_c)$. Giulio Tiozzo and Caroline Davis have independently developed in [Dav+23] an algorithm similar to Algorithm 4.6.1 that uses kneading sequences and itineraries instead of external and dynamical arguments.

4.5 A cell structure

In the following discussion, let $p \in \mathbb{N}^*$ be fixed.

We begin with some observations about the structure of the map $\pi : \mathrm{Cyc}_p(\mathrm{Per}_1) \to \hat{\mathbb{C}}$. Let $B \subset \mathrm{Cyc}_p(\mathrm{Per}_1)$ be the branch locus of π, and let $P = \pi(B) \subset \hat{\mathbb{C}}$ be the ramification locus. Let $P_0 = P \cap \mathbb{C}$ be the set of *finite* ramification points, and let $B_0 = \pi^{-1}(P_0)$ be the set of finite branch points.

Lemma 4.5.1. *P_0 is precisely the set of roots of primitive hyperbolic components of period p in the Mandelbrot set.*

Proof. If π ramifies over f_c, then $f_c^p(z) - z$ has a zero z_0 of multiplicity at least 2. Writing

$$f_c^p(z) - z = (z - z_0)^2 \, g(z),$$

where g is a polynomial, we find that the multiplier of f_c^p at z_0 is

$$
\begin{aligned}
\lambda_c &= \left. \frac{\mathrm{d}}{\mathrm{d}z} f_c^p(z) \right|_{z=z_0} \\
&= \left. \frac{\mathrm{d}}{\mathrm{d}z} \left((z - z_0)^2 \, g(z) + z \right) \right|_{z=z_0} \\
&= 1.
\end{aligned}
$$

It follows that f_c has a parabolic cycle of order dividing p. Since λ_c depends holomorphically on c, the open mapping theorem implies that we can perturb c to make the cycle attracting, implying that f_c lies on the boundary of a hyperbolic component. Thus, since $\lambda_c = 1$, c is the root of a hyperbolic component U.

Since π ramifies over c, two distinct p-cycles come together at c. Thus, by definition, the component U is primitive. $\qquad\square$

We are now prepared to describe the cell structure for marked cycle curves over Per_1. This will consist of a labeling of the faces, edges, and vertices, together with an ordering on the edges around each face.

Definition 4.5.2. Let M_0 denote the path-connected component of $\mathcal{M}$ containing 0.

By Theorem 2.3.33, M_0 contains the root of every hyperbolic component, so in particular, $P_0 \subset M_0$. Also, since M_0 is path-connected and full, it is nullhomotopic.

Definition 4.5.3. The cells in $\text{Cyc}_p(\text{Per}_1)$ are defined as follows:

- A *vertex* is a connected component of $\pi^{-1}(M_0) \smallsetminus B$ containing a lift of f_0.

- An *edge* is a finite branch point of π.

- A *face* is a lift of $\hat{\mathbb{C}} \smallsetminus M_0$.

One may obtain a homotopically equivalent cell structure by contracting each vertex down to a lift of f_0, stretching out the edges to include lifts of principal veins, and expanding the faces into the Mandelbrot set to meet the edges.

Lemma 4.5.4. *Vertices in* $\text{Cyc}_p(\text{Per}_1)$ *are in natural bijection with abstract binary cycles of period* p.

Proof. By definition of Cyc_p, lifts of the polynomial $f_0(z) = z^2$ are in bijective correspondence with cycles of period p under f_0. The result then follows from Lemma 4.3.6. $\square$

We thus label vertices according to abstract binary cycles.

In light of Lemma 4.5.1, edges map under π to roots of primitive hyperbolic components of period p. We may thus label an edge α by the pair (θ_0, θ_1) of external angles whose parameter rays land at $\pi(\alpha)$.

Finally, to label the faces, we use the following result.

Lemma 4.5.5. *Faces in* $\text{Cyc}_p(\text{Per}_1)$ *are in natural bijection with abstract binary cycle classes of period* p. *Moreover, letting* F_C *denote the face corresponding to an ABC class* C, *we have the following dichotomy:*

- *If* C *is reflexive, then the restriction* $\pi : F_C \to \hat{\mathbb{C}} \smallsetminus M_0$ *is a homeomorphism.*

- *Otherwise, if* C *is not reflexive, then the restriction* $\pi : F_C \to \hat{\mathbb{C}} \smallsetminus M_0$ *is a degree 2 branched cover, ramified at* ∞.
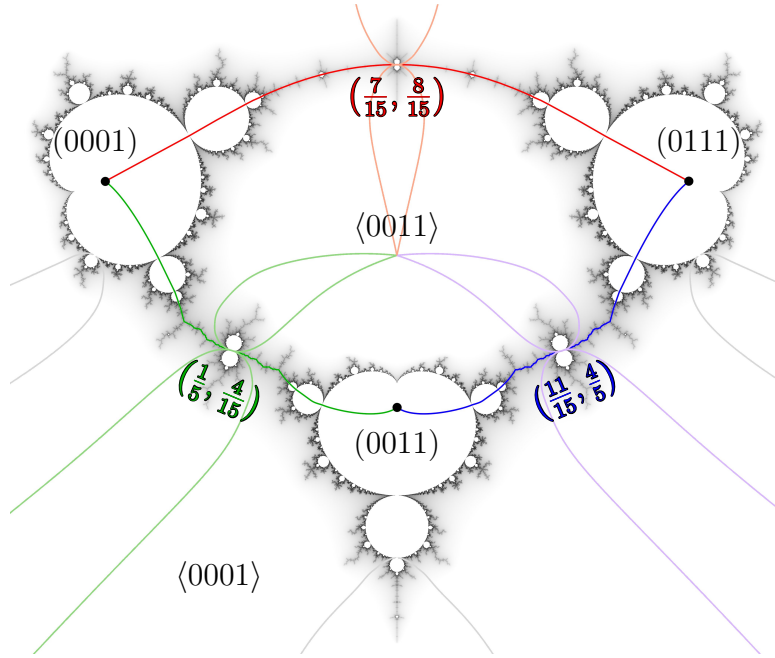
Figure 4.3: Cell structure for $\mathrm{Cyc}_4(\mathrm{Per}_1)$, with vertices, edges, and faces labeled by ABCs, primitive wakes, and ABC classes, respectively. Note that the outer face maps to $\hat{\mathbb{C}} \smallsetminus \mathcal{M}$ with degree 2, while the inner face maps with degree 1.

The active external rays are also shown for reference, since their angles provide the labels for the edges. The active satellite rays, which do not affect the marked cycles, are shown in gray, while the primitive rays are colored according to the corresponding edge. Within the active primitive wakes, the points of the marked cycle have two distinct external arguments. Within the active satellite wakes, the marked cycle has no external argument. Everywhere else, the points of the marked cycle have unique external arguments. These external rays are not part of the cell structure, forming instead a doubled version of the dual graph.

To prove Lemma 4.5.5, we will make use of the following lemma, which describes the monodromy around ∞.

Lemma 4.5.6 (Compare [BDK91], theorem 1.3). *Let $c > 1/4$ be real, and let $\alpha : S^1 \to \mathbb{C} \setminus \mathcal{M}$ be a loop with winding number 1 around 0. Then the monodromy under γ interchanges the point in $J(f_c)$ with external argument $\theta\tau$ with the point of external argument $-\theta\tau$.*

Proof. Since c does not belong to any wake, the landing map $\gamma : \mathbb{Q}/\mathbb{Z} \to J(f_c)$ is injective. It follows that γ is injective on all of S^1, so the language of Lemma 4.5.6 is well-defined.

Up to a homotopy, we may assume that $\alpha(t)$ has external argument $t\tau$ for all $t \in S^1$. Let $z_0 \in \mathcal{J}(f_c)$ have external argument $\theta\tau$, and let $z_t \in \mathcal{J}(f_{\alpha(t)})$ be continuous on $[0, 1]$, starting at the base point z_0. We wish to show that z_1 has external argument $-\theta\tau$.

By Remark 2.3.18, the dynamical rays $R_0(t) = \mathcal{R}_{\gamma(t)}(t/2)$ and $R_1(t) = \mathcal{R}_{\gamma(t)}((1+t)/2)$ land together at the critical point of $f_{\gamma(t)}$, cutting the Julia set $\mathcal{J}(f_{\gamma(t)})$ in half. Since the Julia set never intersects R_0 or R_1, the itinerary of z_t relative to (R_0, R_1) is invariant.

When $\gamma(t)$ makes a full turn around $\mathcal{M}$, R_0 and R_1 make only a half turn, trading places with each other. Thus, the itinerary of z_1 relative to the initial partition $(R_0(0), R_1(0)) = (R_1(1), R_0(1))$ is the exact opposite of the itinerary of z_0 relative to this same partition.

We know another point whose canonical itinerary is the opposite of that of z_0, namely its complex conjugate, $\overline{z_0}$.

Note that the itinerary of an angle relative to the partition $(0, 1/2)$ is precisely its binary expansion. Thus, the dynamical arguments of z_1 and $\overline{z_0}$ have the same binary expansions, so they are equal. The result then follows. $\qquad\square$

Proof of Lemma 4.5.5. Fix any parameter $c_0 > 1/4$. By Lemma 4.3.6, the p-cycles of f_{c_0} are in canonical bijection with ABCs of period p. Two lifts (c_0, ξ) and (c_0, ξ') of c_0 belong to the same face F if and only if they can be connected by a path in F, i.e. if and only if there is some loop in $\mathbb{C} \setminus \mathcal{M}$ based at c_0 whose monodromy takes ξ to ξ'. By Lemma 4.5.6, this occurs if and only if $\xi' \in \{\xi, \overline{\xi}\}$.

We thus have two possibilities:

- If $\xi = \overline{\xi}$, then the face F containing (c_0, ξ) contains only one lift of c_0. Thus, the branched cover $\pi|_F$ has degree 1, so it is a homeomorphism.

- Otherwise, if $\xi \neq \overline{\xi}$, then the face F containing (c_0, ξ) also contains $(c_0, \overline{\xi})$, but it contains no other lifts of c_0. Thus, the branched cover $\pi|_F$ has degree 2, ramifying at

∞.

By Lemma 4.3.6, $\xi = \bar{\xi}$ if and only if the ABC associated to ξ is reflexive. The result then follows. $\qquad\qquad\square$

4.6 Computing the cell structure

We give the following algorithm to compute the cell structure for $\mathrm{Cyc}_p(\mathrm{Per}_1)$ described above:

Algorithm 4.6.1.

1. Enumerate all pairs (θ_0, θ_1) of period p parameter rays in $\hat{\mathbb{C}} \setminus \mathcal{M}$ such that θ_0 and θ_1 land together on $\partial\mathcal{M}$. This can be done using Lavaurs' algorithm [Lav89]. Denote by $\mathcal{A}$ the ordered set of arcs of period p.

2. Denote by P the set of abstract binary cycles of period p. For each endpoint θ of an arc in $\mathcal{A}$, compute a canonical representative (θ) for the associated ABC. One way to do this is to take the minimum over the orbit of θ under angle doubling.

3. Let $\mathcal{A}' = \{(\theta_0, \theta_1) \in \mathcal{A} : (\theta_0) \neq (\theta_1)\}$ be the set of primitive arcs in $\mathcal{A}$.

4. For each p-periodic ABC class $\langle\alpha\rangle$, we *traverse the face* $\langle\alpha\rangle$ as follows:

   4.1 Initialize $k = 0$ and $x_0 = \alpha$. The angle x_k represents the external angle of the parameter c at the kth vertex. We are beginning our journey on the positive real axis, where we are guaranteed to be outside any p-periodic wake.

   4.2 Locate the first arc $(\theta_0, \theta_1) \in \mathcal{A}'$ strictly after x_k in counterclockwise circular order such that either θ_0 or θ_1 belongs to (x_k).

      - If in the process of finding the next arc, we wrap around the end of $\mathcal{A}'$, then we check if $x_k = \alpha$. If so, we terminate the traversal of $\langle\alpha\rangle$ and return the ordered sequence of vertices.

   4.3 If $\theta_0 \in (x_k)$, then set $x_{k+1} = \theta_1$; otherwise, if $\theta_1 \in (x_k)$, then set $x_{k+1} = \theta_0$.

   4.4 Update $k \leftarrow k + 1$ and continue from step 4.2.

5. Glue together all pairs of matching edges in the faces obtained in step 4.

Example 4.6.2 ($\mathrm{Cyc}_5(\mathrm{Per}_1)$)**.** As an example, consider the family of quadratic polynomials $f_c(z) = z^2 + c$ with a marked cycle of period 5. We begin by enumerating the period 5 arcs in QML, together with the ABC associated to the orbit of each angle under doubling.

ID	θ_0	θ_1	(θ_0)	(θ_1)	Knead. Seq.	Primitive?
A_0	1/31	2/31	$(1) = (00001)$	$(1) = (00001)$	0000∗	No
A_1	3/31	4/31	$(3) = (00011)$	$(1) = (00001)$	0001∗	Yes
A_2	5/31	6/31	$(5) = (00101)$	$(3) = (00011)$	0010∗	Yes
A_3	7/31	8/31	$(7) = (00111)$	$(1) = (00001)$	0011∗	Yes
A_4	9/31	10/31	$(5) = (00101)$	$(5) = (00101)$	0000∗	No
A_5	11/31	12/31	$(11) = (01011)$	$(3) = (00011)$	0101∗	Yes
A_6	13/31	18/31	$(11) = (01011)$	$(5) = (00101)$	0100∗	Yes
A_7	14/31	17/31	$(7) = (00111)$	$(3) = (00011)$	0110∗	Yes
A_8	15/31	16/31	$(15) = (01111)$	$(1) = (00001)$	0111∗	Yes
A_9	19/31	20/31	$(7) = (00111)$	$(5) = (00101)$	0101∗	Yes
A_{10}	21/31	22/31	$(11) = (01011)$	$(11) = (01011)$	0000∗	No
A_{11}	23/31	24/31	$(15) = (01111)$	$(3) = (00011)$	0011∗	Yes
A_{12}	25/31	26/31	$(7) = (00111)$	$(11) = (01011)$	0010∗	Yes
A_{13}	27/31	28/31	$(15) = (01111)$	$(7) = (00111)$	0001∗	Yes
A_{14}	29/31	30/31	$(15) = (01111)$	$(15) = (01111)$	0000∗	No

Table 4.1: Period 5 arcs in QML, together with their associated abstract binary cycles. The ABCs are represented using their minimal element under the dictionary ordering. For reference, we also include the kneading sequences, though these are not necessary for the algorithm.

We now proceed to the face traversal stage. For brevity, we will only show the process for the face $\langle 00011 \rangle = \langle 3 \rangle$.

- We begin at some ABC representative for $\langle 3 \rangle$; say, (3). This shall be the "first" vertex v_0 in our face. Since we are starting from the top of the list of edges, we can optionally add an indicator to remember that there is a lift of the positive real axis connecting the center of F to v_0.

- We look for the first primitive arc in our list that is active at (i.e. one of whose angles shares a cycle with) v_0, i.e. one of whose ABCs is (3). This is the second arc on our list, A_1, which connects (3) and (1). We thus set our next vertex to $v_1 = (1)$.

- The next primitive arc after A_1 that is active at $v_1 = (1)$ is A_3, which connects (7) and (1). We thus set our next vertex to $v_2 = (7)$.

- The next primitive arc after A_2 that is active at $v_2 = (7)$ is A_7, which connects (7) and (3). We thus set our next vertex to $v_3 = v_0 = (3)$. Since A_7 crosses the negative real

axis, we can optionally mark the edge connecting v_2 to v_3 as crossing a lift of $\mathbb{R}_-$.

- The next primitive arc after A_7 that is active at $v_3 = (3)$ is A_{11}, which connects (15) and (3). We thus set our next vertex to $v_4 = (15)$.

- The next primitive arc after A_7 that is active at v_4 is A_{13}, which connects (15) and (7). We thus set our next vertex to $v_5 = v_2 = (7)$.

- There are no primitive arcs after A_{13} active at v_5. So, we return to the top of the list. Since v_5 is the marked cycle as we cross the real axis, we can mark a lift of $\mathbb{R}_+$ through v_5. Note that consistently with Lemma 4.5.6, $v_5 = (7)$ and the other positive real vertex $v_0 = (3)$ belong to the same ABC class $\langle 00011 \rangle$.

- Continuing from the top of the list, A_3 connects v_5 to $v_6 = v_1 = (1)$, A_8 connects v_6 to $v_7 = v_4 = (15)$ through $\mathbb{R}_-$, and A_{13} connects v_7 to $v_8 = v_0 = (7)$.

- No more arcs after A_{13} are active at v_8. Since we already crossed the real axis with v_8 active, we close up the face, identifying v_8 with v_0.

The other two faces $\langle 00001 \rangle$ and $\langle 00101 \rangle$ may be computed similarly. In this case, all three faces map to $\hat{\mathbb{C}} \setminus \mathcal{M}$ with degree 2, since no odd period ABC can be reflexive (as the discrepancy between the number of 0s and 1s is always odd).

We can then draw the resulting cell structure:
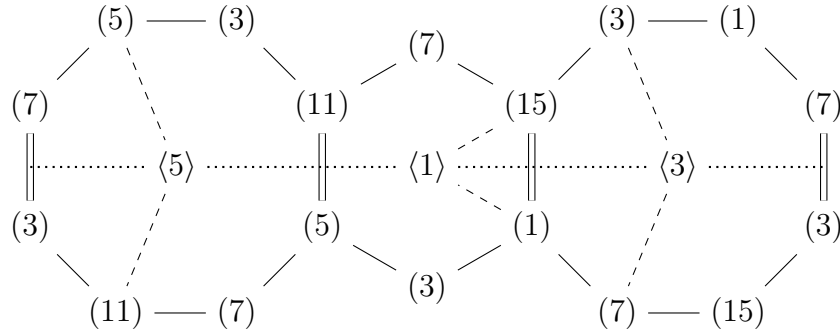
Figure 4.4: Cell structure for the marked cycle curve $\mathrm{Cyc}_5(\mathrm{Per}_1)$, which has genus $g = 2$. The vertex label (α) denotes the orbit of $\alpha/31$ under angle doubling, and the face label $\langle \alpha \rangle$ denotes the orbit of $\alpha/31$ under angle doubling together with angle negation (so, for instance, $\langle 5 \rangle = (5) \cup (11)$). Double edges indicate ray pairings that cross the negative real axis. Dashed lines indicate lifts of the positive real axis, and dotted lines indicate lifts of the negative real axis.

Example 4.6.3 $(\mathrm{Cyc}_6(\mathrm{Per}_1))$. We can use the same procedure to produce the cell structure

for the family of quadratic polynomials with a marked 6-cycle:
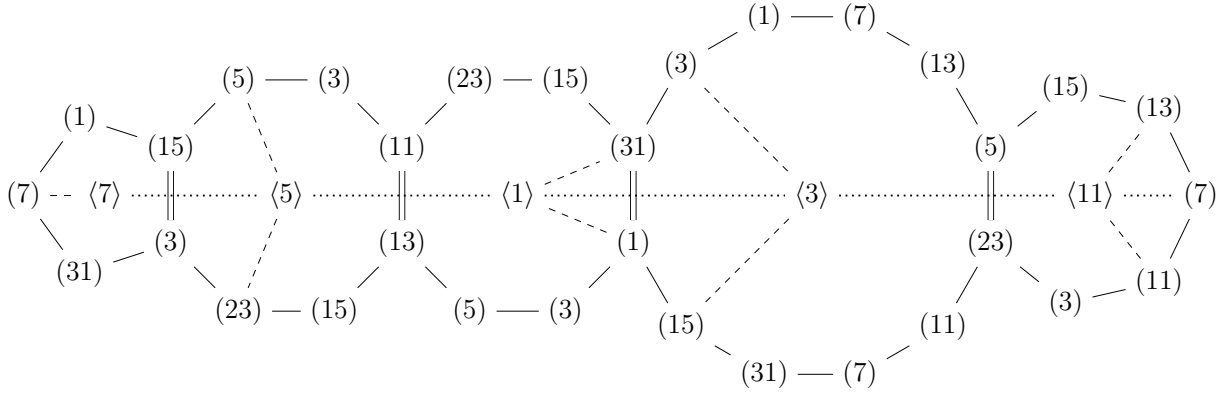
Figure 4.5: Cell structure for the marked cycle curve $\mathrm{Cyc}_6(\mathrm{Per}_1)$, which has genus $g = 4$.

Note that in this case, the faces $\langle 7 \rangle$ and $\langle 11 \rangle$ both have an odd number of edges. The face $\langle 7 \rangle$ is reflexive, while the face $\langle 11 \rangle$ is not.

Lemma 4.6.4 (Edges are realized). *Every primitive arc in* QML *appears as an edge on some face produced by Algorithm 4.6.1.*

Proof. Let $A = (\theta_0, \theta_1)$ be a primitive arc in QML. Starting at $v = (\theta_0)$ and at position A in the list of arcs, we follow the procedure of step 4 in the reverse order. We must eventually reach the top of the list of arcs (i.e. the positive real axis) with some ABC (θ) active. By performing step 4 in the forward direction starting at θ, we find that (θ_0, θ_1) is an edge of the face $\langle \theta \rangle$. $\square$

Corollary 4.6.5 (Edges are doubly realized). *Every primitive arc $A \in$ QML appears either once on two distinct faces, or twice on a single face.*

Proof. Perform the same procedure as in the proof of Lemma 4.6.4, only starting at θ_1 instead of θ_0. Since the procedure is reversible, when we reach the positive real axis, the active ABC is some value (θ') necessarily distinct from (θ). If these two ABCs are bit-flips of each other, then A appears twice on $\langle \theta \rangle$; otherwise, A appears once on $\langle \theta \rangle$ and once on $\langle \theta' \rangle$. $\square$

Proposition 4.6.6 (No isolated vertices). *If $p \neq 2$, then every vertex produced by Algorithm 4.6.1 is connected to some other vertex.*

Theorem 4.6.7. *For $p > 2$, Algorithm 4.6.1 gives rise to a cell structure homeomorphic to* $\mathrm{Cyc}_p(\mathrm{Per}_1)$.

Proof. Let X be the space described by the output of Algorithm 4.6.1. It suffices to show that X is homeomorphic to the cell structure Y described in Definition 4.5.3. As in Definition 4.5.3, let M_0 be the path-connected component of $\mathcal{M}$ containing 0, and let B be the branch locus of the projection map $\pi : \mathrm{Cyc}_p(\mathrm{Per}_1) \to \mathrm{Per}_1$.

Consider a point $c \in \mathbb{C}$, together with a p-cycle ξ of f_c. We will show how to produce a corresponding point $h(c, \xi) \in X$.

Suppose first that (c, ξ) belongs to a "vertex" U of Y, i.e. path-connected component of $M_0 \smallsetminus B$ containing 0. Fix some metric on $\mathrm{Cyc}_p(\mathrm{Per}_1)$ that respects its topology. Let b_0 be the nearest element of B to c, and let b_1 be the second-nearest. Let δ_0 and δ_1 be the corresponding distances (if no such point b_i exists, we set $\delta_i = 0$). Denote by δ be the distance between (c, ξ) and $(0, \xi)$.

Let α be the ABC associated to (c, ξ) according to Lemma 4.5.4. It follows from Corollary 4.1.6 that dynamical rays at angles represented by α land at elements of the marked cycle ξ' for every $(c', \xi') \in U$.

Let A be the primitive arc landing at b_0. Since b_0 is a branch point of π, we know that the p-cycle described by α collides at b_0 with some other p-cycle, described by β, say. It follows from Corollary 4.1.5 and Lemma 4.2.1 that $\pi(b_0)$ is the landing point of the angles in A. By Lemma 4.6.4, there is an edge represented by A, which evidently connects to both α and β. Let $\gamma(t)$ parameterize this edge by arc length (where all edges are defined to have length 1), with $\gamma(0) = \alpha$ and $\gamma(1) = \beta$. We then set

$$h(c, \xi) = \gamma\left(\frac{\delta\,(\delta_1 - \delta_0)}{2\delta\delta_1 + \delta_0}\right).$$

Note that this has value $\gamma(0) = \alpha$, which lies on all edges out of α, whenever there is a tie between the nearest branch points b_0 and b_1. Since no two of $\{\delta, \delta_0, \delta_1\}$ can simultaneously vanish (0 is certainly not the root of a primitive hyperbolic component!), it is easily checked that h is continuous on U and satisfies

$$\lim_{(c,\xi) \to b_0} h(c, \xi) = \gamma(1/2) \tag{4.2}$$

from within U.
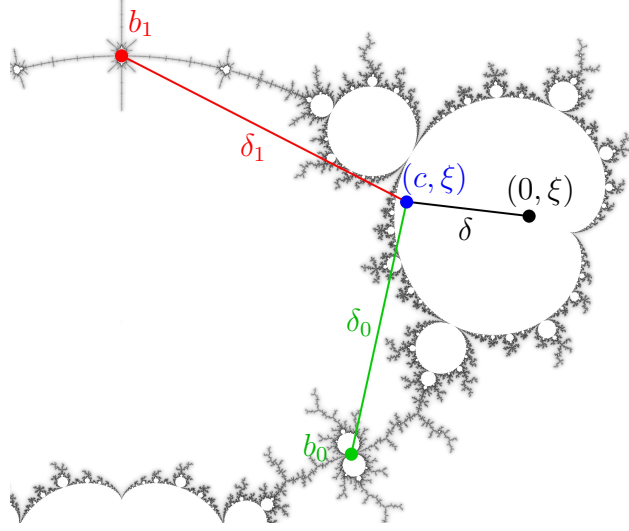
Figure 4.6: The function $h(c, \xi)$ compares the distances δ_0 and δ_1 of (c, ξ) to the nearest two branch points, scaled by the distance δ to $(0, \xi)$ and designed to equal 0 when $\delta_0 = \delta_1$.

If (c, ξ) is an "edge" of Y, i.e. a branch point of π, then by the same reasoning as above, we find that c is the landing point of the rays in an arc $A \in \mathrm{QML}$ active at ξ. We then set $h(c, \xi)$ to be the midpoint of the edge in X represented by A. It follows from eq. (4.2) that this assignment does not introduce any discontinuities.

We have thus defined a map h from the 1-skeleton of Y to the 1-skeleton of X. This map has an inverse up to homotopy, where we send the midpoint m_A of each edge A in X to the branch point (c_A, α) in Y where A lands and is active, and we send points on each half-edge connecting m_A to α in X continuously to points on the vein in Y connecting b_A to $(0, \alpha)$. Thus, the 1-skeletons of X and Y are homotopy equivalent.

It remains to show that the gluing maps for the 2-cells have the same vertex orderings. Consider a loop $\sigma : [0, 1] \to \mathrm{Cyc}_p(\mathrm{Per}_1) \smallsetminus \pi^{-1}(\mathcal{M})$ around a face in Y, based at a point (c_0, ξ_0) on a lift of the positive real axis, chosen up to homotopy so that the external argument of c_t is monotone increasing with respect to circular order. Put $(c_t, \xi_t) = \sigma(t)$.

Since $c_0 \in \mathbb{R}_+$ does not lie within any p-periodic wake, we know by Corollary 4.1.6 that elements of ξ_0 have unique external arguments, which by Proposition 2.3.13 belong to a common orbit (θ_0). Following any path in $\mathbb{C}$ from c_0 to 0 that avoids the ray orbit $\mathcal{O}_{\theta_0}$, by Lemma 4.1.2 we obtain a point $v_0 = (\tilde{c}_0, \tilde{\xi}_0)$ belonging to the Y-vertex labeled by (θ_0).

Proceeding forward along the loop, we know by Lemma 4.1.2 that the dynamical rays $\mathcal{R}_{c_t}(2^k \theta_0)$ continue to land on ξ_t until c_t crosses a ray $\mathcal{R}(\alpha)$ with $\alpha \in (\theta_0)$. When this occurs, there are two possibilities:

53

(1) If α belongs to a satellite arc (α, β), with $\beta \in (\alpha) = (\theta_0)$, then by Section 4.2.2, passing through the wake $\mathcal{W}(\alpha, \beta)$ merely cycles the elements of ξ_t, without changing the external arguments. Thus, the landing vertex $v_t \in Y$ remains invariant.

(2) If α belongs to a primitive arc $A = \{\alpha, \beta\}$, with $\beta \notin (\alpha) = (\theta_0)$, then by Lemma 4.2.1, when c_t lies within the associated wake $\mathcal{W}(A)$, all dynamical rays $\mathcal{R}_{c_t}(\theta)$ with $\theta \in (\alpha) \cup (\beta)$ land on the same cycle $\xi_{\alpha,\beta,t}$.

If $\alpha > \beta$, then when c_t enters $\mathcal{W}(A)$, the dynamical ray $\mathcal{R}_{c_t}(\alpha)$ does not bifurcate. It follows that $\xi_{\alpha,\beta,t} = \xi_t$. When c_t exits the wake $\mathcal{W}(A)$, the dynamical ray $\mathcal{R}_{c_t}(\beta)$ does not bifurcate, so rays in the orbit of β continue to land on ξ_t. Thus, the next associated vertex $v_t \in Y$ is (β).

If $\alpha < \beta$, then when c_t enters $\mathcal{W}(A)$, the dynamical ray $\mathcal{R}_{c_t}(\beta)$, which previously did not land on ξ_t does not bifurcate. It follows that $\xi_{\alpha,\beta,t} \neq \xi_t$. Thus, when c_t exits the wake $\mathcal{W}(A)$, the dynamical ray $\mathcal{R}_{c_t}(\alpha)$ does not bifurcate, so rays in the orbit of α continue not to land on ξ_t. But we know by Corollary 4.1.6 that *some* ray lands on ξ_t, and the only available angles belong to (β). Thus, the next associated vertex $v_t \in Y$ is again (β).

In all cases, the update is consistent with the update rule in Algorithm 4.6.1. It follows that the resulting cell structures are homeomorphic. $\qquad \square$

CHAPTER 5

Marked Cycle Curves over Per_2

As discussed in Section 3.3.2, the dynamical moduli space Per_2 of quadratic rational maps with a superattracting 2-cycle is a natural successor to Per_1, and has been studied extensively. In this chapter, we will show that a small modification to Algorithm 4.6.1 allows us to describe the marked cycle curves over Per_2.

5.1   Structure of Per_2

We first recall some of the basic properties of Per_2.

Proposition 5.1.1 (compare [Mil93])**.** Per_2 *is conformally isomorphic to a one-sided cone with cone angle $\tau/3$. The cone point is the map $[f_\bigcirc] = [z \mapsto z^{-2}]$, which has automorphism group S_3, generated in these coordinates by $z \mapsto 1/z$ and $z \mapsto \omega z$, where ω is a primitive cube root of unity. All other elements of Per_2 have trivial automorphism group.*

Following [Ree90] and [Mil93], subfamilies of $\mathcal{M}_2$ admit four classes of hyperbolic components:

B. *bitransitive* components, in which the critical points are in different components of the immediate basin of the same attracting cycle,

C. *capture* components, in which both critical points are in the basin of the same attracting cycle, but only one is in its immediate basin,

D. *disjoint* type components, in which the critical points belong to basins of disjoint cycles, and

E. *escape* regions, in which both critical points are in the immediate basin of the same attracting fixed point.

Douady and Hubbard's Theorem 2.3.5 states that $\mathbb{C} \smallsetminus \mathcal{M}$ is the only escape region in Per_1, and that all other hyperbolic components are of disjoint type. By contrast, Per_2 has one

bitransitive component, no escape regions, and infinitely many components of types C and D.

Definition 5.1.2. The *filled bifurcation locus* $\mathcal{M}_2$ is the complement of the union of all bitransitive and capture components in Per_2. In other words, $\mathcal{M}_2$ is the set of all $[f] \in \mathrm{Per}_2$ such that the orbit of the free critical point of f is not attracted to the marked superattracting 2-cycle. It is the analogue of the Mandelbrot set in Per_2, and its boundary is the bifurcation locus $\mathcal{B}(\mathrm{Per}_2)$.

5.1.1 Coordinates

There are a number of different sets of coordinates commonly used for Per_2. For our purposes, we will use the following two parameterizations:

Proposition 5.1.3.

- *The dynamical family*

$$\mathcal{G} = \left\{ g_b(z) = b + 1/\left(z^2 - b^2\right) : b \in \mathbb{C} \right\}$$

  is a 3-fold branched cover of Per_2*, branched over the map* $g_0(z) = z^{-2}$*. The moduli space* Per_2 *is the quotient of* $\mathcal{G}$ *by the* $\mathbb{Z}/3\mathbb{Z}$ *action generated by* $b \mapsto \omega b$*.*

- *The dynamical family*

$$\mathcal{H} = \left\{ h_a(z) = \frac{z^2 + a}{1 - z^2} : a \in \mathbb{C} \smallsetminus \{-1\} \right\}$$

  is isomorphic to $\mathrm{Per}_2 \smallsetminus \{[z \mapsto z^{-2}]\}$ *and provides a dynamically meaningful coordinate for* Per_2 *away from the orbifold point* $[z \mapsto z^{-2}]$*. The map* h_a *has critical 2-cycle* $\infty \leftrightarrow -1$*, free critical point* 0*, and free critical value* a*.*

- *For* $b \in \mathbb{C}^*$*,* g_b *is conformally conjugate to* $h_{1-b^{-3}}$ *via the affine conjugacy*

$$-\frac{1}{b} g_b(z) = h_{1-b^{-3}}\left(-\frac{1}{b} z\right).$$

- *The central map* $h_0 \in \mathcal{H}$ *is conjugate to the basilica polynomial* $f_{\text{\large$\infty$}}(z) = z^2 - 1$ *via the Möbius conjugacy* $h_0(1/z) = 1/f_{\text{\large$\infty$}}(z)$*. This represents the unique element of* $\mathrm{Per}_1 \cap \mathrm{Per}_2$*.*

- *The family* $\mathcal{H}$ *has a puncture at* $a = -1$*, where* h_a *degenerates to a constant function.*
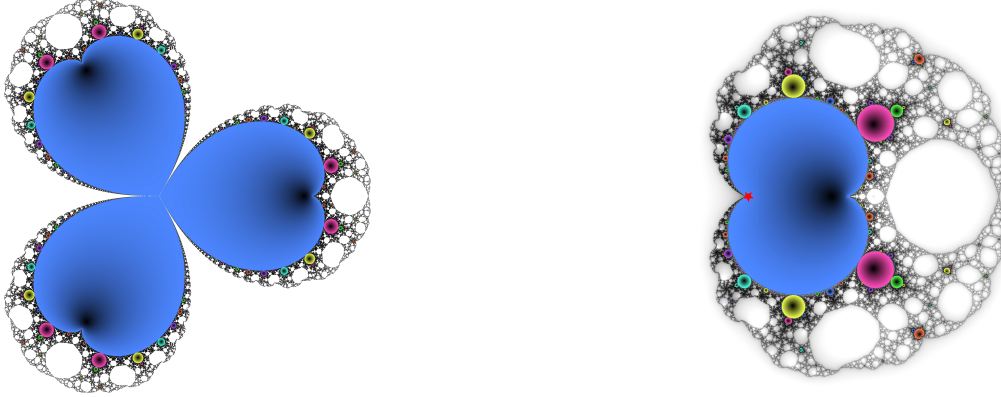
(a) $\mathcal{M}_2$ in the $1/b$ plane, with parameterization $g_b(z) = b + 1/(z^2 - b^2)$. The central point is the puncture $b = \infty$.

(b) $\mathcal{M}_2$ in the a plane, with parameterization $h_a(z) = (z^2 + a)/(1 - z^2)$. The puncture $a = -1$ is marked by a red star.

Figure 5.1: Per_2 in the coordinate systems $\mathcal{G}$ and $\mathcal{H}$. The colored regions are disjoint type components, the bounded white regions are capture components, and the unbounded white region is the unique bitransitive component.

Remark 5.1.4. For $p \neq 2$, the p-cycles of $g_0(z) = z^{-2}$ all have multiplier $(-2)^p$. In particular, g_0 has no indifferent cycles, so there is no cycle monodromy in $\mathcal{G}$ in a neighborhood of g_0.

Among other things, this implies that the number of p-cycles for a generic element of $\mathcal{G}$ (and hence $\mathcal{H}$) is equal to the number of p-cycles of g_0.

We will generally treat the orbifold point as a puncture, identifying Per_2 with $\mathcal{H}$. It should be noted, however, that Per_2 technically contains an additional map $[z \mapsto z^{-2}]$.

5.1.2 Wittner's conjecture

Ben Wittner conjectured in [Wit88] that the connectedness locus in Per_2 is a topological mating of the Mandelbrot set minus the $1/2$ limb with the Julia set of the "basilica" map $f_{\infty}(z) = z^2 - 1$ minus its $1/2$ limb. This was eventually proven by Dzmitry Dudko in [Dud11], building on an extensive theory developed in [Lei92], [Luo95], [AY08], [Tim08], to name a few. We give here a brief summary of the relevant parts of this result.

Let

$$\tilde{\mathbb{C}} = \hat{\mathbb{C}} \smallsetminus \mathcal{W}\left(\frac{1}{3}, \frac{2}{3}\right) / \sim$$

denote the Riemann sphere minus the $(1/3, 2/3)$-wake of the Mandelbrot set, modulo the equivalence relation

$$\gamma_{1/3}(t) \sim \gamma_{2/3}(t),$$

where γ_θ parameterizes the parameter ray $\mathcal{R}_\mathcal{M}(\theta)$ according to the parameterization given in Definition 2.3.7. The topological space $\tilde{\mathbb{C}}$ is a complex orbifold. Let $\widetilde{\mathcal{M}}$ be the image of $\mathcal{M}$ in $\tilde{C}$.

Similarly, let

$$\tilde{B} = \hat{\mathbb{C}} \smallsetminus \mathcal{W}_{\circ}\left(\frac{1}{3}, \frac{2}{3}\right) / \sim$$

denote the Riemann sphere minus the dynamical $(1/3, 2/3)$-wake of $f_{\circ}(z) = z^2 - 1$, modulo the equivalence relation

$$\gamma_{1/3,\circ}(t) \sim \gamma_{2/3,\circ}(t),$$

where γ_θ parameterizes the dynamical ray $\mathcal{R}_{f_{\circ}}(\theta)$ according to the parameterization given in Definition 2.3.8. Let $K_{\circ}$ denote the image of $\mathcal{K}(f_{\circ})$ in $\tilde{B}$.

Denote by $\widetilde{\mathrm{Per}_2}$ the one-point compactification of Per_2, i.e. the teardrop orbifold obtained by filling in the puncture.

We informally define the *topological mating* of $\mathcal{M}$ with $\mathcal{K}_{\circ}$ as the mating of the lamination $\widetilde{\mathrm{QML}}$ with $\mathcal{L}_{\circ}$, where $\widetilde{\mathrm{QML}}$ (resp. $\mathcal{L}_{\circ}$) is the subset of QML (resp. $\mathcal{L}(f_{\circ})$) whose arcs do not belong to $[1/3, 2/3]$, modulo the interval $[1/3, 2/3]$.[1]

Theorem 5.1.5 (Dudko, c.f. [Dud11]). *The topological mating of $\widetilde{\mathcal{M}}$ with $K_{\circ}$ is canonically homeomorphic to $\widetilde{\mathrm{Per}_2}$. The bifurcation locus in Per_2 is the image of $\partial \mathcal{M}$ under this mating. $\mathcal{M}_2$ is the image of $\mathcal{M}$ under this mating.*

In particular, by the mating construction, for any rational angle θ outside $[1/3, 2/3]$, the image in Per_2 of the landing point of $\mathcal{R}_\mathcal{M}(\theta)$ coincides with that of the landing point of $\mathcal{R}_{f_{\circ}}(1 - \theta)$.

While Dudko's structure theorem is deep, it alone does not provide a full analogue of the results in Sections 2.3 and 4.1. However, the remaining theory we require was developed prior to Dudko's result, in the work of Aspenberg-Yampolsky [AY08] and Timorin [Tim08]. The remainder of this section is devoted to describing their results.

By the mating criterion Theorem 2.3.23, every pcf hyperbolic polynomial

$$f \in \mathcal{M} \smallsetminus \mathcal{W}(1/3, 2/3)$$

admits a rational mating with $f_{\circ}$. Since $f_{\circ}$ has a 2-periodic critical point, $f \amalg f_{\circ}$ must

---

[1]In Dudko's construction, care must be taken when handling irrational angles, since $\mathcal{M}$ is not known to be locally connected. Since we only require the mating construction to hold for rational angles, we will avoid going into detail regarding this.

then belong to Per_2. The converse is also true:

Proposition 5.1.6 (Tan Lei, c.f. [Lei92]). *Every postcritically finite map in Per_2 which does not belong to a capture component is the mating of a pcf quadratic polynomial $f \in \mathcal{M} \smallsetminus \mathcal{W}(1/3, 2/3)$ with the basilica polynomial $f_{\bigcirc\!\!\bigcirc}$.*

Corollary 5.1.7. *Hyperbolic components in $\mathcal{M}_2$ are in bijection with hyperbolic components in $\mathcal{M} \smallsetminus \mathcal{W}(1/3, 2/3)$.*

5.1.3 Internal geodesics

Let f be a postcritically finite quadratic[2] polynomial, and let $F_0 \subset \mathcal{K}(f)^\circ$ denote the Fatou component containing the critical point z_0. Let $\phi : F_0 \to \mathbb{D}$ be the Böttcher map of F_0, defined everywhere since F_0 contains no other critical points. Since every Fatou component $F \subset \mathcal{K}(f)^\circ$ is an iterated preimage of F_0, we may extend ϕ to all of $\mathcal{K}(f)^\circ$ by pulling it back under iterates of f.

Definition 5.1.8. Let f be a postcritically finite quadratic polynomial, and let ϕ be as above. Let $\gamma : [0, 1] \to \mathcal{K}(f)$ be a path in the filled Julia set of f. We say that γ is an *internal geodesic* in $\mathcal{K}(f)$ if it satisfies the following properties:

1. γ is injective into $\mathcal{K}(f)$.

2. For every Fatou component F of f, there are at most two values t for which $\gamma(t) \in \partial F$.

3. For any t such that $z = \gamma(t)$ is an interior point of $\mathcal{K}(f)$, either $\phi(z) = 0$ (i.e. z is an iterated preimage of the critical point z_0), or $\gamma'(t)$ is a nonzero real multiple of $\phi'(z)$. Equivalently, γ is orthogonal to the level curves of $\log |\phi|$ wherever the latter is defined.

Proposition 5.1.9. *For any two distinct points $a, b \in \mathcal{K}(f)$, there exists an internal geodesic γ starting at a and ending at b. The choice of γ is unique up to reparameterization by a monotone map on the unit interval.*

Proof. Since $\mathcal{K}(f)$ is simply connected, there is a unique, nonempty homotopy class (rel. endpoints) C_0 of paths connecting a to b. Let $C_1 \subset C_0$ be the subset consisting of all paths γ for which $\gamma^{-1}(\overline{F})$ is connected for every Fatou component F. Since any element of C_0 can be reparameterized to an element of C_1, C_1 is nonempty. Let C_2 be the subset of elements of C_1 that are injective; by the same reasoning, C_2 remains nonempty.

---

[2]The requirement that f be quadratic is unnecessary, but it makes the definition simpler. We will only require this construction for the basilica map $f_{\bigcirc\!\!\bigcirc}(z) = z^2 - 1$.

Up to a monotone reparameterization, any two elements of C_2 are equal outside Fatou components. Thus, it suffices to prove existence and uniqueness when a and b belong to the closure of a single Fatou component F.

Since $\mathcal{K}(f)$ is simply connected, the restriction of ϕ to F extends continuously to an injective map ϕ_F defined on $\overline{F}$ (this may be discontinuous relative the value of ϕ on other Fatou components, but this is irrelevant to us). There are two possibilities:

- If $\phi(a)$ and $\phi(b)$ lie on a single closed ray R from the origin in $\overline{\mathbb{D}}$ (in particular, if either $\phi(a)$ or $\phi(b)$ is zero), then the only injective radial (i.e. orthogonal to circles about 0) path from $\phi(a)$ to $\phi(b)$ is the segment $\tilde{\gamma}$ of R between $\phi(a)$ and $\phi(b)$. The pullback $\phi^{-1} \circ \tilde{\gamma}$ is then the unique path γ connecting a to b.

- Otherwise, if $\arg(\phi(a)) \neq \arg(\phi(b))$, then the only radial paths in $\overline{\mathbb{D}} \smallsetminus \{0\}$ connecting $\phi(a)$ to $\phi(b)$ involve exiting $\mathbb{D}$ to traverse the boundary circle, which would violate condition 2. Thus, the only possibility is that $\phi(\gamma(t)) = 0$ for some $t \in (0, 1)$. Existence and uniqueness then follows by applying the previous case twice. □

Definition 5.1.10. For an internal geodesic γ passing through the center of a Fatou component F at time t_0, the *characteristic angle* of γ at F is the value

$$\underline{\chi}_F(\theta) = \frac{1}{\tau} \arg \phi(t_0 + \varepsilon)$$

which is independent of ε for all sufficiently small $\varepsilon > 0$.

Remark 5.1.11. It is important to distinguish internal angles in $\mathcal{K}(f_{\circ\!\!\circ})$ from external angles to $\mathcal{K}(f_{\circ\!\!\circ})$. Whereas the latter are doubled under the $f_{\circ\!\!\circ}$ itself, the former are doubled under the *square* of $f_{\circ\!\!\circ}$.[3] To preserve this distinction, we notate internal basilica angles with an underline.

5.2 Bubble rays

There are natural analogues for parameter rays as well as dynamical rays for Per_2. These are known as *bubble rays*. To define these, we must first define internal rays for the basilica polynomial $f_{\circ\!\!\circ}(z) = z^2 - 1$.

---

[3]Naively, it may seem contradictory that these two notions of angle can expand at different rates under the same map. As we shall see in Section 5.3.2, this distinction forms a counterpoint that is central to understanding how maps degenerate at the puncture in Per_2.

Since $f_{\circ\!\!\circ}$ is hyperbolic of disjoint type, its Julia set is locally connected. Thus, for any $\theta \in S^1$, the dynamical ray at angle θ lands at some point $\lambda_{\circ\!\!\circ}(\theta) \in \mathcal{J}(f_{\circ\!\!\circ})$.

Definition 5.2.1. The *internal basilica ray* $\mathring{\mathcal{R}}_{\circ\!\!\circ}(\theta)$ at angle $\theta \in S^1$ is the internal geodesic γ from 0 to $\lambda_{\circ\!\!\circ}(\theta)$.

The basilica polynomial has the important property that any two points its Fatou set are connected by a path that visits $\mathcal{J}(f_{\circ\!\!\circ})$ in finitely many points. Thus, for any $\theta \in S^1$, sequence of Fatou components visited by the internal ray $\mathring{\mathcal{R}}_{\circ\!\!\circ}(\theta)$ is either finite or has order type ω.

Definition 5.2.2. For $\theta \in S^1$, let $F_0, F_1, \ldots$ be the (finite or infinite) sequence of Fatou components visited by the internal basilica ray $\gamma = \mathring{\mathcal{R}}_{\circ\!\!\circ}(\theta)$. The *basilica address* of θ is the finite or infinite sequence of characteristic angles along γ:

$$\Gamma(\theta) = \underline{\chi_{F_0}(\gamma), \chi_{F_1}(\gamma), \ldots}$$

Definition 5.2.3. If $h \in \mathrm{Per}_2$ is a mating of a quadratic polynomial $f_c \in \widetilde{\mathcal{M}}$ with $f_{\circ\!\!\circ}$, then the *dynamical bubble ray* $\mathring{\mathcal{R}}_h(\theta)$ at angle $\theta \in S^1$ is the pushforward of the internal basilica ray $\mathring{\mathcal{R}}_{\circ\!\!\circ}(-\theta)$ under the mating of $\mathcal{K}(f_c)$ with $K_{\circ\!\!\circ}$.

Definition 5.2.4. The *parameter bubble ray* $\mathring{\mathcal{R}}(\theta)$ at angle $\theta \in S^1 \smallsetminus (1/3, 2/3)$ is the pushforward of the internal basilica ray $\mathring{\mathcal{R}}_{\circ\!\!\circ}(-\theta)$ under the Wittner mating of $\widetilde{\mathcal{M}}$ with $K_{\circ\!\!\circ}$.

Aspenberg and Yampolsky show that bubble rays inherit most of the properties of external rays in Per_1.

Proposition 5.2.5 (c.f. [AY08], Proposition 6.10)**.** *For $\alpha, \beta \in S^1 \smallsetminus [1/3, 2/3]$, the parameter bubble rays $\mathring{\mathcal{R}}_{\mathcal{M}_2}(\alpha)$ and $\mathring{\mathcal{R}}_{\mathcal{M}_2}(\beta)$ land together at the root of a hyperbolic component V if and only if the corresponding parameter rays in Per_1 land at the root of a hyperbolic component U. If this is the case, then U and V have the same period p, and mating with $f_{\circ\!\!\circ}$ induces a conformal isomorphism between U and V.*

Definition 5.2.6. If α and β land together at a component U, then the component of $\mathrm{Per}_2 \smallsetminus \left(\mathring{\mathcal{R}}_{\mathcal{M}_2}(\alpha) \cup \mathring{\mathcal{R}}_{\mathcal{M}_2}(\beta) \right)$ containing U is known as the *bubble wake* $\mathring{\mathcal{W}}(\alpha, \beta)$. The *closed bubble wake* is the defined to be the set

$$\overline{\mathring{\mathcal{W}}(\alpha, \beta)} = \mathring{\mathcal{W}}(\alpha, \beta) \cup \overline{\mathring{\mathcal{R}}_{\mathcal{M}_2}(\alpha)} \cup \overline{\mathring{\mathcal{R}}_{\mathcal{M}_2}(\beta)}.$$
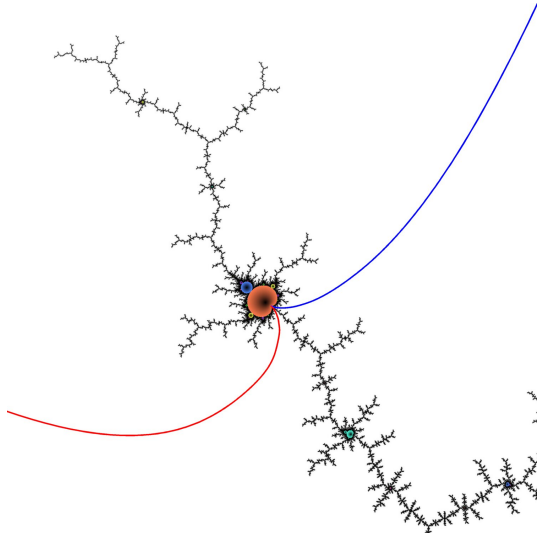
(a) The parameter rays $\mathcal{R}_\mathcal{M}(\frac{1}{5})$ and $\mathcal{R}_\mathcal{M}(\frac{4}{15})$ land together at a period 4 component of $\mathcal{M}$. Call the center of this component f_K.
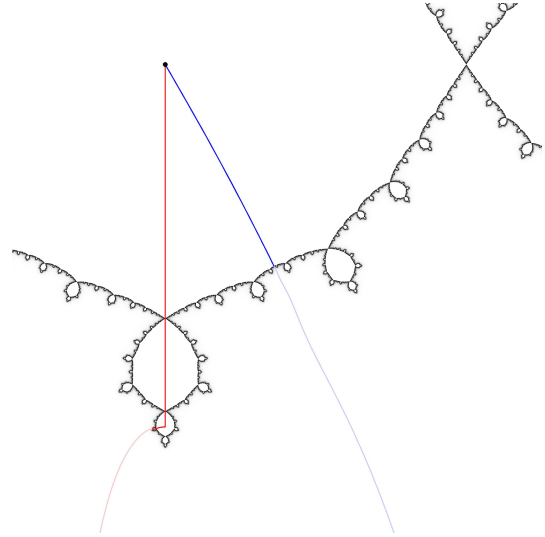
(b) Internal basilica rays at angles $-1/5$ and $-4/15$. The basilica addresses are $\frac{1}{3}$ and $\frac{1}{4}, 0, \frac{1}{4}, 0, \ldots$ respectively (where the critical internal ray segment at angle $\underline{0}$ points to the left, towards the α fixed point). The corresponding external dynamical rays, shown in lighter colors, are pinched to a common point in the Wittner mating with $\widetilde{\mathcal{M}}$.
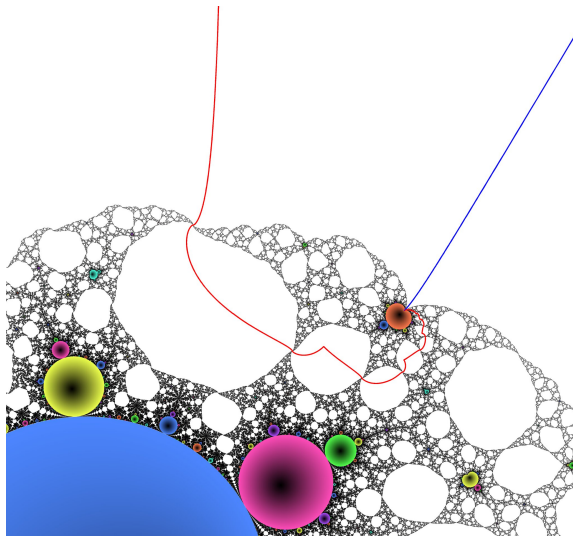
(c) The parameter bubble rays $\mathring{\mathcal{R}}_{\mathcal{M}_2}(\frac{1}{5})$ and $\mathring{\mathcal{R}}_{\mathcal{M}_2}(\frac{4}{15})$ land together at a period 4 component U_K of $\mathcal{M}_2$. The center of U_K is the mating $f_K \amalg f_{\circ\!\circ}$.
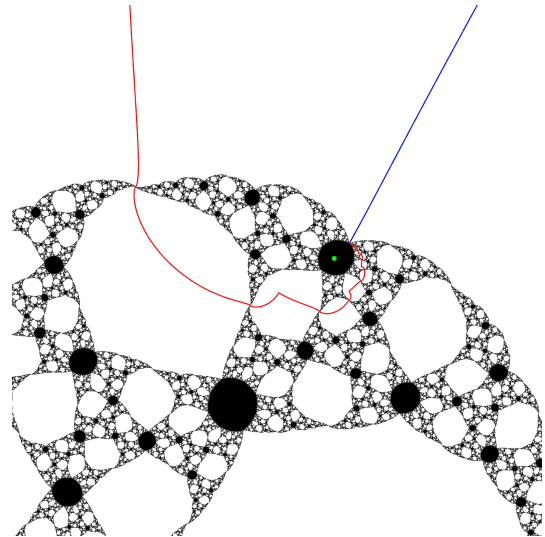
(d) The dynamical bubble rays at angles $1/5$ and $4/15$ land together on the Julia set of $f_K \amalg f_{\circ\!\circ}$. The critical value is shown in green.

Figure 5.2: Correspondence between rays in Per_1 and bubble rays in Per_2.

Remark 5.2.7. Unlike in Per_1, bubble rays may overlap. If $\alpha, \beta \in S^1$ are distinct, then $\overset{\circ}{\mathcal{R}}_{h_a}(\alpha) \cap \overset{\circ}{\mathcal{R}}_{h_a}(\beta)$ (not including the landing points) has a single connected component whose closure contains the 2-periodic critical point, but no element of the Julia set. The analogous statement for parameter bubble rays also holds.

This has the interesting implication that bubble wakes may be bounded. Thus, a closed bubble wake is not simply the closure of the corresponding open bubble wake: the latter may be a proper subset of the former.

5.2.1 Outside $\mathcal{M}_2$

We wish now to extend our definition of dynamical bubble rays to maps outside $\mathcal{M}_2$.

If $h \in \mathcal{H}$ does not belong to $\mathcal{M}_2$, then by definition, h is hyperbolic of either capture type or bitransitive type. Thus, every Fatou component maps after finitely many iterations to the Fatou component F_∞ containing the marked 2-periodic critical point ∞. Let ϕ_h be the Böttcher map, defined on a neighborhood of ∞, and let G_h be the Green's function, defined on all of F_0. By taking iterated pullbacks, we may extend the domain of ϕ_h to an open set containing every iterated preimage of ∞, and we may extend G_h to the entire Fatou set of h.

In fact, the above definitions work for $h \in \mathcal{M}_2$ as well, with the caveat that the domain of G_h only includes the Fatou components that are iterated preimages of the component containing ∞.

We may then define bubble ray segments just as we defined dynamical rays in Section 2.3.

Definition 5.2.8. Let $h \in \mathcal{H}$, with the Böttcher map ϕ_h and Green's function G_h defined as above. Let $z_0 \in \mathbb{C} \setminus \mathcal{J}(h)$ be an iterated preimage of the marked 2-periodic critical point ∞, and let $\underline{\theta} \in S^1$. The *dynamical bubble ray segment*

$$\overset{\circ}{\mathcal{R}}_h^{(z_0)}(\underline{\theta})$$

at angle $\underline{\theta}$ based at z_0 is the unique solution γ to the differential equation

$$\gamma'(t) = \frac{(\nabla G_h)^T}{\|\nabla G_h\|^2}(\gamma(t)), \tag{5.1}$$

defined on a maximal domain (t_0, ∞), such that $\arg \phi_h(\gamma(t)) = \underline{\theta}\tau$ for some (and hence all) sufficiently large $\underline{\theta}$, parameterized such that $G_h(\gamma(t)) = t$ for some (and hence all) $t > t_0$.

Since $\phi(h^2(z)) = \phi(z)^2$, we find that h^2 acts on bubble ray segments at ∞ by angle doubling.

We say a dynamical ray segment $\overset{\circ}{\mathcal{R}}_h^{(z_0)}(\underline{\theta})$, parameterized by $\gamma(t)$, *bifurcates* if $\gamma(t)$ is not defined for all $t > 0$, and we say it *lands* if $\lim_{t\to 0} \gamma(t)$ exists.

Proposition 5.2.9 (c.f. [TY96]). *Every hyperbolic rational map has locally connected Julia set.*

Corollary 5.2.10. *If $h \in \mathcal{H} \smallsetminus \mathcal{M}_w$, then every dynamical bubble ray segment either bifurcates or lands.*

Proposition 5.2.11. *The critical points of G_h are precisely the precritical points of h.*

Proof. This follows by taking the gradient of the functional equation $G_h(h^2(z)) = 2G_h(z)$. $\qquad\square$

Proposition 5.2.12. *For $a \in \mathbb{C} \smallsetminus (-\infty, -1]$, the dynamical bubble ray segment $\overset{\circ}{\mathcal{R}}_{h_a}^{(\infty)}(0)$ lands at a fixed point of h_a.*

Definition 5.2.13. For a as above, we refer to the landing point of $\overset{\circ}{\mathcal{R}}_{h_a}^{(\infty)}(0)$ as the α-*fixed point α_a.*

The α-fixed point lies on the boundary of two canonical Fatou components F_∞ and F_{-1}, containing respectively the 2-periodic critical point ∞ and its associated critical value -1.

We can now define the dynamical bubble ray using the internal basilica address.

Definition 5.2.14. Let $h \in \mathcal{H}$ be arbitrary, and let $\theta \in S^1$. Let $\Gamma(\theta) = \underline{\chi_0, \chi_1, \ldots}$ be the basilica address of $-\theta$. The *dynamical bubble ray*

$$\overset{\circ}{\mathcal{R}}_h(\theta)$$

is constructed as follows:

1. Let $z_0 = \infty$ be the preperiodic critical point, and let

$$\gamma_0^+ = \overset{\circ}{\mathcal{R}}_h^{(z_0)}(\underline{\chi_0}).$$

If γ_0^+ runs into a critical point of G_h (i.e. an iterated preimage of the free critical point), we halt the process and say that $\overset{\circ}{\mathcal{R}}_h(\theta)$ *bifurcates*. Otherwise, let z_0^+ be the landing point of γ_0^+. If χ_0 is the last entry in the basilica address of θ, then terminate the process and say that $\overset{\circ}{\mathcal{R}}_h(\theta)$ *lands* at z_0^+. Otherwise, since the internal basilica ray

64

at angle θ passes through the boundaries of exactly two Fatou components, it follows from the capture construction in [Wit88] that z_0^+ belongs to the boundary of exactly one other Fatou component F_1.

2. Let U be a neighborhood of z_0, and let $V = U \cap F_1$. Consider the family of solutions to (5.1) passing through z, where z varies through V. If this family is normal for sufficiently small V, then we let γ_1^- be the limit of this family as z tends to z_0. Otherwise, we say that $\mathring{\mathcal{R}}_h(\theta)$ bifurcates in F_1.

   Running γ_1^- for decreasing t, normality implies that γ_1^- cannot run into a saddle point of G_h. Thus, γ_1^- must terminate at an iterated preimage of z_∞. We call this point z_1.

3. We now repeat this procedure, using α_1 to seed the next bubble ray segment at angle $\underline{\chi}_1$ from z_1, and continuing the process forever or until we halt.

$\mathring{\mathcal{R}}_h(\theta)$ is then defined to be the concatenation

$$\gamma_0^+ \cdot \hat{\gamma}_1^- \cdot \gamma_1^+ \cdot \hat{\gamma}_2^- \cdot \ldots,$$

stopping early as described above if the process terminates. In the above, $\hat{\gamma}$ denotes the time-reversal of γ.

Proposition 5.2.15. *When $h = f_c \amalg f_{\circlearrowleft\circ}$ is a mating, Definitions 5.2.3 and 5.2.14 are equivalent up to a re-parameterization.*

Proof. Since the dynamics of h in the image of $\mathcal{K}(f_{\circlearrowleft\circ})^\circ$ are conformally conjugate to those of $f_{\circlearrowleft\circ}$, the interior Green's functions on corresponding Fatou components are equivalent. The result then follows by existence and uniqueness. $\qquad\square$

Dynamical and parameter bubble rays satisfy almost all the same properties as their Per_1 analogues. In lieu of repeating much of Section 2.3.1, we state the following fundamental property and refer the reader to [AY08] and [Tim08] for a thorough investigation of the properties of bubble rays.

Proposition 5.2.16 (c.f. [AY08]). *For $h \in \mathcal{H}$ and $\theta \in S^1$, if the dynamical bubble ray $\mathring{\mathcal{R}}_h(\theta)$ lands at some $z \in \mathcal{J}(h)$, then $\mathring{\mathcal{R}}_h(2\theta)$ lands at $h(z)$.*

We remark that Lemma 4.1.2 holds for dynamical bubble rays as well, with essentially the exact same proof (modulo passing to another limit). The analogues of the other results in Sections 4.1 and 4.2 then follow by similar arguments. In other words, the *local monodromy* of maps in Per_2 is exactly analogous to that of maps in Per_1.

5.3 Monodromy

If two p-periodic points degenerate into each other in a neighborhood of some $h \in \mathrm{Per}_2$, then those periodic points must have multiplier p^{th} root of unity at h. It follows that h must be a root of a hyperbolic component of period p, and hence the monodromy is described by Lemma 4.2.1 as discussed above.

A crucial difference between Per_1 and Per_2 comes from the fact that Per_2 has an orbifold point and a puncture. To obtain a complete description of cycle monodromy in Per_2, it is therefore necessary to understand the monodromy about these two exceptional points.

5.3.1 The orbifold point

We first study the monodromy of cycles around the orbifold point $[f_\circlearrowright]$, where $f_\circlearrowright(z) = z^{-2}$. Using the 3-fold branched cover $\mathcal{G}$, with $g_b(z) = b + 1/(z^2 - b^2)$, observe that

$$
\begin{aligned}
g_{\omega b}(z) &= \omega b + \frac{1}{z^2 - \overline{\omega} b^2} \\
&= \omega b + \frac{\omega}{\omega z^2 - \omega b^2} \\
&= \omega \left(b + \frac{1}{(\overline{\omega} z)^2 - \omega b^2} \right) \\
&= \omega g_b(\overline{\omega} z),
\end{aligned}
$$

where ω is a primitive cube root of unity. Thus, $g_{\omega b}(\omega z) = \omega g_b(z)$. In particular, z is p-periodic under g_b if and only if ωz is p-periodic under $g_{\omega b}$.

Proposition 5.3.1. *For b in a neighborhood U of 0, the Julia set $\mathcal{J}(g_b)$ is a quasicircle, and there is a quasisymmetric homeomorphism $\psi_b : S^1 \to \mathcal{J}(g_b)$ conjugating the angle anti-doubling map $\theta \mapsto -2\theta$ to g_b. The map $(b, \theta) \mapsto \psi_b(\theta)$ is continuous on $U \times S^1$.*

Proof. Note that $g_0^2(z) = z^4$. Since g_b varies continuously in $(L_\infty(\hat{\mathbb{C}}))$ with b, it follows that g_b^2 is polynomial-like of degree 4 for b in a neighborhood of 0. Let U be a neighborhood of 0 such that for $b \in U$, g_b^2 has three critical points in $\mathbb{D}$ counted with multiplicity, all of which converge under forward iteration toward the same attracting fixed point. Evidently, this is an open condition which is satisfied for g_0.

By Douady and Hubbard's straightening theorem [DH85], for $b \in U$, g_b^2 is hybrid equivalent to a degree 4 polynomial with three critical points in the immediate basin of an attracting fixed point. It follows that $\mathcal{J}(g_b^2) = \mathcal{J}(g_b)$ is a quasicircle, and the landing of dynamical

rays induces a quasisymmetric homeomorphism $\psi_b : \mathcal{J}(g_b) \to S^1$, conjugating g_b^2 to $z \mapsto z^{-4}$. Since the landing points of external rays change continuously as we move within a hyperbolic component, we know that ψ_b is continuous.

In the case $b = 0$, $\psi_0(\theta) = \exp(\theta\tau i)$ plainly conjugates the angle anti-doubling map to $g_0(z) = z^{-2}$. Thus, the map $\vartheta = \psi_b^{-1} \circ g_b \circ \psi_b$ is quasisymmetric with winding number -2, and satisfies $\vartheta^2(\theta) = 4\theta$. Since the unique quasisymmetric square root of $\theta \mapsto 4\theta$ with winding number -2 is the angle anti-doubling map, the result follows. □

Theorem 5.3.2. *Fix any $p \in \mathbb{N}^* \smallsetminus \{2\}$. Let γ be a loop in $\mathrm{Per}_2 \smallsetminus \{f_\bigcirc\}$ with winding number 1 about $f_\bigcirc$. If γ is chosen to be sufficiently small, then all orbits of p-periodic points of $f = \gamma(0)$ under the monodromy action $\mathrm{mon}_p(\gamma)$ induced by γ have exact cardinality 3.*

Proof. Note that all p-periodic points of $g_0(z) = z^{-2}$ lie on the unit circle, and hence are repelling with multiplier $(-2)^p$. Furthermore, g_0 has no indifferent periodic points.

It follows that the p-periodic points of g_b move continuously and remain bounded away from one another for b in some neighborhood of 0. Thus, the 3-fold cover $\mathcal{G}$ exhibits no monodromy around $[f_\bigcirc]$, implying that all orbits of $\mathrm{mon}_p(\gamma)$ have cardinality dividing 3. It remains to show that no point is fixed under $\mathrm{mon}_p(\gamma)$.

Let A denote the (finite) set of p-periodic points of $f_\bigcirc$, and let $\delta > 0$ be sufficiently small such that:

(1) the distance between any two elements of A is at least 3δ, and

(2) for all $z \in A$, $\mathrm{dist}(z, \omega z) > 5\delta$.

Property (2) holds for sufficiently small δ since $0 \notin A$, as 0 has period 2 under $g_0 = f_\bigcirc$. Let V be the neighborhood of radius δ around A, so by (1) no two elements of A are connected by a path in V. We may then choose $\varepsilon > 0$ sufficiently small such that all p-periodic points of g_b belong to V for all $b \in \mathbb{D}_\varepsilon(0)$.

Now let $\tilde{\gamma}(t) = \frac{\varepsilon}{2}\exp(3t\tau i)$ for $t \in [0, 1]$, so that $\tilde{\gamma}(0) = \varepsilon/2$ and $\tilde{\gamma}(1) = \omega\varepsilon/2$. Suppose z is a p-periodic point of $g_{\gamma(0)}$. Let w be the image of z under the monodromy induced by γ. Since z and w are connected by a path, we know that both z and w belong to the same component V_0 of V.

Also, if $z_0 \in \mathcal{J}(f_\bigcirc)$ is the image of z under the monodromy induced by the radial path $\rho(t) = \frac{\varepsilon}{2}(1 - t)$, then the same reasoning implies $z_0 \in V_0$.

Since $V_0 = B_\delta(z_0)$ has diameter δ, we see that $\text{dist}(z_0, z) < 2\delta$ and $\text{dist}(z_0, w) < 2\delta)$. The triangle inequality then gives

$$\begin{aligned}
\text{dist}(\omega z, w) &\geq \text{dist}(z_0, \omega z_0) - \text{dist}(\omega z, \omega z_0) - \text{dist}(z_0, w) \\
&= \text{dist}(z_0, \omega z_0) - \text{dist}(z, z_0) - \text{dist}(z_0, w) \\
&> 5\delta - 2\delta - 2\delta = \delta.
\end{aligned}$$

Thus, it cannot be the case that $\omega z = w$. Now $g_{\gamma(0)}$ is uniquely conjugate to $g_{\gamma(1)}$ via

$$g_{\omega(1)}(\omega z) = \omega g_{\omega(0)}(z),$$

with uniqueness holding since $g_\omega(0) \neq f_\bigcirc$ (as $\varepsilon > 0$), where $f_\bigcirc$ is the unique element of $\mathcal{M}_2$ commuting with an order 3 Möbius transformation [Mil00]. It follows that z and w represent distinct periodic points of the conjugacy class $[f_{\gamma(0)}]$, proving that the monodromy action on z has exact order 3. $\qquad\square$

Corollary 5.3.3. *If γ is a small counterclockwise loop around $[f_\bigcirc]$, based at some $b \in \text{Per}_2$, then under the coordinates ψ_b of Proposition 5.3.1, the monodromy under γ maps $\psi_b(\theta)$ to $\psi_b(\theta + \omega)$.*

5.3.2   The puncture

We now study the monodromy of cycles around the puncture in Per_2. Throughout, we will use the coordinates $h_a(z) = (z^2 + a)/(1 - z^2)$, for which the puncture is located at $a = -1$.

Proposition 5.3.4. *For $z \in \hat{\mathbb{C}}$, the map h_a^2 converges pointwise on $\hat{\mathbb{C}}$ as $a \to -1$ to the map $\hat{h}(z) = -\frac{1}{2}(z^2 + 1)$, which is in turn conjugate to the "cauliflower" map $f_\clubsuit(z) = z^2 + \frac{1}{4}$.*

Proof. Computing, for $a \neq -1$ and $z^2 \neq 1$ we have

$$\begin{aligned}
h_a^2(z) &= \frac{\left(\frac{z^2+a}{1-z^2}\right)^2 + a}{1 - \left(\frac{z^2+a}{1-z^2}\right)^2} \\
&= \frac{(z^2 + a)^2 + a(1 - z^2)^2}{(1 - z^2)^2 - (z^2 + a)^2} \\
&= \frac{(a + 1)(z^4 + a)}{(a + 1)(1 - a - 2z^2)} \\
&= \frac{z^4 + a}{1 - a - 2z^2}. \qquad\qquad (*)
\end{aligned}$$

Plugging in $a = -1$, the above expression becomes

$$\frac{(z^2 + 1)(z^2 - 1)}{-2(z^2 - 1)}$$

The final expression is well-defined and equal to $\hat{h}(z) = -\frac{1}{2}(z^2 + 1)$ when $z \neq \pm 1$.

It remains to check the case $z = \pm 1$. For $a \neq -1$, note that $h_a^2(\pm 1) = h_a(\infty) = -1$ (independent of a), while also $\hat{h}(-1) = -1$. The claim then follows.

The conjugacy to $f_{\clubsuit}$ is given by

$$\hat{h}(-2z) = -2f_{\clubsuit}(z). \qquad \qquad \square$$

Remark 5.3.5. For $a \neq -1$, the formula $(*)$ for $h_a^2(z)$ holds for all $z \in \hat{\mathbb{C}}$, including ± 1. Indeed, plugging $z = \pm 1$ into $(*)$ yields the expression

$$\frac{(\pm 1)^4 + a}{1 - a - 2(\pm 1)^2} = \frac{1 + a}{-1 - a} = -1,$$

consistent with the value of $h_a^2(\pm 1)$ as established above.

Proposition 5.3.6. *Fix any $p \geq 3$. Let γ be a loop in* Per_2 *with winding number 1 about the puncture. If γ is chosen to be sufficiently small, then the p-periodic points of f exhibit no monodromy under γ.*

Proof. The angles $1/3$ and $2/3$ both have period 2 under angle doubling. Thus, if $p \geq 3$, then the (finite) set of p-periodic angles in $S^1 \smallsetminus (1/3, 2/3)$ is bounded away from $\{1/3, 2/3\}$. It follows that the union of all p-periodic parameter bubble rays is bounded away from the puncture $a = -1$. Thus, if γ is chosen to be sufficiently small, then γ does not cross any p-periodic parameter bubble ray. It then follows from the Per_2 analogue of Lemma 4.1.2 that for ant p-periodic angle θ, the landing point of

$$\overset{\circ}{\mathcal{R}}_{\gamma(t)}(\theta)$$

moves continuously with t.

It remains only to show that every p-periodic point is the landing point of a p-periodic dynamical bubble ray. Since γ does not cross any parameter bubble rays and passes inside the period 1 component of $\mathcal{M}_2$, we see that no point on γ lies inside a p-periodic bubble wake. Thus, each p-periodic dynamical bubble ray lands at a unique point of period p. Since

there are the same number of p-periodic angles as p-periodic points ($p \geq 3$), the result then follows.

$\square$

5.4   A cell structure

We may now define a cell structure for $\mathrm{Cyc}_p(\mathrm{Per}_2)$ just as we did for Per_1 in Section 4.5. To this end, we let $p \neq 2$ be fixed.

As with Per_1, we begin by understanding the branch locus of the map $\pi : \mathrm{Cyc}_p(\mathrm{Per}_2) \to \overline{\mathrm{Per}_2}$. Let $B \subset \mathrm{Cyc}_p(\mathrm{Per}_2)$ be the branch locus of π, and let $P = \pi(B) \subset \hat{\mathbb{C}}$ be the ramification locus. Let $P_0 = P \smallsetminus \{[z \mapsto z^2]\}$ be the set of "finite" ramification points, and let $B_0 = \pi^{-1}(P_0)$ be the set of "finite" branch points.

Definition 5.4.1. Let M_0 denote the path-connected component of $\mathcal{M}$ containing 0, and let A be the smallest path-connected subset of M_0 containing 0 and the roots of all p-periodic hyperbolic components. Denote by A_2 the image of A under the Wittner mating.

Proposition 5.4.2. A_2 is simply connected.

Proof. Since A is simply connected, it suffices to show that for every $\alpha, \beta \in S^1 \smallsetminus [1/3, 2/3]$ whose dynamical rays land together on $\mathcal{J}(f_{\circ\!\!\circ})$, the parameter rays $\mathcal{R}_{\mathcal{M}}(\alpha)$ and $\mathcal{R}_{\mathcal{M}}(\beta)$ do not land on A.

Assume that the dynamical rays $\mathcal{R}_{f_{\circ\!\!\circ}}(\alpha)$ and $\mathcal{R}_{f_{\circ\!\!\circ}}(\beta)$ land together. It follows that for some $k \in \mathbb{N}$, $2^k \alpha = 1/3$ and $2^k \beta = 2/3$. Since α and β do not belong to $\{1/3, 2/3\} \subset [1/3, 2/3]$, we conclude that α and β are strictly preperiodic with period 2. Thus, the parameter rays in Per_1 at angles α and β land at Misiurewicz points of period 2.

Suppose for the sake of contradiction that $\mathcal{R}_{\mathcal{M}}(\alpha)$ lands at some Misiurewicz point $c \in A$. It follows that c is not a tip, since otherwise $A \smallsetminus \{c\}$ would be a smaller path-connected set, containing all the same hyperbolic component roots as A. Thus, there is different angle α' such that $\mathcal{R}_{\mathcal{M}}(\alpha')$ also lands at c. Theorem 3.1 of [Mil93] then implies that c belongs to a 2-periodic wake, a contradiction since the only 2-periodic wake is $\mathcal{W}(1/3, 2/3)$. The reasoning for β is identical. $\square$

By Theorem 2.3.33 and the fact that all disjoint type hyperbolic components in Per_2 arise from matings [Lei92], $M_0^{(2)}$ contains the root of every hyperbolic component in Per_2, so in particular, $P_0 \subset M_0^{(2)}$, except in the case $p = 1$, where the puncture also belongs to P_0.

Definition 5.4.3. The cells in $\mathrm{Cyc}_p(\mathrm{Per}_2)$ are defined as follows:

- A *vertex* is a lift of A_2.

- An *edge* is a branch point of π, excluding the orbifold point $[f_{\bigcirc}]$.

- A *face* is a lift of $\hat{\mathbb{C}} \smallsetminus A_2$.

As in the case of Per_1, a homotopically equivalent, and more geometrically clear, cell structure may be obtained by contracting each vertex down to a lift of $[f_{\bigcirc\!\bigcirc}]$, stretching out the edges to include lifts of veins in Per_2, and expanding the faces into A_2 to meet the edges.

Lemma 5.4.4. *Vertices in* $\mathrm{Cyc}_p(\mathrm{Per}_1)$ *are in natural bijection with p-cycles of* $f_{\bigcirc\!\bigcirc}$. *If* $p \geq 3$, *then vertices are in natural bijection with p-cycles of angles under doubling.*

Proof. By definition of Cyc_p, lifts of $h_0 \sim f_{\bigcirc\!\bigcirc}$ are in bijective correspondence with cycles of period p under h_0. If $p \geq 3$, then no pairs of p-periodic dynamical rays of $f_{\bigcirc\!\bigcirc}$ land together, so p-cycles of $f_{\bigcirc\!\bigcirc}$ are in natural bijection with p-cycles of angles under doubling. $\qquad\square$

We thus label vertices according to p-cycles of angles under doubling, treating $p = 1$ as a special case.

As discussed in Section 5.3, the ramification points of π_p are the roots of disjoint type hyperbolic components in Per_2 (or equivalently $\mathcal{M} \smallsetminus \mathcal{W}(1/3, 2/3)$), the puncture if $p = 1$, and $[f_{\bigcirc}]$. We may thus label an edge α by the pair (θ_0, θ_1) of angles in $S^1 \smallsetminus [1/3, 2/3]$ whose parameter rays land at $\pi(\alpha)$.

Finally, to label the faces, we use the following result.

Lemma 5.4.5. *Faces in* $\mathrm{Cyc}_p(\mathrm{Per}_2)$ *are in natural bijection with orbits of p-periodic angles under the operations* $\theta \mapsto -2\theta$ *and* $\theta \mapsto \theta + 1/3$. *Moreover, letting* F_C *denote the face corresponding to an orbit* C, *we have the following dichotomy:*

- *If* C *contains only a single p-cycle under anti-doubling (we say* C *is* reflexive*), then the restriction* $\pi : F_C \to \hat{\mathbb{C}} \smallsetminus A_2$ *is a homeomorphism.*

- *Otherwise, if* C *is not reflexive, then the restriction* $\pi : F_C \to \hat{\mathbb{C}} \smallsetminus A_2$ *is a degree 3 branched cover, ramified at* $[f_{\bigcirc}]$.

Proof. Fix a sufficiently large real parameter a_0 (any value greater than 2 will suffice) such that the Julia set of h_{a_0} is a quasicircle. By Proposition 5.3.1, labeling a p-cycle of h_{a_0} is equivalent under the coordinate ψ_{a_0} to labeling a p-cycle of angles under the anti-doubling

map $\theta \mapsto -2\theta$. By Corollary 5.3.3, a large counterclockwise loop around $\mathcal{M}_2$ (which is a clockwise loop around $[f_{\bigcirc}]$) will induce a monodromy action that adds $-1/3$ to every angle.

The p-cycles of h_{a_0} are in canonical bijection with ABCs of period p. Two lifts (a_0, ξ) and (a_0, ξ') of c_0 belong to the same face F if and only if they can be connected by a path in F, i.e. if and only if there is some loop in $\mathrm{Per}_2 \smallsetminus A_2$ based at a_0 whose monodromy takes ξ to ξ'.

Let $O = (\theta_0, \ldots, \theta_{p-1})$ be the p-cycle of angles under anti-doubling associated to ξ under the coordinate ψ_{a_0}. There are two possibilities:

- If $\theta_k = \theta_0 - 1/3$ for some k, then $\theta_{2k \pmod p} = \theta_0 + 1/3$ (and $\theta_{3k \pmod p} = \theta_0$, so that p is a multiple of 3), so the face F containing (a_0, ξ) contains only one lift of a_0. Thus, the branched cover $\pi|_F$ has degree 1, so it is a homeomorphism.

- Otherwise, if $\theta_0 - 1/3$ does not belong to O, then neither does $\theta_0 + 1/3$. In this case, the face F containing (a_0, ξ) also contains $(a_0, \xi + 1/3)$ and $(a_0, \xi - 1/3)$ (where adding arithmetic is done on the ψ_{a_0} coordinate), but F contains no other lifts of a_0. Thus, the branched cover $\pi|_F$ has degree 3, ramifying at $[f_{\bigcirc}]$.

$\square$

5.5 Computing the cell structure

The algorithm to describe the cell structure for $\mathrm{Cyc}_p(\mathrm{Per}_2)$ is nearly identical to Algorithm 4.6.1, with the only real difference being that we remove the $\frac{1}{3}$ limb.

Instead of using our knowledge of the monodromy about infinity to predict which faces will ramify, it suffices to keep track of which angles have been active when crossing the positive real axis. This allows us to use the external arguments of $f_{\bigcirc}$, which are covariant under angle doubling, instead of the "argument at infinity" ψ, which is covariant under angle anti-doubling. This is useful because the Per_2 analogue of Lemma 4.2.1 describes monodromy to dynamical arguments of $f_{\bigcirc}$ (i.e. arguments of bubble rays), not in terms of ψ.

Algorithm 5.5.1.

1. Enumerate all pairs (θ_0, θ_1) of period p parameter rays in $\hat{\mathbb{C}} \smallsetminus \mathcal{M}$ such that θ_0 and θ_1 land together on $\partial \mathcal{M}$, and such that θ_0 and θ_1 do not belong to $[1/3, 2/3]$. This can be done using Lavaurs' algorithm [Lav89]. Denote by $\mathcal{A}$ the ordered set of arcs of period p.

2. Denote by P the set of p-cycles of angles under doubling. For each endpoint θ of an

arc in $\mathcal{A}$, compute a canonical representative (θ) for the associated ABC. One way to do this is to take the minimum over the orbit of θ under angle doubling.

3. Let $\mathcal{A}' = \{(\theta_0, \theta_1) \in \mathcal{A} : (\theta_0) \neq (\theta_1)\}$ be the set of primitive arcs in $\mathcal{A}$.

4. For each p-periodic ABC $\langle \alpha \rangle$ which is not marked as visited, we *traverse the face $\langle \alpha \rangle$* as follows:

   4.1 Initialize $k = 0$ and $x_0 = \alpha$. The angle x_k represents the bubble ray argument of the parameter a at the kth vertex. We are beginning our journey on the positive real axis, where we are guaranteed to be outside any p-periodic wake.

   4.2 Locate the first arc $(\theta_0, \theta_1) \in \mathcal{A}'$ strictly after x_k in counterclockwise circular order such that either θ_0 or θ_1 belongs to (x_k).

   - If in the process of finding the next arc, we wrap around the end of $\mathcal{A}'$, then we mark x_k as visited and check if $x_k = \alpha$. If so, we terminate the traversal of $\langle \alpha \rangle$ and return the ordered sequence of vertices.

   4.3 If $\theta_0 \in (x_k)$, then set $x_{k+1} = \theta_1$; otherwise, if $\theta_1 \in (x_k)$, then set $x_{k+1} = \theta_0$.

   4.4 Update $k \leftarrow k + 1$ and continue from step 4.2.

5. Glue together all pairs of matching edges in the faces obtained in step 4.

Example 5.5.2 $(\mathrm{Cyc}_5(\mathrm{Per}_2))$**.** As an example, consider the family of maps in Per_2 with a marked cycle of period 5. We begin by enumerating the period 5 arcs in $\widetilde{\mathrm{QML}}$, together with the ABC associated to the orbit of each angle under doubling.

ID	θ_0	θ_1	(θ_0)	(θ_1)	Knead. Seq.	Primitive?
A_0	1/31	2/31	$(1) = (00001)$	$(1) = (00001)$	0000*	No
A_1	3/31	4/31	$(3) = (00011)$	$(1) = (00001)$	0001*	Yes
A_2	5/31	6/31	$(5) = (00101)$	$(3) = (00011)$	0010*	Yes
A_3	7/31	8/31	$(7) = (00111)$	$(1) = (00001)$	0011*	Yes
A_4	9/31	10/31	$(5) = (00101)$	$(5) = (00101)$	0000*	No
A_5	21/31	22/31	$(11) = (01011)$	$(11) = (01011)$	0000*	No
A_6	23/31	24/31	$(15) = (01111)$	$(3) = (00011)$	0011*	Yes
A_7	25/31	26/31	$(7) = (00111)$	$(11) = (01011)$	0010*	Yes
A_8	27/31	28/31	$(15) = (01111)$	$(7) = (00111)$	0001*	Yes
A_9	29/31	30/31	$(15) = (01111)$	$(15) = (01111)$	0000*	No

Table 5.1: Period 5 arcs in $\widetilde{\mathrm{QML}}$, together with their associated abstract binary cycles. The ABCs are represented using their minimal element under the dictionary ordering. For reference, we also include the kneading sequences, though these are not necessary for the algorithm.

We now proceed to the face traversal stage. For brevity, we will only show the process for the face $\langle 00001 \rangle = \langle 1 \rangle$.

- We begin at (1), according to the label of our face. This shall be the "first" vertex v_0 in our face. Since we are starting from the top of the list of edges, we can optionally add an indicator to remember that there is a lift of the positive real axis connecting the center of F to v_0.

- We look for the first primitive arc in our list that is active at v_0, i.e. one of whose ABCs is (1). This is the second arc on our list, A_1, which connects (3) and (1). We thus set our next vertex to $v_1 = (3)$.

- The next primitive arc after A_1 that is active at $v_1 = (3)$ is A_2, which connects (5) and (3). We thus set our next vertex to $v_2 = (5)$.

- There are no primitive arcs after A_5 active at v_2. So, we return to the top of the list. Since we passed $1/2$ *and* returned to the top of the list, v_2 was the marked cycle as we crossed both the negative and positive the real axis. Thus, we can mark a lift of $\mathbb{R}_-$ through v_2 followed by a lift of $\mathbb{R}_+$ through v_2. We also mark $v_2 = (5)$ as visited.

- Continuing from the top of the list, A_2 (again) connects v_2 to $v_3 = v_1 = (3)$.

- The next primitive arc after A_2 that is active at $v_3 = (3)$ is A_{11}, which is after the

74

negative real axis. So, we can mark a lift of $\mathbb{R}_-$ at v_3. Since A_{11} connects (15) to (3), we set $v_4 = (15)$.

- A_{13} connects v_4 to $v_5 = (7)$.

- After passing through $\mathbb{R}_+$ and marking $v_5 = (7)$ as visited, A_3 connects v_5 to $v_6 = v_0 = (1)$.

- No more arcs after A_3 are active at $v_6 = (1)$. Since we return to the real axis with the initial vertex (1) active, we close up the face, identifying v_6 with v_0.

The other face $\langle 3 \rangle$ turns out to be equivalent to $\langle 1 \rangle$ under bit flip. Thus, we obtain the following structure:
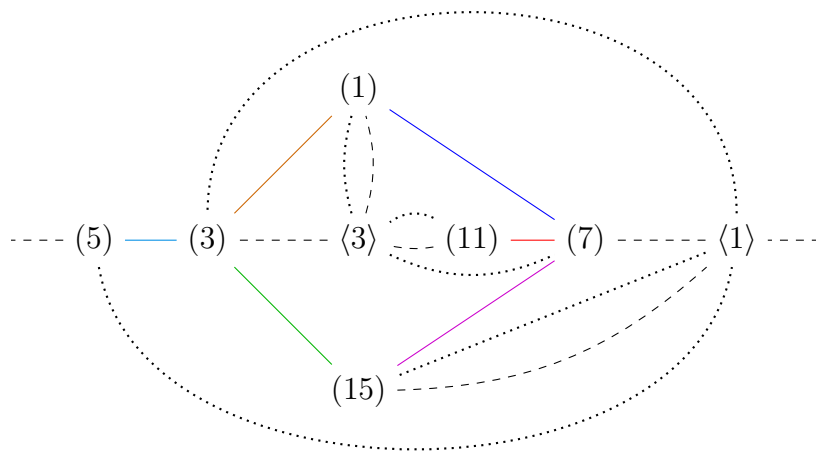
(a) Cell structure for the marked cycle curve $\mathrm{Cyc}_5(\mathrm{Per}_2)$, which has genus $g = 0$. Angle brackets denote face centers, and parentheses denote vertices. Solid, colored lines are edges. Dashed lines indicate lifts of the positive real axis, and dotted lines indicate lifts of the negative real axis.
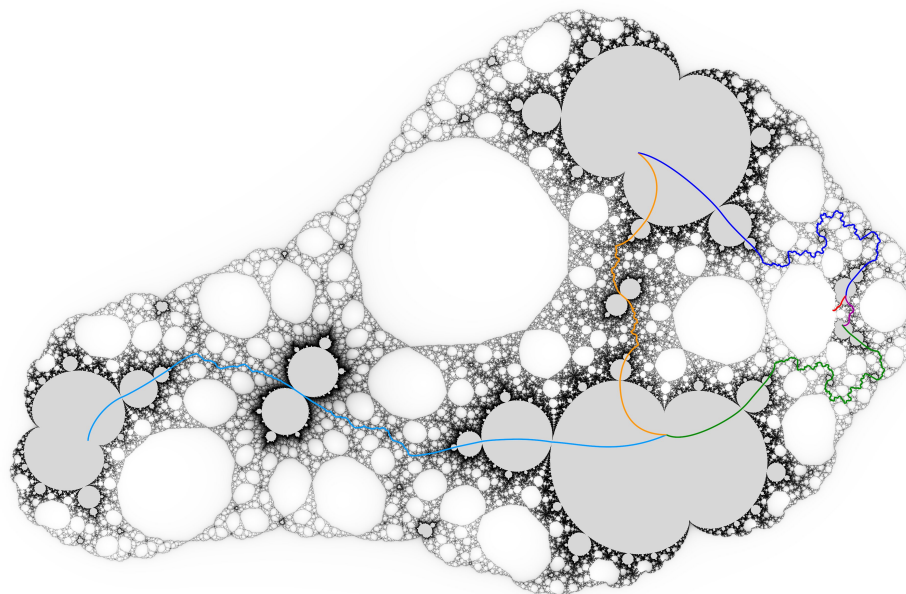
(b) Embedding of cells in $\mathrm{Cyc}_5(\mathrm{Per}_2)$.

Figure 5.3: Comparison of combinatorial structure of $\mathrm{Cyc}_5(\mathrm{Per}_2)$ to geometric structure.

CHAPTER 6

Dynatomic Curves

The cell structures for marked cycle curves can be extended to describe dynatomic curves defined in Chapter 3 as well.

6.1 Cell Structure

Definition 6.1.1. The cells in $\mathrm{Dyn}_p(\mathrm{Per}_m)$ are defined as follows for $m = 1, 2$:

- A *vertex* is an angle in $\mathbb{Q}/\mathbb{Z}$ that is p-periodic under doubling.

- An *edge* is a (bubble) wake W in Per_m, together with a choice of *shift* $\ell \in \mathbb{Z}/p\mathbb{Z}$. If θ_0 and θ_1 are the angles defining W, then the edge connects the vertices $2^\ell \theta_0$ and $2^\ell \theta_1$.

- A *primitive face* is a sequence of vertices as constructed as in Algorithm 6.1.2.

- For each satellite (bubble) wake $W = \mathcal{W}(\theta, 2^\ell\theta)$ in Per_m, and each $j \in [\gcd(p, \ell)]$,[1] there is a *satellite face* whose vertices are given by the sequence

$$F^{\mathrm{sat}}(\theta, j) = \left(2^{j+k\ell}\theta : k \in \left[\frac{p}{\gcd(p, \ell)} \right] \right). \tag{6.1}$$

As in the case of Per_1, a homotopically equivalent, and more geometrically clear, cell structure may be obtained by contracting each vertex down to a lift of $[f_{\circ\!\!\!\circ}]$, stretching out the edges to include lifts of veins in Per_2, and expanding the faces into A_2 to meet the edges.

Algorithm 6.1.2. For simplicity, we only describe the case of dynatomic curves over Per_1. As in Algorithm 5.5.1, we can obtain the corresponding algorithm for Per_2 by removing all subarcs of $[1/3, 2/3]$ from the Mandelbrot lamination QML.

---

[1]Recall that $[k] \stackrel{\text{def}}{=} \{0, 1, \ldots, k-1\}$.

1. Enumerate all pairs (θ_0, θ_1) of period p arcs in QML. This can be done using Lavaurs' algorithm [Lav89]. Denote by $\mathcal{A}$ the ordered set of arcs of period p.

2. For each p-periodic angle α which is not marked as visited, we *traverse the face* $[\alpha]$ as follows:

   2.1 Initialize $k = 0$ and $x_0 = \alpha$. The angle x_k represents the external argument of the parameter a at the kth vertex. We are beginning our journey on the positive real axis, where we are guaranteed to be outside any p-periodic wake.

   2.2 Locate the first arc $(\theta_0, \theta_1) \in \mathcal{A}$ strictly after x_k in counterclockwise circular order such that either θ_0 or θ_1 belongs to (x_k).

      - If in the process of finding the next arc, we wrap around the end of $\mathcal{A}$, then we mark x_k as visited and check if $x_k = \alpha$. If so, we terminate the traversal of $\langle \alpha \rangle$ and return the ordered sequence of vertices.

   2.3 If $\theta_0 \in (x_k)$; say, $x_k = 2^r \theta_0$, then set $x_{k+1} = 2^r \theta_1$.

      Otherwise, if $\theta_0 \notin (x_k)$ but $\theta_1 \in (x_k)$; say, $x_k = 2^r \theta_1$ then set $x_{k+1} = 2^r \theta_0$.

   2.4 Update $k \leftarrow k + 1$ and continue from step 2.2.

3. Construct all satellite faces as in (6.1).

4. Glue together all pairs of matching edges in the primitive and satellite faces.

Example 6.1.3 ($\mathrm{Dyn}_4(\mathrm{Per}_1)$). As an example, consider the family of quadratic polynomials with a marked point of period 4. We begin by enumerating the period 4 arcs in QML, together with the ABP associated to the orbit of each angle under doubling.

| ID	θ_0	θ_1	ABP (θ_0)	ABP (θ_1)	Knead. Seq.	Type
A_0	1/15	2/15	0001	0010	000*	Satellite
A_1	3/15	4/15	0011	0100	001*	Primitive
A_2	2/5	3/5	0110	1001	010*	Satellite
A_3	7/15	8/15	0111	1000	011*	Primitive
A_4	11/15	12/15	1011	1100	001*	Primitive
A_5	13/15	14/15	1101	1110	000*	Satellite

Table 6.1: Period 4 arcs in QML, together with their associated abstract binary points (ABPs). The ABPs are represented using their minimal element under the dictionary ordering.

We now proceed to the face traversal stage. For brevity, we will only show the process for the primitive face [0100].

- We begin at [0100], according to the label of our face. This will be the "first" vertex v_0 in our face F. Since we are starting from the top of the list of edges, we can optionally add an indicator to remember that there is a lift of the positive real axis connecting the center of F to v_0.

- We look for the first arc in our list that is active at v_0, i.e. one of whose ABPs shares a cycle with 0100. This is the very first on our list, A_0. Since A_0 is a satellite arc, both defining angles θ_0, θ_1 are in the orbit of v_0. Since θ_1 differs from θ_0 by a left shift, we obtain v_1 from v_0 by applying a left shift, yielding $v_1 = 1000$.

- The next arc in our list that is active at v_1 is A_1, which connects 0011 and 0100. This arc is primitive, and v_1 differs from the active angle 0100 by a left shift. We thus obtain v_2 by applying a left shift to the other angle 0011, so that $v_2 = 0110$.

- The next arc after A_2 active at $v_2 = 0110$ is A_2, which is a satellite arc with a relative shift of 2. We thus obtain our next vertex by applying two left (or right) shifts to v_2, yielding $v_3 = 1001$. Since A_2 crosses over $1/2$, we can mark the edge (v_2, v_3) as crossing the negative real axis.

- The next arc after A_2 that is active at $v_3 = 1001$ is the primitive arc A_4. The ABP of A_4 that is active at v_3 is 1100, from which v_3 differs by a left shift. So, the next vertex is obtained by applying a left shift to the other angle 1011 of A_4, yielding $v_4 = 0111$.

- The next arc after A_4 active at $v_4 = 0111$ is the satellite arc A_5. This arc is characterized by a right shift, so we obtain $v_4 = 1011$ by applying a right shift to v_3.

- There are no primitive arcs after A_5 active at v_3. So, we return to the top of the list, and we can mark a lift of the positive real axis at v_4. Note that $v_4 = 1011$ differs from $v_0 = 0100$ by a bit-flip, consistent with Lemma 4.5.6.

- Continuing from the top of the list, the next arc active at v_4 is the primitive arc A_3, which connects $\theta_0 = 0111$ to $\theta_1 = 1000$. Since v_4 differs from θ_0 by a right shift, v_5 is obtained by applying a right shift to θ_1, so that $v_5 = v_0 = 0100$.

- No more arcs after A_3 are active at v_5. Since we return to the real axis with the initial vertex 0100 active, we close up the face, identifying v_5 with v_0.

We may similarly fill in the other satellite faces. The resulting cell structure has genus 2, so it cannot be drawn in the plane without duplicating some vertices.

Over Per_2, on the other hand, the dynatomic curve of period 4 is rational, and its cell structure can be drawn on the plane:
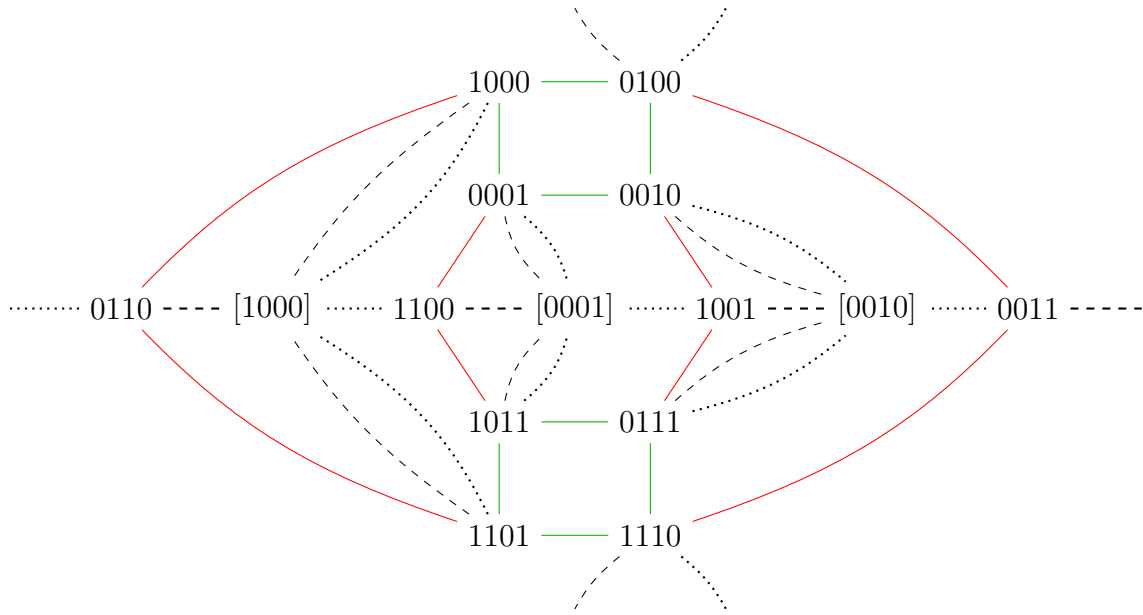
(a) Cell structure for the dynatomic curve $\mathrm{Dyn}_4(\mathrm{Per}_2)$, which has genus $g = 0$. Square brackets denote face centers (ABP classes), while bare sequences denote vertices (ABPs). The face [0100] is centered at infinity. Red lines are primitive edges, and green lines are satellite edges. Dashed lines indicate lifts of the positive real axis, and dotted lines indicate lifts of the negative real axis.
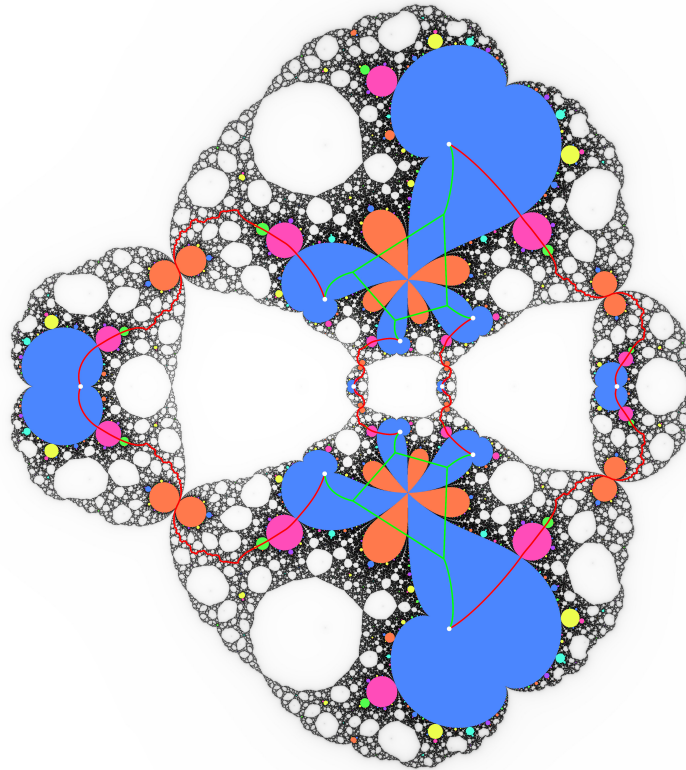
(b) Embedding of cells in $\mathrm{Dyn}_4(\mathrm{Per}_2)$, with satellite faces partially collapsed. Vertices aare shown in white, primitive edges are shown in red, and satellite edges are shown in green.

Figure 6.1: Comparison of combinatorial structure of $\mathrm{Dyn}_4(\mathrm{Per}_2)$ to geometric structure.

CHAPTER 7

Combinatorics

7.1 Dirichlet convolutions

The present chapter makes repeated use of Dirichlet convolutions, introducing some new notation that may collide with notation from previous sections.

Throughout this chapter, μ will denote the Möbius function

$$\mu(n) = \begin{cases} (-1)^k & \text{if } n \text{ is the product of } k \text{ distinct primes;} \\ 0 & \text{otherwise.} \end{cases}$$

Definition 7.1.1. If f and g are two functions from $\mathbb{N}^*$ to some field F, then the Dirichlet convolution of f and g is the function $(f * g) : \mathbb{N}^* \to F$ defined by

$$(f * g)(n) = \sum_{d|n} f(d)g(n/d).$$

It is readily checked that the operation of Dirichlet convolution is commutative, associative, and bilinear with respect to its input functions.

Definition 7.1.2. If f is a function from $\mathbb{N}^*$ to some field, then the *Möbius transform* of f is the Dirichlet convolution of f with μ:

$$(f * \mu)(n) = \sum_{d|n} f(d)\mu(n/d).$$

The Möbius transform is linear with respect to f and satisfies the well-known *Möbius inversion formula*:

$$(f * \mu) * \mathbf{1} = (f * \mathbf{1}) * \mu = f,$$

where $\mathbf{1}$ is the constant function $\mathbf{1}(n) = 1$.

The Möbius transform of an arithmetic function f should not be confused with the notion of a Möbius transformation on $\hat{\mathbb{C}}$.

7.2   Cell counts for Marked Cycle Curves

In this section, we will derive formulas for the number of cells in our decompositions of $\mathrm{Cyc}_p(\mathrm{Per}_m)$ for $m = 1, 2$. We begin by studying the dynamics of two maps:

- $h_1(z) = z^2$, which is the map at the origin in $\mathrm{Per}_1(0)$, and

- $h_2(z) = z^{-2}$, which is conjugate in the limit to the map at infinity in $\mathrm{Per}_2(0)$, as discussed in Section 5.1.1.

Lemma 7.2.1. *The number of points on S^1 of period dividing p under $h_1(z) = z^2$ is*

$$\tilde{v}_1(p) = 2^p - 1$$

The number of points on S^1 of period dividing p under $h_2(z) = z^{-2}$ is

$$\tilde{v}_2(p) = 2^p - (-1)^p.$$

Proof. A point $z = \exp(\tau i \theta)$ is periodic of period dividing p under h_1 if and only if $2^p \theta = \theta$ (mod 1), i.e. θ is of the form $\frac{j}{2^p - 1}$.

Similarly, a point $z = \exp(\tau i \theta)$ is periodic of period dividing p under h_2 if and only if $(-2)^p \theta = \theta$ (mod 1), i.e. θ is of the form

$$\frac{j}{(-2)^p - 1} = \frac{(-1)^p j}{2^p - (-1)^p}. \qquad \square$$

Applying the Möbius inversion formula, we obtain the following:

Corollary 7.2.2. *For $m = 1, 2$, the number of points on S^1 of period p under $h_m(z)$ is*

$$v_m(p) = (\mu * \tilde{v}_m)(p) = \sum_{d \mid p} \mu\left(\frac{p}{d}\right) \tilde{v}_m(d),$$

where μ is the Möbius function and $*$ denotes Dirichlet convolution.

Corollary 7.2.3. *The number of p-cycles under* $h_m(z) = z^{\pm 2}$ *is*

$$c_m(p) = \frac{1}{p} v_m(p) = \frac{1}{p} \sum_{d \mid p} \mu\left(\frac{p}{d}\right) \tilde{v}_m(d),$$

Remark 7.2.4. The values $c_1(p)$ and $c_2(p)$ are equal for $p \geq 3$. This is most easily seen since the Möbius transform is additive, and the Möbius transform of $\sigma(p) = \tilde{v}_2(p) - \tilde{v}_1(p) = 1 - (-1)^p$ is

$$(\mu * \sigma)(p) = \begin{cases} 2 & p = 1 \\ -2 & p = 2 \\ 0 & p \geq 3. \end{cases}$$

Dynamically, the fact that these sequences are eventually equal should come as no surprise. Indeed, for any degree d branched self-cover f of the sphere, there are only finitely many p for which f has a critical p-cycle. For all other p, the Lefschetz fixed point theorem implies that the number of p-cycles depends only on d.

These cycle counts are closely related to the number of hyperbolic components in the corresponding parameter spaces. Indeed, we have the following:

Lemma 7.2.5. *The number of hyperbolic components of period p in the Mandelbrot set is*

$$\mathrm{Hyp}_1(p) = \frac{1}{2} v_1(p).$$

The number of hyperbolic components of period p outside the $\frac{1}{2}$-limb is

$$\mathrm{Hyp}_2(p) = \frac{1}{3} v_2(p).$$

Proof. By Theorem 2.3.27, every period $p \geq 2$ hyperbolic component in the Mandelbrot set is the landing point of two parameter rays of period p under f_1, and conversely every period p parameter ray lands at a period p hyperbolic component of $\mathcal{M}$. It follows that the number of hyperbolic components of period dividing p is

$$\widetilde{\mathrm{Hyp}}_1(p) = \frac{1}{2}(2^p - 1) = \frac{1}{2}\tilde{v}_1(p).$$

To count the number of hyperbolic components outside the $\frac{1}{2}$-limb, we must determine the number N of points of period dividing p under f_1 (i.e., multiples of $\frac{1}{2^p-1}$) which lie outside

84

$\left(\frac{1}{3}, \frac{2}{3}\right)$. We thus have

$$N = \begin{cases} \frac{2}{3}\left(2^p + 1\right) & p \text{ odd} \\ \frac{2}{3}\left(2^p - 1\right) & p \text{ even} \end{cases}$$
$$= \frac{2}{3}\tilde{v}_2(p).$$

It follows that the number of hyperbolic components of period dividing p outside the $\frac{1}{2}$-limb is

$$\widetilde{\mathrm{Hyp}_2}(p) = \frac{N}{2} = \frac{1}{3}\tilde{v}_2(p).$$

Applying the Möbius inversion formula, the result follows. □

Corollary 7.2.6. *The number of* primitive *hyperbolic components of period p in the Mandelbrot set (for $m = 2$, outside the $\frac{1}{2}$-limb) is*

$$\mathrm{Prim}_m(p) = (2\,\mathrm{Hyp}_m - \varphi * \mathrm{Hyp}_m)(p),$$

where φ denotes Euler's totient function.

Proof. We first count the number of satellite components. Since a hyperbolic component of period d has $\varphi(p/d)$ tunings of period p, the number of satellite hyperbolic components of period p is

$$\mathrm{Sat}_1(p) = \sum_{d|p, d\neq p} \varphi\left(\frac{p}{d}\right) \mathrm{Hyp}_1(d) = \varphi * \mathrm{Hyp}_m(p) - p,$$

and the number outside the $\frac{1}{2}$-limb is

$$\mathrm{Sat}_2(p) = \sum_{d|p, d\neq p} \varphi\left(\frac{p}{d}\right) \mathrm{Hyp}_2(d) = \varphi * \mathrm{Hyp}_m(p) - p.$$

Subtracting these from the total count yields the result. □

Lemma 7.2.7. *If a p-cycle $z_0 \to z_1 \to \cdots \to z_p = z_0$ under a map h is invariant under another map σ, where σ commutes with h and satisfies $\sigma^d = \mathrm{id}$, then either σ acts trivially on the cycle, or $\gcd(d, p) > 1$.*

Proof. Since our cycle is invariant under σ, we have $\sigma(z_0) = z_k$ for some $k \in \{0, 1, \ldots, p-1\}$. Thus, $f(z_i) = z_{i+k}$ for all i, where addition is mod p. Since $\sigma^d(z_0) = z_0$, it follows that $kd \equiv 0$

mod p. If we assume d is coprime to p, then necessarily $k \equiv 0 \mod p$. Since $k < p$, we have $k = 0$, so that σ fixes all points in the cycle. $\qquad\square$

Lemma 7.2.8. *The number of $2k$-cycles of $h_1(z) = z^2$ invariant under $z \mapsto z^{-1}$ is*

$$Q_1(2k) = \frac{1}{2k} \sum_{d|k,\ 2 \nmid \frac{k}{d}} \mu\left(\frac{k}{d}\right) 2^d.$$

The number of $3k$-cycles of $h_2(z) = z^{-2}$ invariant under $z \mapsto \omega z$, where ω is a primitive cube root of unity, is

$$Q_2(3k) = \frac{2}{3k} \sum_{d|k,\ 3 \nmid \frac{k}{d}} \mu\left(\frac{k}{d}\right) \tilde{v}_2(d).$$

Remark 7.2.9. The cases of periods 1 and 2 warrant special consideration.

Note that $\sigma_1(z) = z^{-1}$ has two fixed points, namely ± 1. Among these, 1 is fixed by $h_1(z) = z^2$, and -1 is not periodic. In light of Lemma 7.2.7, all cycles of period $p > 1$ invariant under σ_1 are of even order. The fixed point 1 is thus the only σ_1-invariant cycle of h_1.

In spite of this, the face of $\mathrm{Cyc}_1(\mathrm{Per}_1)$ corresponding to this fixed point still maps to Per_1 with local degree 2. This is because the two fixed points of h_1 have the same kneading sequence, so even though they are each invariant under σ_1, they ultimately lie in the same cycle class.

From another perspective, this exception arises because for all other cycles, there is a canonical path in $z \mapsto z^2 + c$ parameter space from $h_1(z) = z^2$ at $c = 0$ to the puncture at $c = \infty$ (where the face ramifies) by following the positive real axis. However, when following this path for period 1, the fixed points collide at $c = \frac{1}{4}$ and our argument breaks down.

For this reason, we make an exception to the definition of Q_1 by setting

$$Q_1(1) = 0.$$

In the case of Per_2, h_2 has three fixed points, namely 1, ω and $\bar{\omega}$, none of which are invariant under $\eta_2(z) = \omega z$. In the coordinates $z \mapsto \frac{z^2 + a}{1 - z^2}$, two of these fixed points collide at the puncture $a = -1$, which, like in Per_1, lies on the canonical path from the basilica "vertex center" $a = 0$ to the cone point $a = \infty$, where the face ramifies. Unlike in the case of Per_1, though, our analysis is unaffected, since the model map $h_2(z) = z^{-2}$ describes f near the

ramification point $c = \infty$, not near the face center $a = 0$.

Also in Per_2, the critical 2-cycle $0 \leftrightarrow \infty$ of $h_2(z) = z^{-2}$ is invariant under $\eta_2(z) = \omega z$. As 0 and ∞ are the only fixed points of η_2, Lemma 7.2.7 implies that this 2-cycle is the unique η_2-invariant cycle of period not divisible by 3.

A philosophical discussion may be had as to the "correct" definition for the curve $\mathrm{Cyc}_2(\mathrm{Per}_2)$. On the one hand, maps in Per_2 already have a marked 2-cycle, so one approach would be to identify $\mathrm{Cyc}_2(\mathrm{Per}_2)$ trivially with itself. On the other hand, the critical 2-cycle does not vary as we move around Per_2, and defining $\mathrm{Cyc}_2(\mathrm{Per}_2)$ as such would be inconsistent with our definition of $\mathrm{Cyc}_1(\mathrm{Per}_1)$, in which we disregarded the fixed point at ∞. Thus, an alternate definition of $\mathrm{Cyc}_2(\mathrm{Per}_2)$ is as the empty set. When such definitional ambiguities arise in pathological cases, it is the author's belief that one should always choose the definition "suggested by the mathematics", i.e. the one whose implications are consistent with simpler and more general formulae. Since the latter definition is more consistent with every result in this thesis, we elect to define $\mathrm{Cyc}_2(\mathrm{Per}_2) \stackrel{\mathrm{def}}{=} \varnothing$.

For the above reasons, we leave $Q_2(1) = 0$ and set $Q_2(2) = 0$, consistent with the pattern that $Q_2(p) = 0$ when p is not a multiple of 3.

The following technical lemma will also be useful in proving Lemma 7.2.8:

Lemma 7.2.10. *Let ℓ be prime, let $\tilde{g}$ be an arbitrary function from $\mathbb{N}^* \to \mathbb{C}$, and suppose that $\tilde{q}$ is a function on $\mathbb{N}^*$ satisfying the recurrence*

$$\tilde{q}(p) = \begin{cases} \tilde{q}(k) + \tilde{g}(k) & \text{if } p = \ell k \text{ is divisible by } \ell, \\ 0 & \text{otherwise.} \end{cases}$$

Then the Möbius transform of $\tilde{q}$ is given by

$$q(p) = \begin{cases} \sum_{d|k,\ \ell \nmid d} \mu\left(\frac{k}{d}\right) \tilde{g}(d) & \text{if } p = \ell k \text{ is divisible by } \ell, \\ 0 & \text{otherwise.} \end{cases}$$

Proof. For brevity, let us write

$$\chi(p) = \begin{cases} 0 & \text{if } p \equiv 0 \mod \ell, \\ 1 & \text{otherwise.} \end{cases}$$

Note that since ℓ is prime, $\mu(\ell d) = -\chi(d)\mu(d)$ for all $d \in \mathbb{Z}$. Define also

$$\alpha(k) = \sum_{d|k} \chi(d)\,\mu(d)\,\tilde{g}(k/d)$$

$$= \sum_{d|k,\ \ell \nmid \frac{k}{d}} \mu\left(\frac{k}{d}\right)\tilde{g}(d),$$

and let

$$g(k) = \sum_{d|k} \mu(d)\tilde{g}(k/d)$$

be the Möbius transform of $\tilde{g}$.

By linearity of the Möbius transform, $q(\ell k) = q(k) + g(k)$ for all k, and $q(p) = 0$ for p coprime to ℓ.

We will argue by induction on $r = \mathrm{ord}_\ell(k)$ that $q(\ell k) = \alpha(k)$ for all k. In the base case $r = 0$, for $k \not\equiv 0 \pmod{\ell}$, we have

$$q(\ell k) = q(k) + \sum_{d|k} \mu\left(\frac{k}{d}\right)\tilde{g}(d)$$

$$= 0 + \sum_{d|k} \chi\left(\frac{k}{d}\right)\mu\left(\frac{k}{d}\right)\tilde{g}(d)$$

$$= \alpha(k),$$

where the second equality follows since all divisors of k are coprime to ℓ.

Suppose now that for some $r \geq 0$, $\alpha(\ell^{r+1}p) = q(\ell^r p)$ for all p coprime to ℓ. For $p \not\equiv 0 \pmod{\ell}$, putting $k = \ell^r p$, we then have

$$\alpha(\ell k) - \alpha(k) = \sum_{d|\ell k} \chi(d)\mu(d)\tilde{g}(\ell k/d) - \sum_{d|k} \chi(d)\mu(d)\tilde{g}(k/d)$$

$$= \sum_{d|\ell k} \chi(d)\mu(d)\tilde{g}(\ell k/d) + \sum_{d|k} \mu(\ell d)\tilde{g}(\ell k/\ell d)$$

$$= \sum_{d|\ell k} \mu(d)\tilde{g}(\ell k/d)$$

$$= g(\ell k).$$

Thus,
$$\alpha(\ell k) = \alpha(k) + g(\ell k) = q(\ell k) + g(\ell k) = q(\ell^2 k),$$

so by induction on r, $q(\ell k) = \alpha(k)$ for all k. $\qquad \square$

Proof of Lemma 7.2.8, Per_1 *case.* A point z_0 is periodic under $h_1(z) = z^2$ of period dividing $p = 2k$ if and only if $z_0 = \exp\left(\tau i \frac{m}{M}\right)$, where $M := 2^{2k} - 1$ and $m \in \mathbb{Z}/M\mathbb{Z}$. The cycle is invariant under $\eta_1(z) = z^{-1}$ if and only if either

(a) $f^k(z_0) = z_0^{-1}$, or

(b) $f^k(z_0) = z_0$ and the k-cycle $z_0 \to \cdots \to z_k = z_0$ is invariant under η_1.

Condition (a) is equivalent to

$$(2^k + 1)m \equiv 0 \mod M.$$

Since $2^k + 1$ divides $M = (2^k - 1)(2^k + 1)$, the above has exactly $2^k + 1$ solutions in $\mathbb{Z}/M\mathbb{Z}$. One of these solutions, however, is the fixed point 0 (corresponding to $1 \in \mathbb{C}$), which we discount as per Remark 7.2.9. Thus, the number of relevant solutions to (a) is 2^k.

Adding in the solutions for (b), we find that the number $\tilde{q}_1(p)$ of points of period dividing p whose cycle is invariant under η_1 is given by the recurrence

$$\tilde{q}_1(p) = \begin{cases} \tilde{q}_1(k) + 2^k & \text{if } p = 2k \text{ is even,} \\ 0 & \text{if } p \text{ is odd.} \end{cases}$$

The number $q_1(p)$ of such points whose period is exactly p is then given by the Möbius transform of $\tilde{q}_1$. By Lemma 7.2.10, this is given by

$$q_1(p) = \begin{cases} \sum_{d|k,\ 2 \nmid d} \mu\left(\frac{k}{d}\right) 2^d & \text{if } p = 2k \text{ is even,} \\ 0 & \text{if } p \text{ is odd.} \end{cases}$$

The number $Q_1(p)$ of invariant cycles is then obtained by dividing the number $q_1(p)$ of p-periodic points by the period p, yielding the desired result. $\qquad \square$

Proof of Lemma 7.2.8, Per_2 *case.* A point $z_0 \in S^1$ is periodic under $h_2(z) = z^{-2}$ of period dividing $p = 3k$ if and only if $z_0 = \exp\left(\tau i \frac{m}{M}\right)$, where $M := 2^{3k} - (-1)^k$ and $m \in \mathbb{Z}/M\mathbb{Z}$. The cycle is invariant under $\eta_2(z) = \omega z$ if and only if one of the following holds:

(a) $f^k(z_0) = \omega z_0$,

(b) $f^k(z_0) = \bar{\omega} z_0$, or

(c) $f^k(z_0) = z_0$ and the k-cycle $z_0 \to \cdots \to z_k = z_0$ is invariant under η_2.

Condition (a) is equivalent to

$$\left((-2)^k - 1\right) m \equiv \frac{M}{3} \quad \mathrm{mod}\ M, \tag{7.1}$$

or equivalently

$$\left(2^k - (-1)^k\right) m \equiv (-1)^k \frac{M}{3} \quad \mathrm{mod}\ M. \tag{7.2}$$

Note that $\tilde{p}_2(k) = 2^k - (-1)^k$ divides

$$\frac{M}{3} = \frac{2^{2k} + (-2)^k + 1}{3} \left(2^k - (-1)^k\right),$$

where the first factor above is an integer as seen by reducing the numerator mod 3. It follows that equation (7.2) has exactly $\tilde{v}_2(k) = 2^k - (-1)^k$ solutions in $\mathbb{Z}/M\mathbb{Z}$.

Analogously, condition (b) produces another $\tilde{v}_2(k)$ solutions.

Adding in the solutions for (c), we find that the number $\tilde{q}_2(p)$ of points on S^1 of period dividing p whose cycle is invariant under η_2 is given by the recurrence

$$\tilde{q}_2(p) = \begin{cases} \tilde{q}_2(k) + 2\tilde{v}_2(k) & \text{if } p = 3k \text{ is divisible by 3,} \\ 0 & \text{otherwise.} \end{cases}$$

The number $q_2(p)$ of such points whose period is exactly p is then given by the Möbius transform of $\tilde{q}_2$. By Lemma 7.2.10, this is given by

$$q_2(p) = \begin{cases} 2\sum_{d|k,\ 2\nmid d} \mu\left(\frac{k}{d}\right) \tilde{v}_2(d) & \text{if } p = 3k \text{ is divisible by 3,} \\ 0 & \text{otherwise.} \end{cases}$$

The number $Q_2(p)$ of invariant cycles is then obtained by dividing the number $q_2(p)$ of p-periodic points by the period p, yielding the desired result. $\qquad\square$

Theorem 7.2.11. *The combinatorics of the marked cycle curve of period p over Per_m are as follows for $m = 1, 2$:*

- *The number of vertices is $c_m(p)$.*

- *The number of edges is $\mathrm{Prim}_m(p)$, except in the case $m = 2$, $p = 1$, where an extra edge exists due to monodromy around the puncture.*

- *The number of faces is $\frac{1}{m+1}\left(c_m(p) + mQ_m(p)\right)$.*

Thus, the genus is given by

$$g_1(p) = 1 + \frac{1}{4}\left(2\,\mathrm{Prim}_1 - 3\,c_1 - Q_1\right)(p)$$

$$g_2(p) = 1 + \frac{1}{6}\left(3\,\mathrm{Prim}_2 - 4\,c_2 - 2Q_2\right)(p).$$

Proof. The edge and vertex counts follow directly from the algorithm.

To count the faces, recall that faces of $\mathrm{Cyc}_p(\mathrm{Per}_m)$ are in natural bijection with orbits $\tau^*(\zeta)$ under τ_{m+1} of p-cycles ζ of f_m, where τ_{m+1} is element-wise incrementation mod $m + 1$.

A given cycle ζ has an orbit of size $m + 1$ if it is not fixed by τ_{m+1}, and 1 otherwise. It follows that the total number of faces in $\mathrm{Cyc}_p(\mathrm{Per}_m)$ is

$$\frac{1}{m+1}\left(c_m(p) - Q_m(p)\right) + Q(p) = \frac{1}{m+1}\left(c_m(p) + mQ_m(p)\right)$$

as desired. $\qquad\square$

Corollary 7.2.12. *In particular, if p is an odd prime, then the genus of $\mathrm{Cyc}_p(\mathrm{Per}_m)$ for $m = 1, 2$ is given by*

$$g_1(p) = \frac{1}{2p}\left(2^{p-1}(p - 3) - p^2 + 2p + 3\right),$$

$$g_2(p) = \frac{1}{6p}\left(2^p(p - 4) - 3p^2 + 7p + 8\right).$$

The face count for marked cycle curves over Per_1 has a number of different dynamical interpretations. We summarize them in the following statement,

Proposition 7.2.13 (Compare [Buf+23])**.** *The following values are equal:*

(1) *the number of ABC classes of period p,*

(2) *the number of faces in $\mathrm{Cyc}_p(\mathrm{Per}_1)$,*

(3) $\frac{1}{2}\left(c_1(p) + Q_1(p)\right),$

(4) the number of hyperbolic components of period p on the real axis, and

(5) the number of factors of the Gleason polynomial

$$G_p(c) = \prod_{d|p} \left(f_c^d(0)\right)^{\mu(p/d)}$$

when factored over $\mathbb{F}_2$.

Proof. Lemma 4.5.5 shows that (1) and (2) are equal. Theorem 7.2.11 shows that (2) and (3) are equal. Corollary 4.1.9 shows that (1) and (4) are equal. Finally, it is a theorem of Xavier Buff, William Floyd, Sarah Koch, and Walter Parry [Buf+23] that (4) and (5) are equal. □

While there are no real hyperbolic components in Per$_2$, the above statement suggests there may be a relationship between the number of faces in $\mathrm{Cyc}_p(\mathrm{Per}_2)$ and the number of factors of the "Per$_2$ Gleason polynomial"

$$G_p^{(2)}(a) = \prod_{d|p} \left(\nu\left(h_a^d(0)\right)\right)^{\mu(p/d)} \qquad \text{(where } \nu \text{ denotes the numerator in reduced form)}$$

when factored over $\mathbb{F}_2$. Numerical experiments up through period 18 suggest that such a relationship indeed holds.

Conjecture 7.2.14. *For all $p \geq 2$, the number $N_2(p)$ of factors of $G_p^{(2)}(a)$ over $\mathbb{F}_2$ is related to the number $F_2(p) = \frac{1}{3}(c_2 + 2Q_2)(p)$ of faces of $\mathrm{Cyc}_p(\mathrm{Per}_2)$ by the following formula:*

$$N_2(p) = \begin{cases} \frac{1}{2}F_2(p) & \text{if } p \text{ is odd,} \\ F_2(p) & \text{if } p \equiv 0 \pmod 4, \\ F_2(p) - Q_1(p) & \text{if } p \equiv 2 \pmod 4. \end{cases}$$

92

The following tables summarize the counts derived above:

Table 7.1: Cell counts for marked cycle curves over Per_1.

period	vertices (c_1)	edges (Prim_1)	refl. faces (Q_1)	faces ($\frac{c_1+Q_1}{2}$)	genus (g_1)
1	2	1	0	1	0
2	1	0	1	1	0
3	2	1	0	1	0
4	3	3	1	2	0
5	6	11	0	3	2
6	9	20	1	5	4
7	18	57	0	9	16
8	30	108	2	16	32
9	56	240	0	28	79
10	99	472	3	51	162
11	186	1013	0	93	368
12	335	1959	5	170	728
13	630	4083	0	315	1570
14	1161	8052	9	585	3154
15	2182	16315	0	1091	6522

Table 7.2: Cell counts for marked cycle curves over Per_2. An extra edge has been added in period 1 due to the puncture monodromy.

period	vertices (c_2)	edges (Prim_2)	refl. faces (Q_2)	faces ($\frac{c_2+2Q_2}{3}$)	genus (g_2)
1	3	$1+1=2$	0	1	0
2	0	0	0	0	0
3	2	0	2	2	-1
4	3	2	0	1	0
5	6	6	0	2	0
6	9	14	0	3	2
7	18	36	0	6	7
8	30	72	0	10	17
9	56	158	2	20	42
10	99	316	0	33	93
11	186	672	0	62	213
12	335	1306	2	113	430
13	630	2718	0	210	940
14	1161	5370	0	387	1912
15	2182	10874	4	730	3982

7.3 Cell counts for Dynatomic Curves

Theorem 7.3.1. *The combinatorics of the dynatomic curve of period $p \geq 2$ over Per_m are as follows for $m = 1, 2$:*

- *The number of vertices is $v_m(p)$.*

- *The number of edges is $p\,\mathrm{Hyp}_m(p)$.*

- *The number of primitive faces is $\frac{1}{m+1}v_m(p)$.*

- *The number of satellite faces is*

$$S(p) = \sum_{d|p} d\,\mathrm{Hyp}_m(d)\varphi\left(\frac{p}{d}\right) - p\,\mathrm{Hyp}_m(p).$$

Thus, the genus is given by

$$G_m(p) = 1 + \frac{1}{2}\left(p\,\mathrm{Hyp}_m(p) - \frac{m+2}{m+1}v_m(p) - S(p)\right)$$

$$= 1 + p\,\mathrm{Hyp}_m(p) - \frac{1}{2}\left(\frac{m+2}{m+1}v_m(p) - \sum_{d|p} d\,\mathrm{Hyp}_m(d)\varphi\left(\frac{p}{d}\right)\right)$$

Proof. The edge and vertex counts follow directly from the algorithm.

To count the primitive faces, recall that over Per_1, monodromy about infinity acts on the set of p-periodic angles by bit-flip. Since the bit-flip map $\eta_1 : \Sigma_p \to \Sigma_p$ is an involution without fixed points, it follows that the number of η_1-orbits is half the number $v_1(p)$ of p-periodic angles.

Similarly, over Per_2, monodromy about infinity acts on the set of p-periodic angles by $\eta_2(\theta) = \theta + \frac{1}{3}$, which has order 3 with no fixed points. Thus, the number of η_2-orbits is one third of the number $v_2(p)$ of p-periodic angles.

To count the satellite faces, we note that the number of faces arising from a given satellite hyperbolic component U is equal to the period of the component on which U is tuned. Thus, the satellite face count is derived just as in Corollary 7.2.6, except with an additional factor of d to account for the tuning period. $\square$

Corollary 7.3.2. *In particular, if p is an odd prime, then the genus of $\mathrm{Dyn}_p(\mathrm{Per}_m)$ for*

$m = 1, 2$ *is given by*

$$G_1(p) = (2^{p-2} - 1)(p - 3),$$

$$G_2(p) = \frac{1}{6} \left(2^p(p - 4) - 5p + 17\right).$$

Of interest also is the distribution of *face sizes*, i.e. the number of edges buonding each face, counted with multiplicity. The following conjectures descring the maximal face size of $\mathrm{Cyc}_p(\mathrm{Per}_m)$ $(m = 1, 2)$ have been verified for $p \leq 26$.[1]

Conjecture 7.3.3. *For $p \geq 5$, the largest face of $\mathrm{Cyc}_p(\mathrm{Per}_1)$ has $\Phi(p) + 2$ edges, where*

$$\Phi(p) = \sum_{0 \leq k < p} \varphi(k),$$

and where φ denotes Euler's totient function. This face is unique unless $p = 7$.

Conjecture 7.3.4. *For $p \geq 9$ odd (and for $p = 5$), the largest face of $\mathrm{Cyc}_p(\mathrm{Per}_2)$ has edge count $\Phi(p)$. For $p \geq 6$ even, the largest face of $\mathrm{Cyc}_p(\mathrm{Per}_2)$ has edge count*

$$\Phi(p) + 1 - \frac{1}{2}\varphi\left(\frac{p}{2}\right).$$

In all cases except for $p = 8$ and $p = 10$, there is a unique largest face of $\mathrm{Cyc}_p(\mathrm{Per}_2)$ up to complex conjugation.

Heuristically, since *irreflexive* (i.e., not reflexive) faces of $\mathrm{Cyc}_p(\mathrm{Per}_m)$ map to Per_m with degree $m + 1$ $(m = 1, 2)$, we expect a generic reflexive face of $\mathrm{Cyc}_p(\mathrm{Per}_m)$ to be smaller than a generic irreflexive face by a factor of $1/(m + 1)$. Thus, when considering the smallest face in $\mathrm{Cyc}_p(\mathrm{Per}_m)$, it makes sense to exclude the reflexive faces, which only exist when $(m + 1) \mid p$.

Experimentally, the size of the smallest irreflexive face of $\mathrm{Cyc}_p(\mathrm{Per}_m)$ appears to grow asymptotically linearly with p, with the same growth rate for $m = 1, 2$. However, the growth is not monotone, and the data currently available is too small to conjecture a linear asymptotic growth rate with any degree of confidence. We propose instead the following:

Conjecture 7.3.5. *For $m = 1, 2$, the size $\kappa_m(p)$ of the smallest face in $\mathrm{Cyc}_p(\mathrm{Per}_m)$ tends to infinity as $p \to \infty$. Moreover, if $\kappa_m^+(p) \geq \kappa_m(p)$ denotes the size of the smallest* irreflexive

---

[1] Since Algorithm 4.6.1 uses $O(2^p)$ space, it quickly becomes infeasible as a means to determine the distribution of face sizes for larger values of p.

face, then the limit

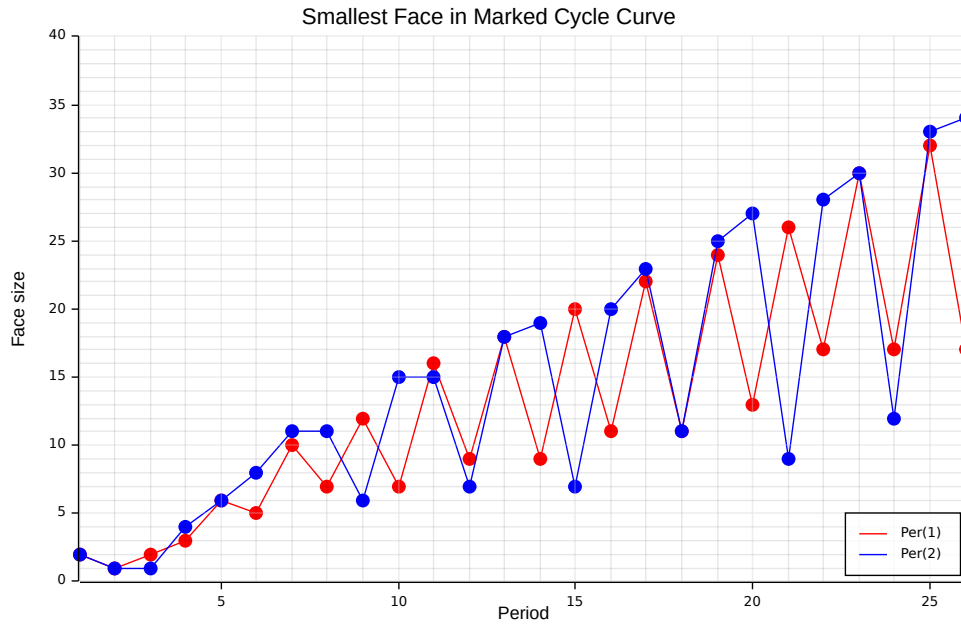$$\lim_{p \to \infty} \frac{\kappa_1^+(p)}{\kappa_2^+(p)}$$

exists and is equal to 1.

Figure 7.1: Number $\kappa_m(p)$ of (not necesssarily distinct) edges bounding the smallest face in $\mathrm{Cyc}_p(\mathrm{Per}_m)$, $m = 1, 2$.
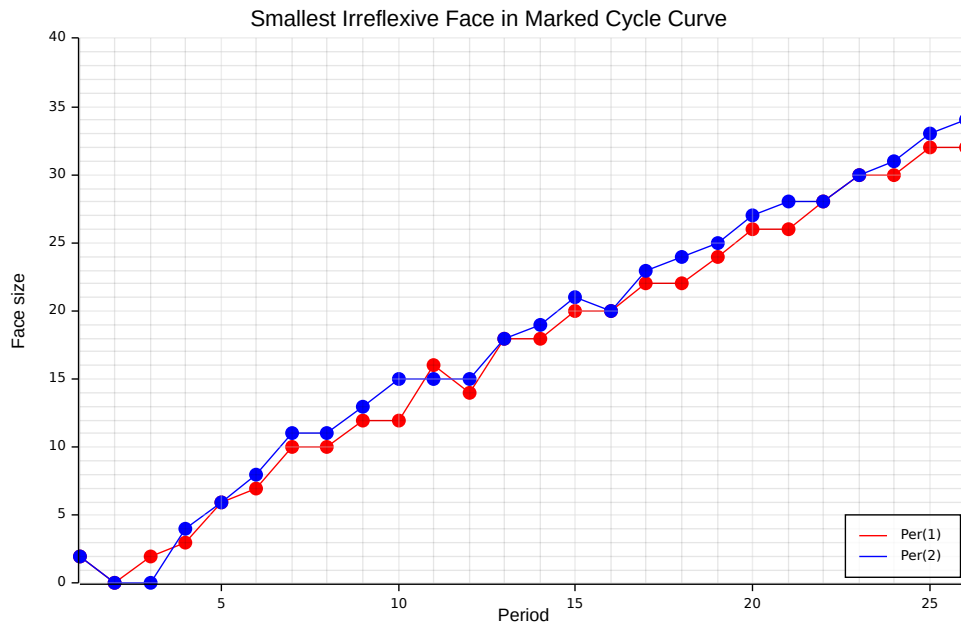
Figure 7.2: Number $\kappa_m^+(p)$ of (not necesssarily distinct) edges bounding the smallest irreflexive face in $\mathrm{Cyc}_p(\mathrm{Per}_m)$, $m = 1, 2$.

CHAPTER 8

Further Dynamical Varieties

8.1 Marked cycle curves over Per_3

The family Per_3 of quadratic rational maps with a superattracting 3-cycle has been studied extensively, but many fundamental questions remain open. Unlike in the case of Per_2, every element of whom is a mating of a quadratic polynomial with $f_B(z) = z^2 - 1$, the situation in Per_3 is much more complicated.

Up to affine conjugacy, there are three quadratic polynomials with a superattracting 3-cycle:

- The *rabbit* polynomial, $f_R(z) = z^2 + c_R$, where c_R is the root of the Gleason polynomial $G_3(c) = \frac{1}{c} f_c^3(0) = c^3 + 2c^2 + c + 1$ near $c = -0.12256 + 0.74486i$,

- the *corabbit* polynomial, $f_{\bar{R}}(z) = z^2 + \bar{c}_R$, and

- the *airplane* polynomial, $f_A(z) = z^2 + c_A$, where $c_A \approx -1.75488$ is the unique real root of G_3.

One might therefore hope to partition of Per_3 into a disjoint union of three components, corresponding to the subsets of Per_3 that arise from matings of arbitrary admissible quadratic polynomials with the maps f_R, $f_{\bar{R}}$, and f_A respectively. Unfortunately, two major complicating factors render this task impossible:

1. There exist *shared matings* in Per_3, i.e. maps which can be decomposed as matings of quadratic polynomials in two or more distinct ways. For instance, the mating $f_A \sqcup f_K$ of the airplane with the *kokopelli* polynomial (the unique quadratic polynomial $f_K(z) = z^2 + c_K$ at the center of a primitive 4-periodic hyperbolic component in the upper half plane).

   It is conjectured that there are always only finitely many ways to decompose a quadratic rational map g as a mating of polynomials. While this is trivial in the case that g is

hyperbolic, it is not known for general g (even if we restrict to the case of Misiurewicz maps).

2. Some hyperbolic maps in Per_3 do not arise as matings. For instance, using the coordinates

$$f_c(z) = \frac{z^2 + c^3 - c - 1}{z^2 - c^2},$$

which has critical 3-cycle $\infty \mapsto 1 \mapsto -c$ and free critical point 0, there are 13 values of c for which 0 is periodic of period 4, corresponding to the roots of

$$\nu(f_c^4(0))/\nu(f_c^2(0)),$$

where ν denotes the numerator of a rational expression. The map f_c corresponding to the unique real solution $c_* \approx 0.623061$ corresponds to a map f_c which is not a mating of quadratic polynomials.
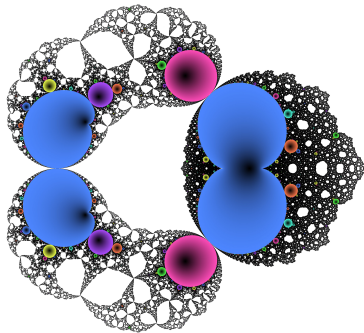
(a) The moduli space Per_3 of quadratic rational maps with a superattracting 3-cycle.
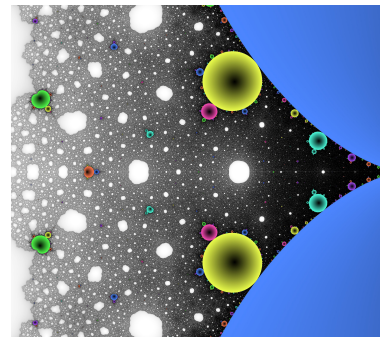
(b) Detail of Hubbard's "zone of ignorance", in which not all postcritically finite maps arise from matings. The map f_{c_*} described above appears at the center of the orange hyperbolic component on the left.
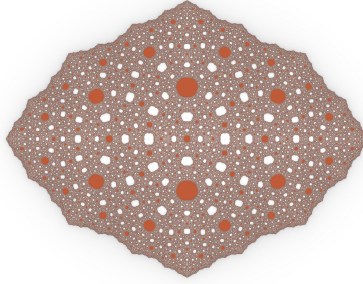
Figure 8.2: Julia set for the non-mating f_{c_*}. Both critical orbits lie on the real axis, with itineraries 110* and 10* with respect to the imaginary axis. The white Fatou components converge toward the superattracting 3-cycle, while the orange Fatou components converge toward the superattracting 4-cycle.

Much is not known about non-matings and the structure of parameter space around them. Marked cycle curves over Per_3 may therefore provide a lens through which study the structure and distribution of non-mating components. Unfortunately, since the algorithms developed in this thesis rely on the assumption that all postcritically finite maps come from matings, they are inapplicable to Per_3. The marked cycle curves do still exist, though, and they may be computed.

The moduli space $\mathrm{Cyc}_4(\mathrm{Per}_3)$ is the simplest dynamical variety that ramifies over a non-mating component in Per_3. It is a genus 1 curve with 5 punctures, coming from the lifts of the two punctures $c = \pm 1$ in Per_3. The branched cover

$$\pi : \mathrm{Cyc}_4(\mathrm{Per}_3) \longrightarrow \mathrm{Per}_3$$

has 6 branch points: five coming from the five primitive period 4 components in Per_3 (including the non-mating component), and one coinciding with one of the lifts of the puncture $c = 1$.

The ramification over this puncture is a phenomenon new to Per_3: by Proposition 5.3.6 $\mathrm{Cyc}_p(\mathrm{Per}_2)$ does not ramify over the puncture in Per_2 for any $p > 1$.

Question 8.1.1. Does $\mathrm{Cyc}_p(\mathrm{Per}_3)$ ramify over a puncture for all p other than 2 and 3?

Question 8.1.2. Can we develop an algorithm for the cell structure, or just a formula for the genus, of $\mathrm{Cyc}_p(\mathrm{Per}_3)$? Can this then be used to understand the distribution of non-mating components?
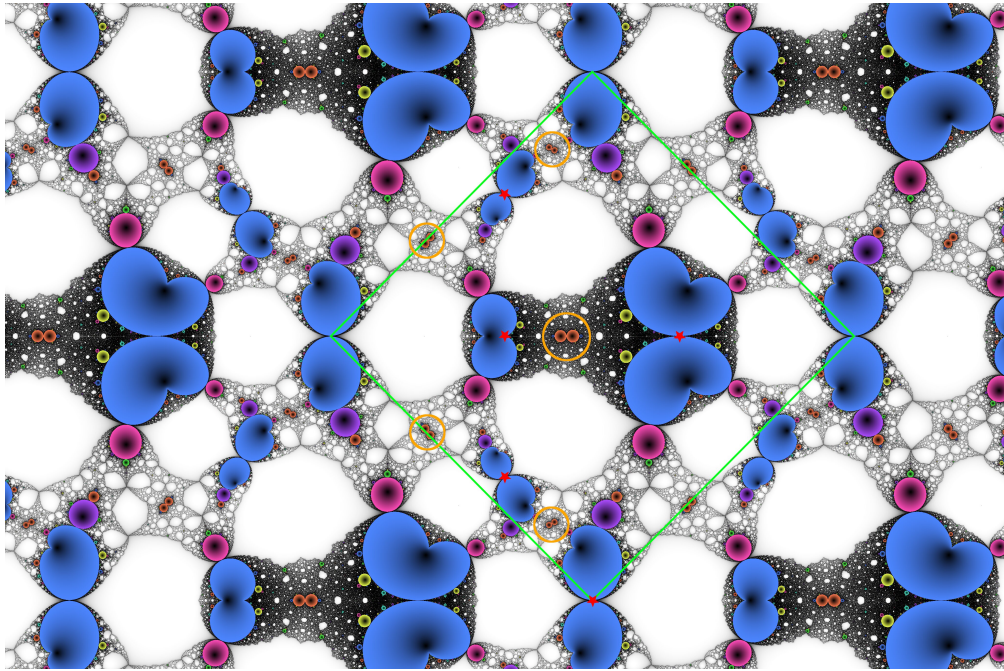
Figure 8.3: Universal cover of $\mathrm{Cyc}_4(\mathrm{Per}_3)$. The green rhombus denotes a fundamental domain (it is *almost* a square — the j-invariant is $2^{15}/19 \approx 1724.6$, as shown in Appendix B.2. The red stars denote the lifts of the two punctures in Per_3. Circled in orange are the five branch points coming from the four period 4 primitive mating components, together with the one non-mating component. The rightmost puncture is also a branch point, for a total of 6 branch points.

8.2 Misiurewicz curves

As discussed in Chapter 3, a third type of dynamical variety may be obtained by marking a preperiodic point instead of a periodic point or cycle.

Definition 8.2.1. For an algebraic dynamical family $\mathcal{F}$ on a Riemann surface S, the *Misiurewicz variety* $\text{Mis}_{k,p}(\mathcal{F})$ of preperiod k and period p is the Zariski closure of the quasi-projective variety

$$V_{k,p}(\mathcal{F}) = \{(f, z) : f \in \mathcal{F} \text{ and } z \in S \text{ has exact preperiod } k \text{ and period } p \text{ under } f\}.$$

If $\mathcal{F}$ consists of rational maps on $\hat{\mathbb{C}}$, then $\text{Mis}_p(\mathcal{F})$ is the vanishing locus in $\mathcal{F}$ of the *predynatomic polynomial*[1], defined recursively by $\varphi_{-1,p}(f, z) = 1$, and by

$$\varphi_{k,p}(f, z) = \frac{1}{\varphi_{k-1,p}(f, z)} \prod_{d|p} \left[\nu\left(f^{d+k}(z) - f^k(z)\right)\right]^{\mu(d/p)}$$

for $k \in \mathbb{N}$, where μ is the Möbius function and where ν denotes the numerator of a rational expression in reduced form.

Gao Yan in [Gao16] shows that Misiurewicz curves over the quadratic family $\mathcal{P}_2$ are smooth and irreducible and provides a formula for their genus.

Question 8.2.2. Can we describe a cell structure for Misiurewicz curves over Per_1 and Per_2 similar to the cell structures for marked cycle curves and dynatomic curves?

8.3 Dynamical covers over other base curves

The definitions of $\text{Cyc}_p, \text{Dyn}_p$, and Mis_p are extremely general and can be applied to any discrete-time dynamical system. This suggests a research program toward investigating the structure of these dynamical varieties over various bases.

We show here a collection of figures of dynamical varieties over various bases. It would be interesting to know of a dynamical cell structure for such varieties analogous to those developed in Chapters 4 to 6.

---

[1]The term *Misiurewicz polynomial* is already in use and refers to a slightly different object, namely a "one-variable" regular function $G_{k,p,\mathcal{F}} : \mathcal{F} \to \mathbb{C}$ that vanishes at all parameters where $\mathcal{F}$ has a critical point of exact preperiod k and period p. The vanishing locus of $G_{k,p,\mathcal{F}}$ is a subset of the ramification locus of $\text{Mis}_p(\mathcal{F})$; the latter also branches over certain parabolic parameters and, in particular cases depending on p and $\mathcal{F}$, certain critically periodic parameters. A detailed analysis of this phenomenon may be found in section 5 of [Gao16].
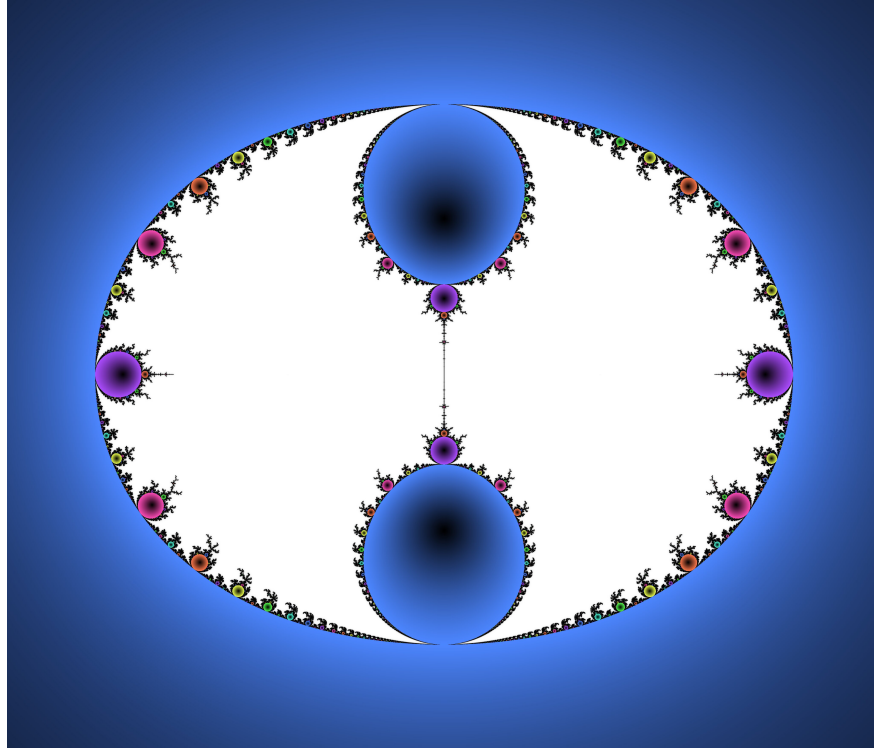
Figure 8.4: $\mathrm{Mis}_{2,1}(\mathrm{Per}_1)$: Quadratic polynomials with a marked point of preperiod 2 and period 1. The branch point at infinity is "spurious", ramifying over the pcf hyperbolic map $f_0(z) = z^2$.
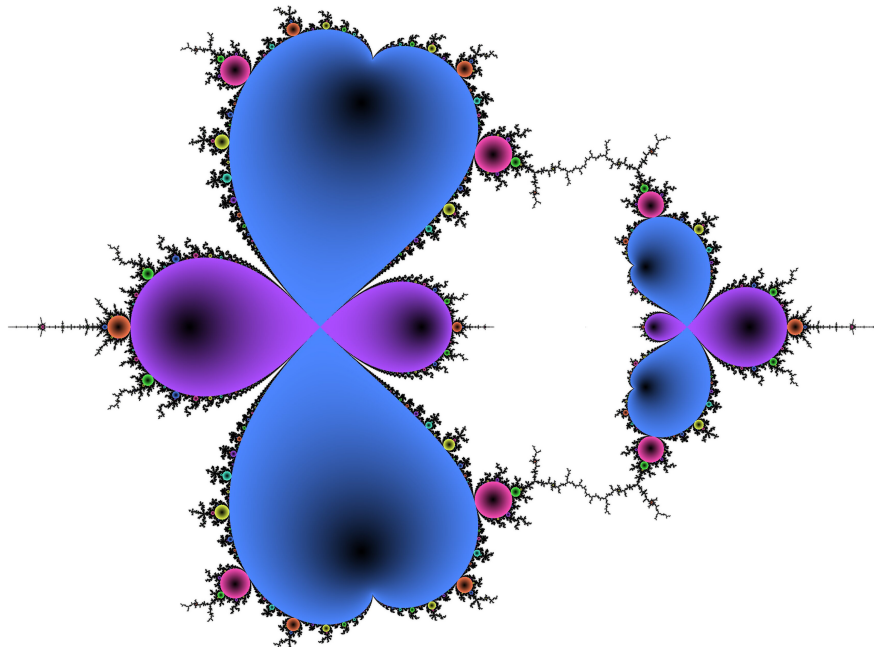

Figure 8.5: $\mathrm{Mis}_{2,2}(\mathrm{Per}_1)$: Quadratic polynomials with a marked point of preperiod 2 and period 2.
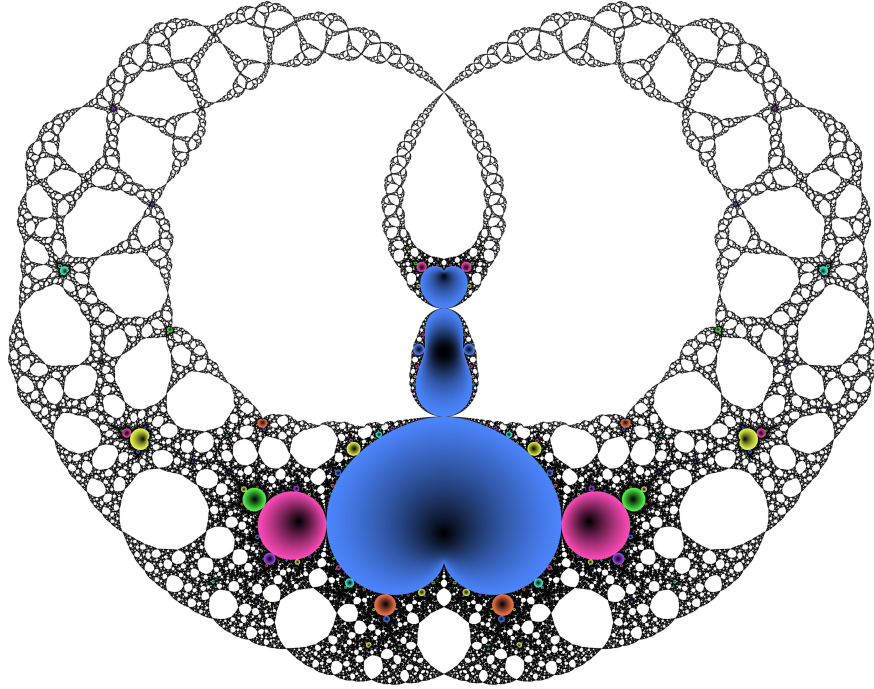
Figure 8.6: $\mathrm{Mis}_{2,1}(\mathrm{Per}_2)$: Quadratic rational maps with a 2-periodic critical point and a marked point of preperiod 2 and period 1.
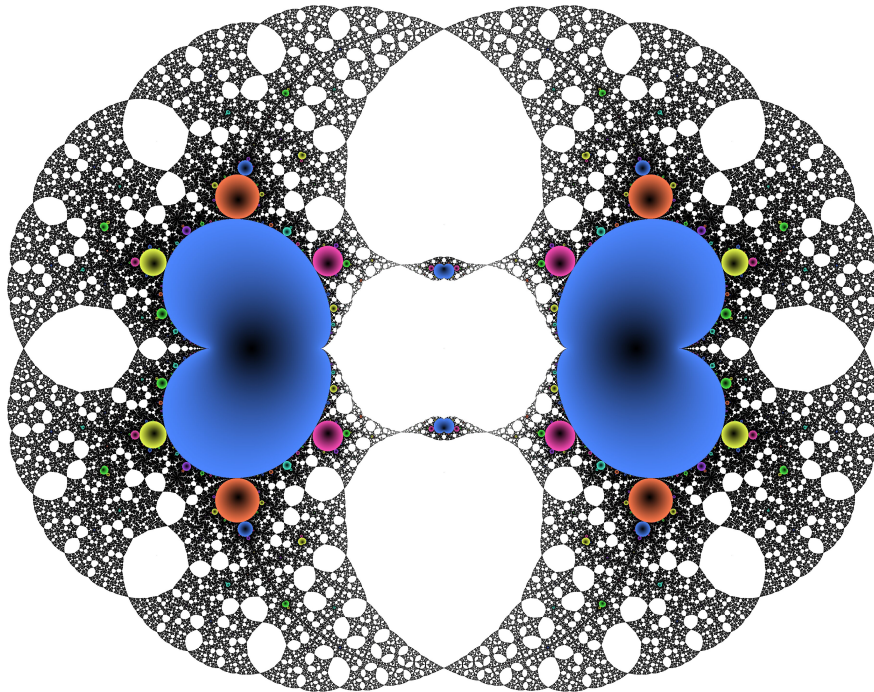
Figure 8.7: $\mathrm{Mis}_{2,2}(\mathrm{Per}_2)$: Quadratic rational maps with a 2-periodic critical point and a marked point of preperiod 2 and period 2.

8.3.1 Per_4

The natural next step after studying $\mathrm{Cyc}_p(\mathrm{Per}_3)$ woudl be to try to understand $\mathrm{Cyc}_p(\mathrm{Per}_m)$ for all n. Unfortunately, the case $p = 3$, $m = 4$ is the only other nontrivial case for which the resulting curve has genus ≤ 1.
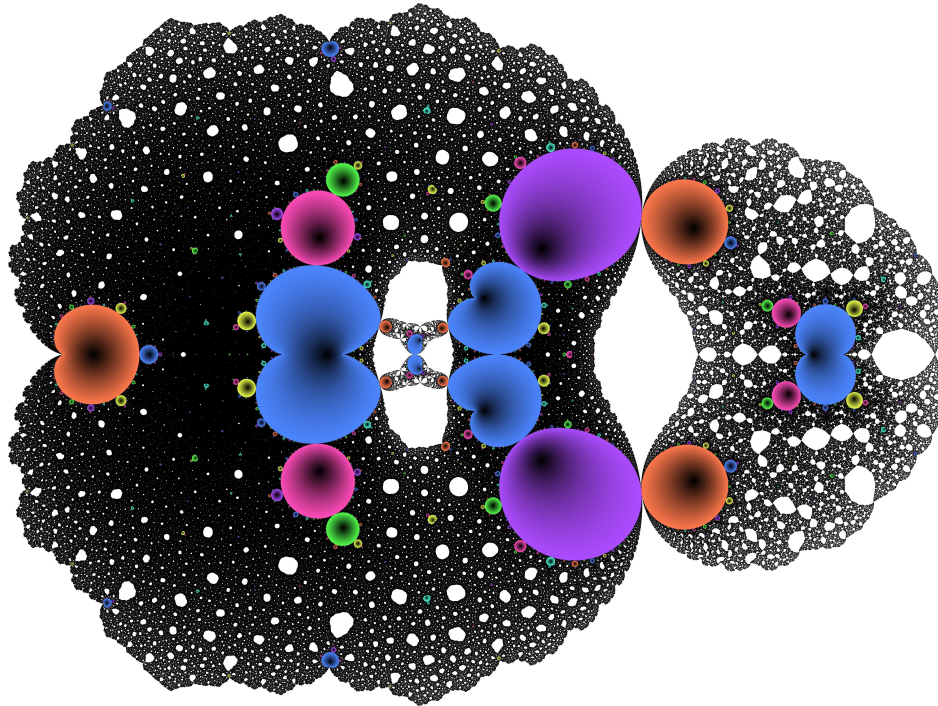
Figure 8.8: The dynamical family Per_4 of quadratic rational maps with a critical point of period 4.
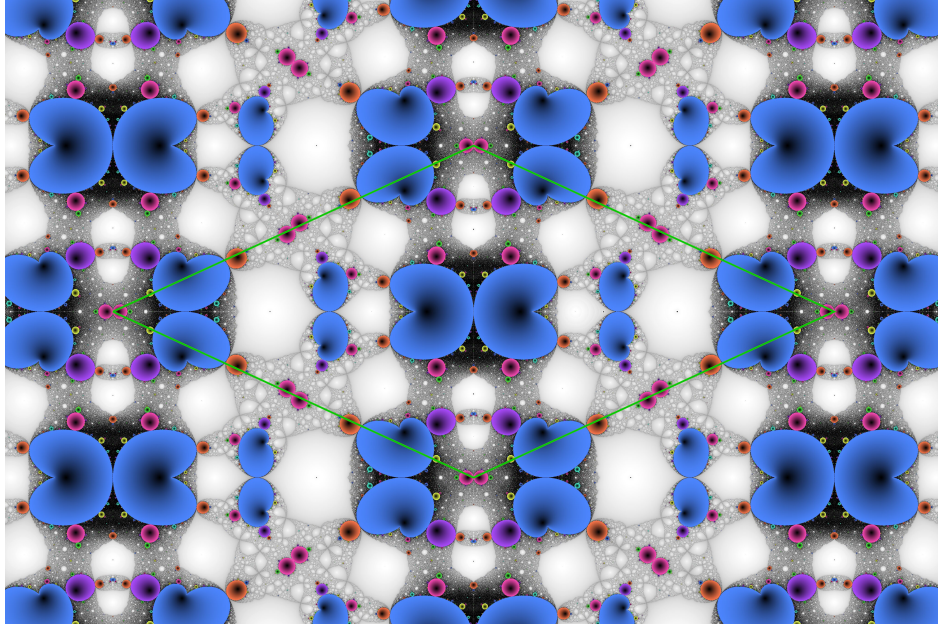
Figure 8.9: $\mathrm{Cyc}_3(\mathrm{Per}_4)$: Quadratic rational maps with a critical point of period 4 with a marked 3-cycle. A fundamental domain is shown in green. All branch points lie on the boundary of this fundamental domain.

8.3.2 PrePer$_{2,1}$

The Milnor curves Per_n can be generalized by instead applying pre-periodic critical orbit relations. The simplest nontrivial case is the family $\mathrm{PrePer}_{2,1}$ of quadratic rational maps with a critical point of preperiod 2, period 1.
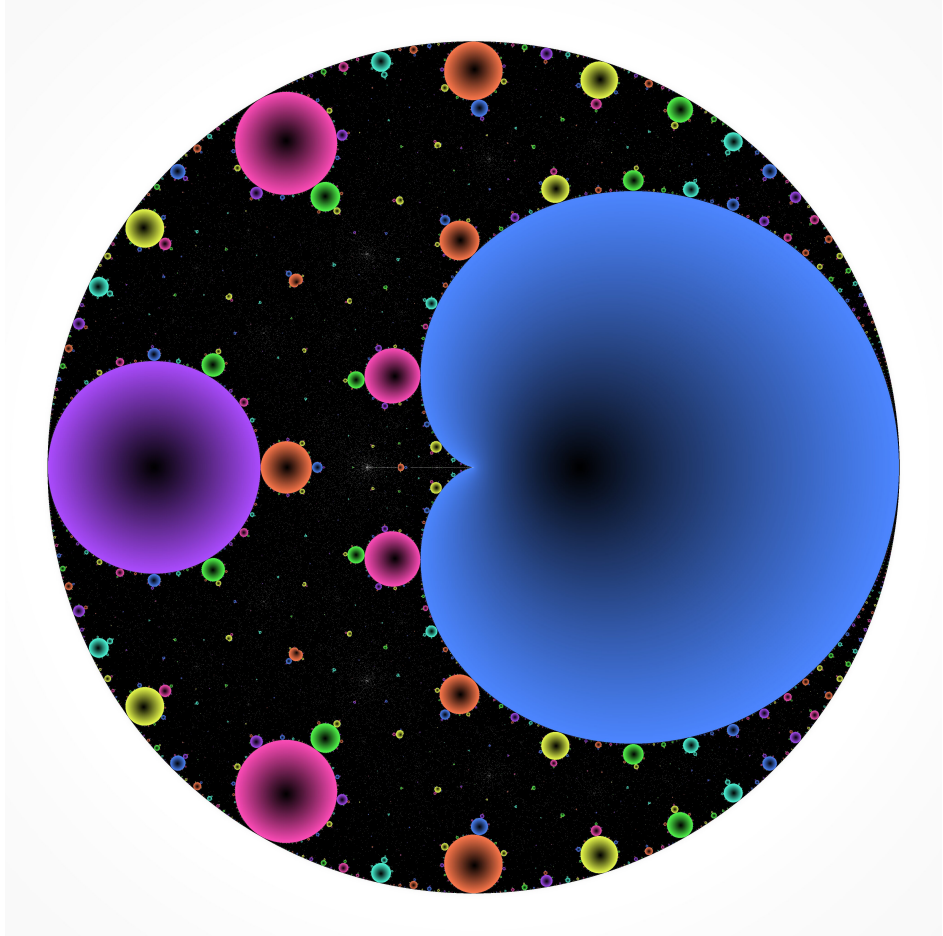
Figure 8.10: The dynamical moduli space PrePer$_{2,1}$.
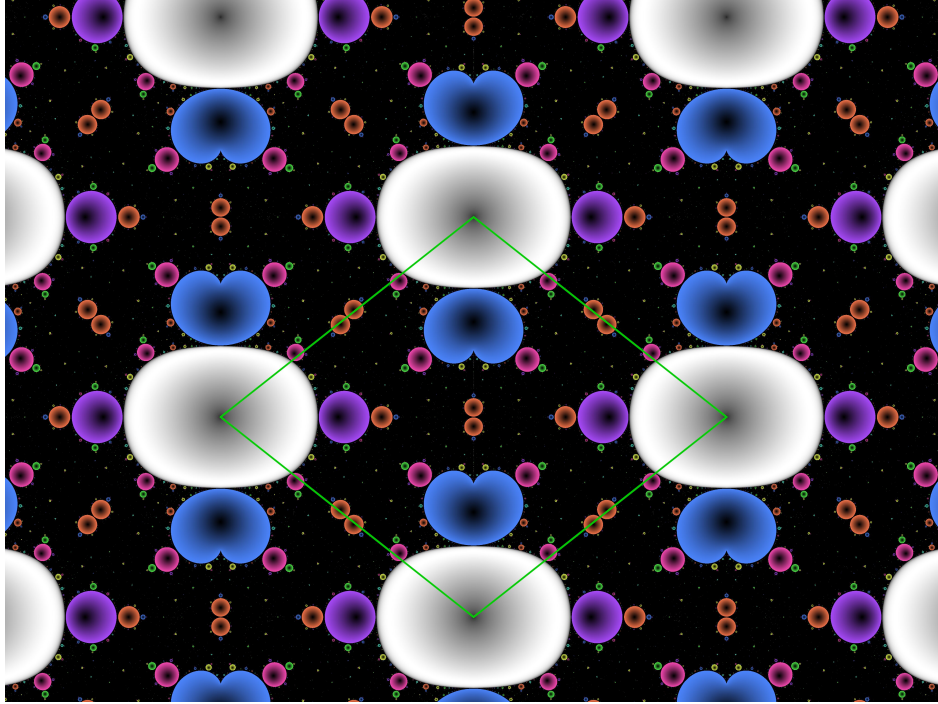
Figure 8.11: $\mathrm{Cyc}_4(\mathrm{PrePer}_{2,1})$: Maps in $\mathrm{PrePer}_{2,1}$ with a marked 4-cycle. A fundamental domain is shown in green. The j-invariant is $j = 2^{13}/11$.

8.3.3   Cubic polynomials

The dynamical moduli space $\mathcal{P}_3$ of cubic polynomials has complex dimension 2, and thus is difficult to visualize. However, we can draw dynamical varieties over various dynamically meaningful sllices of $\mathcal{P}_3$.

8.3.3.1   Unicritical Cubics

The family $\mathcal{U}_3$ of cubic polynomials with a unique (finite) critical point is the clearest generalization of the quadratic family to a one-parameter family of cubics.
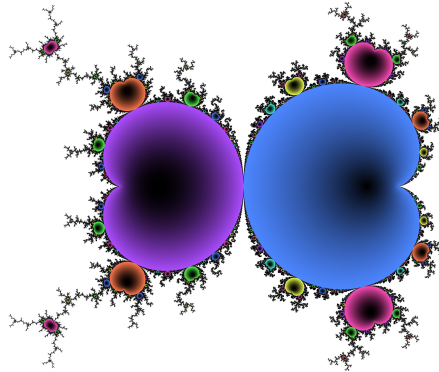
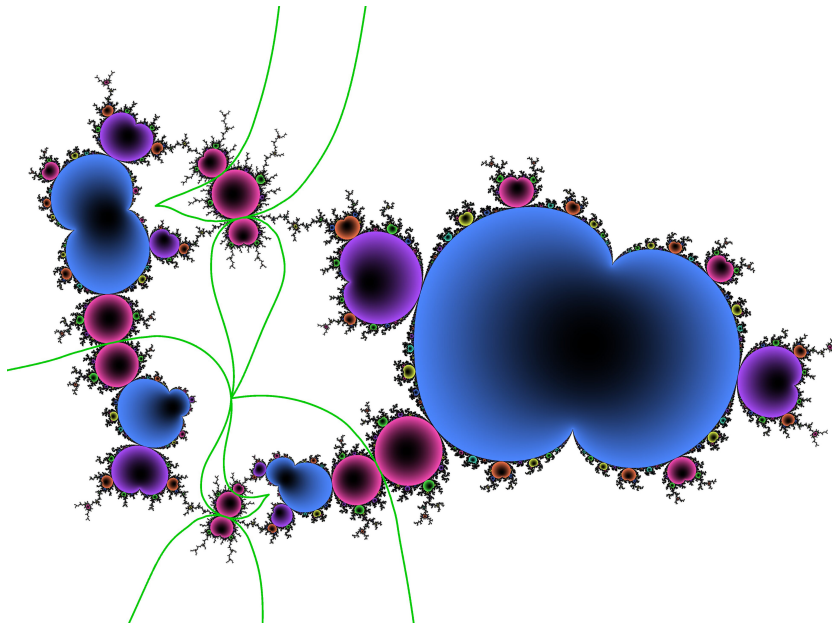Figure 8.12: The family $\mathcal{U}_3$ of unicritical cubic polynomials.

Figure 8.13: $\mathrm{Cyc}_3(\mathcal{U}_3)$: Unicritical cubic polynomials with a marked 3-cycle. The relevant external rays are shown in green. Two escape regions have local degree 3, while the other two have local degree 1.

8.3.3.2 Cubic Per_1

The family $\mathrm{Per}_1(\mathcal{P}_3)$ of cubic polynomials with a critical fixed point provides another dynamically natural base curve.[2]

---

[2]The parameterization of $\mathrm{Per}_1(\mathcal{P}_3)$ used here is actually a 2-fold branched cover of moduli space. In the coordinates $f_c(z) = z^2(z + c)$ used here, the maps f_c and f_{-c} are affine conjugate via $z \mapsto -z$.
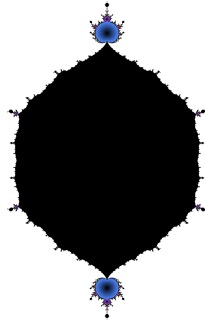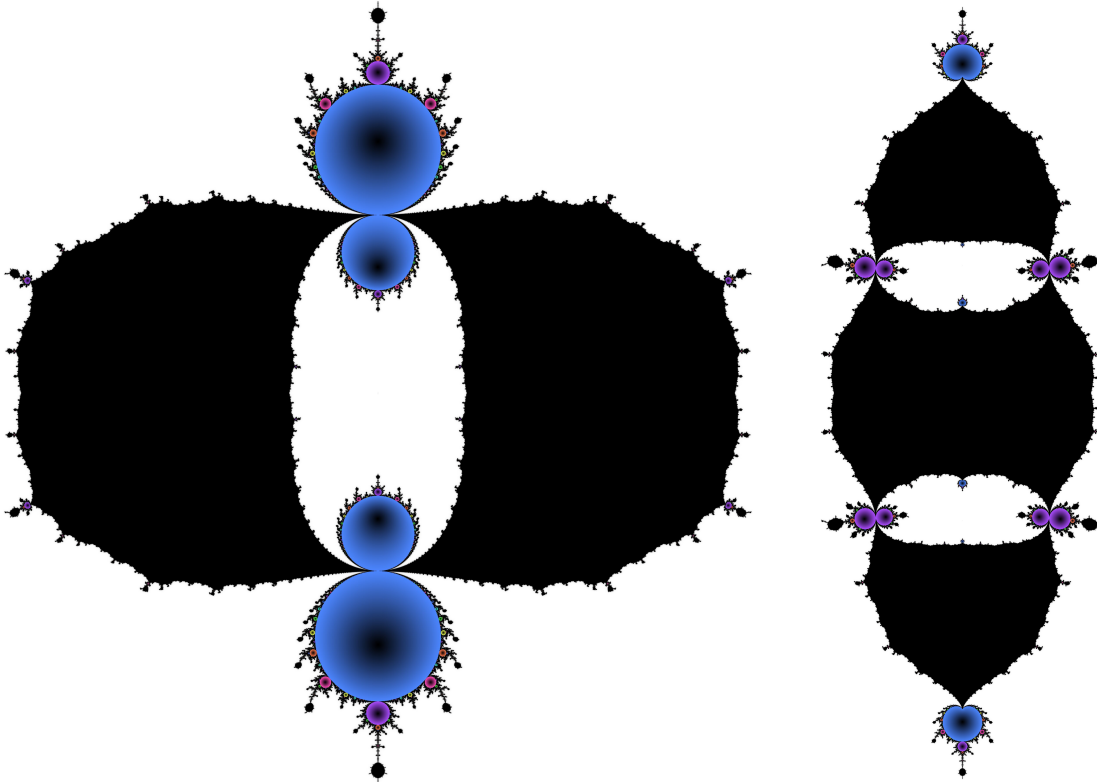
Figure 8.14: The family $\mathrm{Per}_1(\mathcal{P}_3)$ of cubic polynomials with a fixed critical point.

(a) $\mathrm{Cyc}_1(\mathrm{Per}_1(\mathcal{P}_3))$: Maps in $\mathrm{Per}_1(\mathcal{P}_3)$ with a marked (non-critical) fixed point.

(b) $\mathrm{Cyc}_2(\mathrm{Per}_1(\mathcal{P}_3))$: Maps in $\mathrm{Per}_1(\mathcal{P}_3)$ with a marked 2-cycle.

8.3.3.3 Cubic $\mathrm{Per}_1(1)$

A related family is the locus $\mathrm{Per}_1(\mathcal{P}_3, 1)$ of cubic polynomials with a fixed point of multiplier 1. As above, we work in a 2-fold branched cover of moduli space, with coordinates
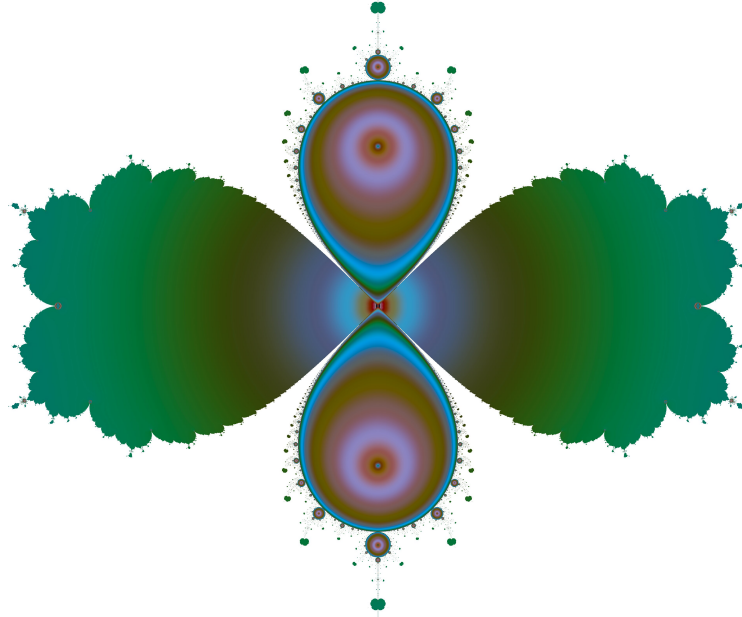
$$f_c(z) = z(z^2 + cz + 1).$$

Figure 8.16: The family $\mathrm{Per}_1(\mathcal{P}_3, 1)$ of cubic polynomials with a fixed point of multiplier 1. To better distinguish components, points outside the excaping locus are colored according to the internal potential of the critical point (the Kœnigs coordinate for hyperbolic components, and the Leau-Fatou coordinate for parabolic components).
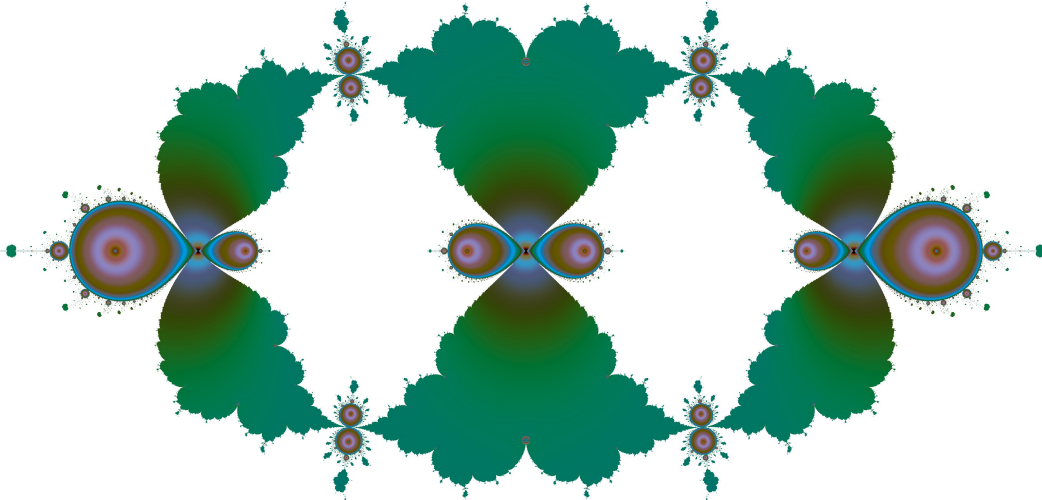

Figure 8.17: $\mathrm{Cyc}_2(\mathrm{Per}_1(\mathcal{P}_3, 1))$: Maps in $\mathrm{Per}_1(\mathcal{P}_3, 1)$ with a marked 2-cycle.
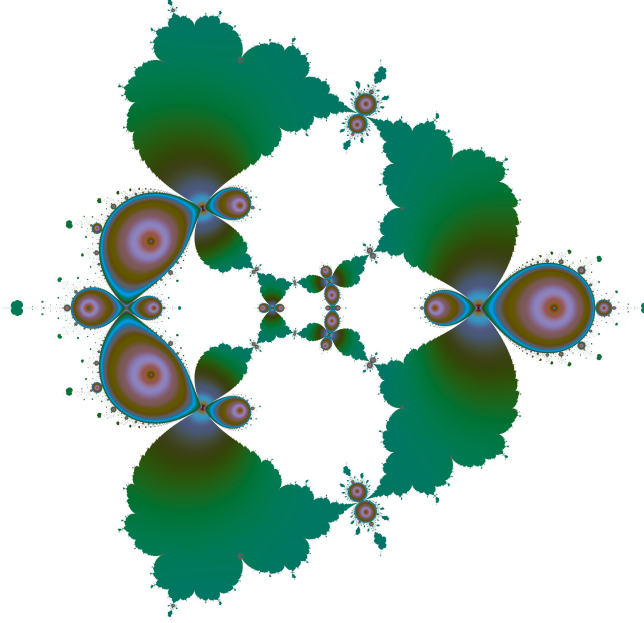
Figure 8.18: $\mathrm{Dyn}_2(\mathrm{Per}_1(\mathcal{P}_3, 1))$: Maps in $\mathrm{Per}_1(\mathcal{P}_3, 1)$ with a marked point of period 2.
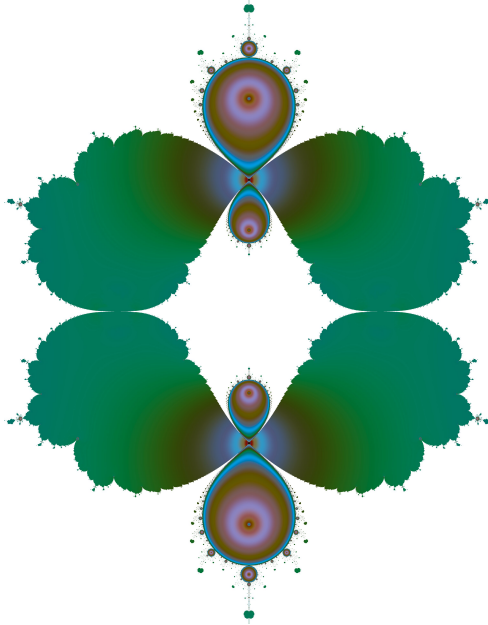

Figure 8.19: $\mathrm{Mis}_{1,1}(\mathrm{Per}_1(\mathcal{P}_3, 1))$: Maps in $\mathrm{Per}_1(\mathcal{P}_3, 1)$ with a marked point of preperiod 1 and period 1.

8.3.3.4 Cubic Per_2

We can similarly compute dynamical varieties over the family $\mathrm{Per}_2(\mathcal{P}_3)$ of cubic polynomials with a superattracting 2-cycle.
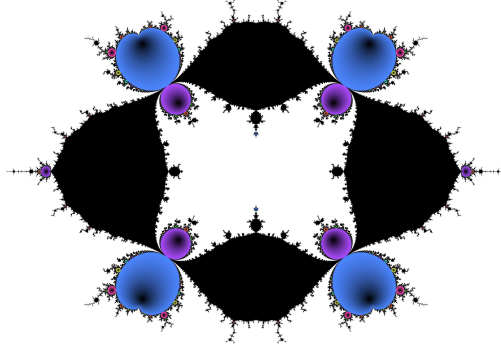
Figure 8.20: The family $\mathrm{Per}_2(\mathcal{P}_3)$ of cubic polynomials with a critical point of period 2.
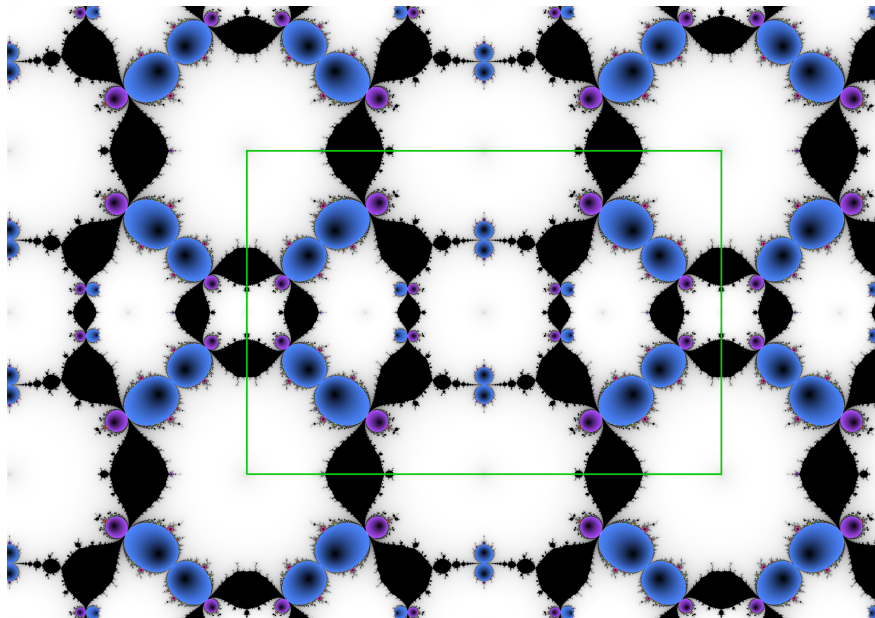
Figure 8.21: $\mathrm{Cyc}_1(\mathrm{Per}_2(\mathcal{P}_3))$: Maps in $\mathrm{Per}_2(\mathcal{P}_3)$ with a marked fixed point. A fundamental domain is shown in green. The j-invariant is $\frac{32}{5} \cdot 1728$.
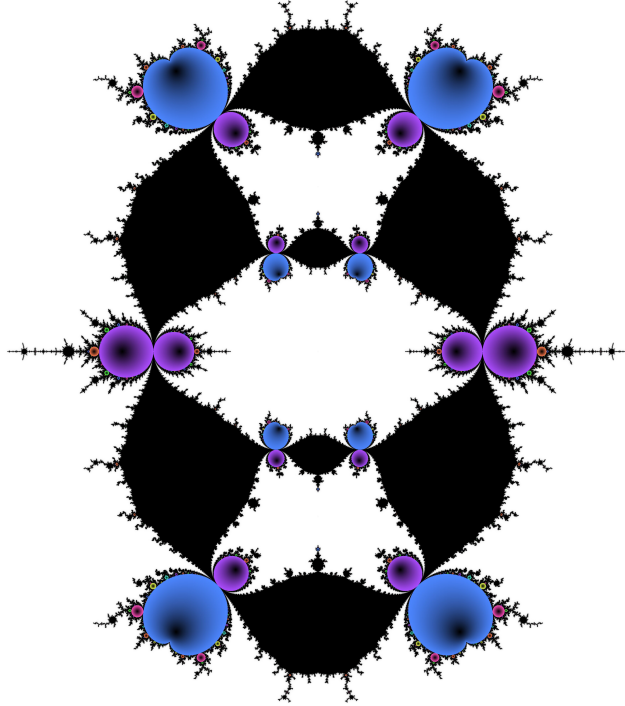
Figure 8.22: $\mathrm{Cyc}_2(\mathrm{Per}_2(\mathcal{P}_3))$: Maps in $\mathrm{Per}_2(\mathcal{P}_3)$ with a marked (non-critical) 2-cycle.

8.3.3.5 Odd Cubics

A third interesting one parameter subspace of the cubic family $\mathcal{P}_3$ is the moduli space Odd_3 of cubic polynomials that commute with an order 2 affine symmetry.
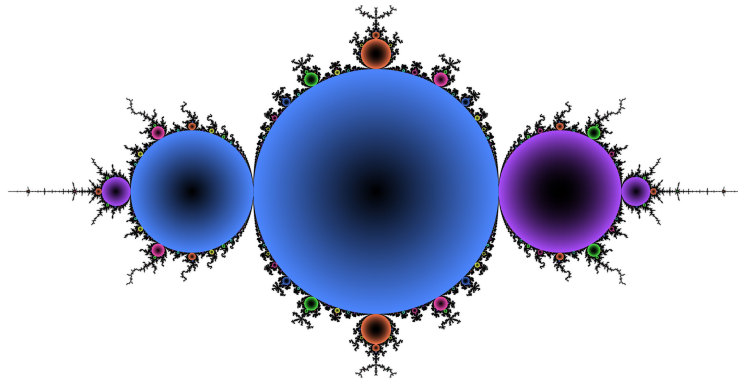
Figure 8.23: The family Odd_3 of odd cubic polynomials.
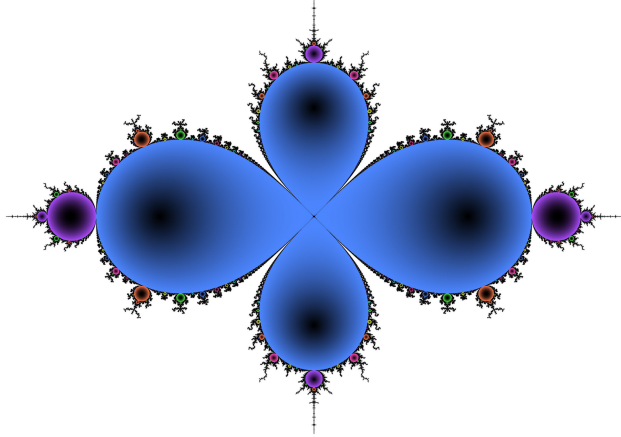
Figure 8.24: $\mathrm{Cyc}_1(\mathrm{Odd}_3)$: Odd cubic polynomials with a marked fixed point.
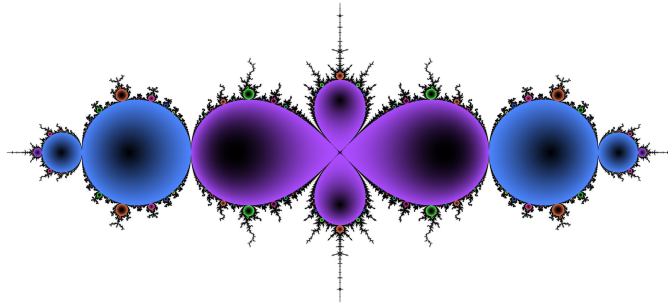
Figure 8.25: $\mathrm{Cyc}_2(\mathrm{Odd}_3)$: Odd cubic polynomials with a marked 2-cycle.
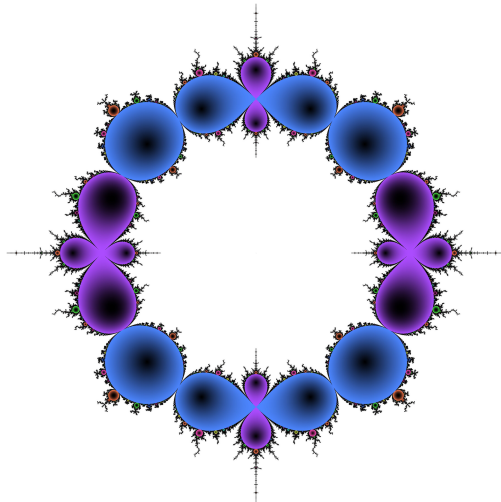
Figure 8.26: $\mathrm{Dyn}_2(\mathrm{Odd}_3)$: Odd cubic polynomials with a marked point of period 2.
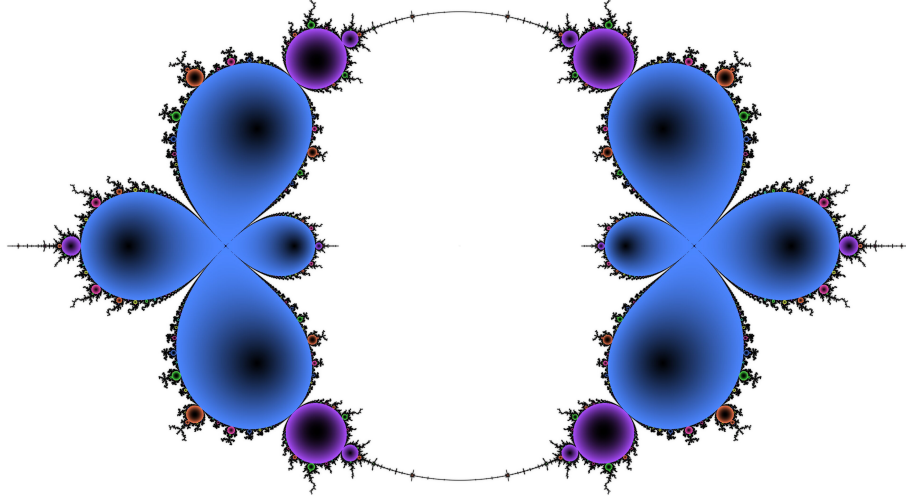
Figure 8.27: $\mathrm{Mis}_{1,1}(\mathrm{Odd}_3)$: Odd cubic polynomials with a marked point of preperiod 1 and period 1.
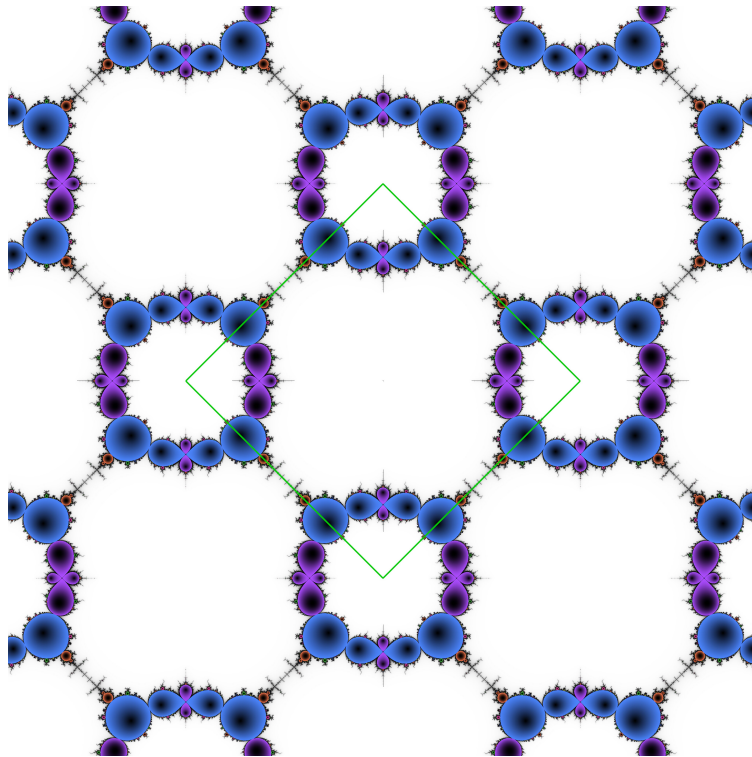
Figure 8.28: $\mathrm{Mis}_{1,2}(\mathrm{Odd}_3)$: Odd cubic polynomials with a marked point of preperiod 1 and period 2. A fundamental domain is drawn in green. The j-invariant is 1728.

APPENDIX A

Algorithm Implementations

In this appendix, we provide an implementation for Algorithm 4.6.1 to compute a cell structure for the marked cycle curve over Per_1 or Per_2.

A.1 Marked Cycle Cell Structure

We begin with the face traversal step, which is the key component of Algorithm 4.6.1. This implementation can be made more efficient by using an adjacency map instead of looping through every arc, but we provide the latter implementation here for clarity. A thorough, optimized implementation in *Rust* is available at [Sto23b].

Face Computation for Marked Cycle Curve

1: **function** COMPUTEFACES(V, E) ▷ *We input the sets of vertices and edges. For marked cycle curves, edges are just primitive lamination arcs in counterclockwise order.*
2:      $visited\_vertices \leftarrow \varnothing$
3:      $F \leftarrow$ empty array
4:      **for** each v_0 in V **do**
5:          **if** $v_0 \in visited\_vertices$ **then continue** ▷ *Avoid traversing the same face multiple times*
6:          **else**
7:            Add v_0 to $visited\_vertices$
8:          $v \leftarrow v_0$
9:          Initialize an array $vs \leftarrow [v_0]$ ▷ *Circularly ordered list of vertices on the boundary of the face*
10:          $degree \leftarrow 1$ ▷ *Local degree of the map $\pi : F \rightarrow \mathrm{Per}_m$*
11:          **loop**
12:              **for** each (θ_0, θ_1) in $\mathcal{A}$ **do** ▷ *Traverse through wakes in counterclockwise order, starting from the positive real axis*
13:                  **if** $v = \theta_0$ **then**
14:                      $v \leftarrow \theta_1$
15:                      $vs.\mathrm{PUSH}(v)$
16:                  **else if** $node = \theta_1$ **then**
17:                      $v \leftarrow \theta_0$
18:                      Push v onto vs
19:              **if** $v = v_0$ **then**
20:                  **if** LENGTH(vs) > 1 **then** pop vs ▷ *Remove the extra copy of the starting vertex*
21:                  Push FACE($\langle v_0 \rangle$, vs, $face\_degree$) to F ▷ *$\langle v_0 \rangle$ denotes the cycle class of v_0, which is our label for F*
22:                  **break** 11
23:              **else**
24:                  Add v to $visited\_vertices$ ▷ *We are crossing the positive real axis, so the current vertex is also a representative for the same face.*
25:              $degree \leftarrow degree + 1$
     return F

We may now put the face traversal step in context by constructing the entire cell structure

for $\mathrm{Cyc}_p(\mathrm{Per}_m)$, $m = 1, 2$.

Cell Structure for Marked Cycle Curves

1: **function** COMPUTECYCLES(p)

2:     $N \leftarrow 2^p - 1$ ▷ *Denominator of angles in Mandelbrot lamination*

3:     $\mathcal{C} \leftarrow$ array of `null` of size N

4:     **for** $k = 1$ through $N - 1$ such that $\mathcal{C}[k]$ is `null` **do**

5:        $\mathcal{O} \leftarrow$ ORBIT(k/N)   ▷ *Orbit of $\theta = k/N$ under angle doubling*

6:        **if** $|\mathcal{O}| = p$ **then**   ▷ *Exclude cycles of lower period*

7:           $\theta_0 \leftarrow \min(\mathcal{O})$ ▷ *Choose a representative for the cycle*

8:           **for** each $\alpha \in \mathcal{O}$ **do**

9:              $\mathcal{C}[N\alpha] \leftarrow \theta_0$

10:    **return** $\mathcal{C}$

11: **procedure** MARKEDCYCLECELLSTRUCTURE(p, *is_per2*)

12:     $\mathcal{C} \leftarrow$ COMPUTECYCLES(p)   ▷ *Array mapping angles to cycle representatives*

13:     $V \leftarrow$ values of $\mathcal{C}$, sorted and deduplicated ▷ *Each vertex corresponds to a lift of f_0, and may be labeled by a p-cycle of f_0*

14:     $\mathcal{A} \leftarrow$ LAVAURS(p, *is_per2*) ▷ *Period p arcs in the Mandelbrot lamination, excluding arcs in $[1/3, 2/3]$ if the base curve is Per_2 (as the corresponding basilica matings are obstructed)*

15:     $E \leftarrow \{(\theta_0, \theta_1) \in \mathcal{A} : \mathcal{C}[\theta_0] \neq \mathcal{C}[\theta_1]\}$ ▷ *Non-satellite ray pairings, which land at roots of primitive hyperbolic components*

16:     $F \leftarrow$ COMPUTEFACES($V, \mathcal{A}$)

17:     **return** V, E, F

A.2   Dynatomic Cell Structure

The cell structure for dynatomic curves over Per_1 and Per_2 is computed using a similar algorithm, with a few modifications. Instead of using ABCs to encode vertices, we now use ABPs.

To avoid having to separately consider satellite edges and primitive edges, we no longer identify edges with wakes, and instead simply identify them with pairs of vertices. This means that when computing edges from wakes, we must account for all of the ABP pairs represented by that wake:

Dynatomic Edges

1: **function** COMPUTEEDGES($\mathcal{A}$)   ▷ *Input the set of arcs in the lamination of $\mathcal{M}$ or $\widetilde{\mathcal{M}}$*

2:     $E \leftarrow$ empty array

3:     **for** each $(\theta_0, \theta_1) \in \mathcal{A}$ **do**

4:        $\mathcal{O}_0 \leftarrow$ ORBIT(θ_0)   ▷ *Orbit under angle doubling*

5:        $\mathcal{O}_1 \leftarrow$ ORBIT(θ_1)

6:        **for** each $(\alpha, \beta) \in \mathcal{O}_0 \times \mathcal{O}_1$ **do**   ▷ *Create an edge for each shift of the arc.*

7:           push (α, β) to E ▷ *Note that crucially, edges are ordered not according to their own endpoints, but according to the wakes in $\mathcal{A}$ from which they originate.*

8:     **return** E

Finally, faces now fall into two categories: primitive faces, which are analogous to the faces in marked cycle curves, and satellite faces, which describe lifts of the roots of satellite hyperbolic components. Primitive faces are computed as in Appendix A.1. Satellite faces are computed by connecting shifts:

Dynatomic Satellite Faces

1: **function** SATELLITEFACES(p, $\mathcal{A}_{\text{sat}}$, $\mathcal{S}$) ▷ *p is the period, $\mathcal{A}_{\text{sat}}$ is the set of satellite arcs in the lamination of $\mathcal{M}$ or $\widetilde{\mathcal{M}}$, and $\mathcal{S}$ is an array encoding the shift of each ABP θ relative to the minimum of the ABC (θ).*

2:     $F_{\text{sat}} \leftarrow$ empty array

3:     **for** each $(\alpha, \beta) \in \mathcal{A}_{\text{sat}}$ **do**

4:        $\sigma \leftarrow \mathcal{S}[\beta] - \mathcal{S}[\alpha]$ ▷ *Rotation number of the satellite component*

5:        $N_\alpha \leftarrow \gcd(\sigma, p)$ ▷ *Number of faces represented by the current satellite component*

6:        **for** i from 0 to N_α **do**

7:           $F \leftarrow (2^{i+j\sigma}\alpha \mid 0 \leq j < N_\alpha)$ ▷ *Note that the relative shift between adjacent vertices is σ*

8:           push F to F_{sat}

9:     **return** F_{sat}

We may now put everything together to obtain a cell structure for $\mathrm{Dyn}_p(\mathrm{Per}_m)$, $m = 1, 2$.

Cell Structure for Dynatomic Curves

1: **function** COMPUTECYCLESANDSHIFTS(p)
2:     $N \leftarrow 2^p - 1$ ▷ *Denominator of angles in Mandelbrot lamination*
3:     $\mathcal{C} \leftarrow$ array of `null` of size N
4:     $\mathcal{S} \leftarrow$ array of `null` of size N
5:     **for** $k = 1$ through $N - 1$ such that $\mathcal{C}[k]$ is `null` **do**
6:        $\mathcal{O} \leftarrow$ ORBIT(k/N)   ▷ *Orbit of $\theta = k/N$ under angle doubling*
7:        **if** $|\mathcal{O}| = p$ **then**   ▷ *Exclude cycles of lower period*
8:           **for** each $\theta_i \in \mathcal{O}$ **do**   ▷ *Enumerate elements of $\mathcal{O}$, starting from $\theta_0 = k/N$*
9:              $\mathcal{C}[N\theta_i] \leftarrow \theta_0$ ▷ *θ_0 is the minimum of the cycle, serving as a representative*
10:              $\mathcal{S}[N\theta_i] \leftarrow i$ ▷ *Shift of θ_i relative to θ_0*
11:     **return** $\mathcal{C}$
12: **procedure** DYNATOMICCELLSTRUCTURE(p, *is_per2*)
13:     $\mathcal{C}, \mathcal{S} \leftarrow$ COMPUTECYCLESANDSHIFTS(p) ▷ *Arrays mapping angles to cycle representatives and shifts relative to the latter*
14:     $V \leftarrow$ keys of $\mathcal{C}$ whose values are not `null` ▷ *Each vertex corresponds to a lift of f_0, and thus may be labeled by a p-periodic angle*
15:     $\mathcal{A} \leftarrow$ LAVAURS(p, *is_per2*)
16:     $E \leftarrow$ COMPUTEEDGES($\mathcal{A}$)
17:     $F_{\mathrm{prim}} \leftarrow$ PRIMITIVEFACES(V, E)   ▷ *Same as* COMPUTEFACES *in Appendix A.1*
18:     $F_{\mathrm{sat}} \leftarrow$ SATELLITEFACES(V, E)
19:     **return** $V, E, F_{\mathrm{prim}} \cup F_{\mathrm{sat}}$

A.3   Lavaurs' Algorithm for Laminations

The above implementations make use of Lavaurs' algorithm [Lav89] to compute ray pairings in the Mandelbrot set. For completeness, we include an implementation of this algorithm as well.

1: **procedure** Lavaurs(max_period, is_per2)

2: $\quad \mathcal{L} \leftarrow (\varnothing, \{(0,1)\})$ $\qquad\qquad\qquad\qquad\qquad$ ▷ *Arcs arranged by period*

3: $\quad E \leftarrow ((0,1),(1,0))$ ▷ *Sorted array of all arc endpoints, together with their companion angles*

4: $\quad$ **for** n from 1 through max_period **do** $\qquad$ ▷ *Iteratively compute arcs of each period*

5: $\quad\quad N \leftarrow 2^n - 1$

6: $\quad\quad S \leftarrow$ empty stack $\qquad\qquad$ ▷ *We employ a stack to track connectivity of regions*

7: $\quad\quad E' \leftarrow$ empty array $\qquad\qquad$ ▷ *New arc endpoints, which will later be added to E*

8: $\quad\quad (\alpha, \beta) \leftarrow E[0]$ $\qquad\qquad\qquad$ ▷ *Earliest unvisited pre-existing arc endpoint*

9: $\quad\quad j \leftarrow 1$ $\qquad\qquad\qquad\qquad$ ▷ *Iterator for pre-existing arc endpoints*

10: $\quad\quad$ **for** k from 1 to N **do**

11: $\quad\quad\quad \theta \leftarrow \frac{k}{N}$ $\qquad\qquad\qquad\qquad$ ▷ *New angle under consideration*

12: $\quad\quad\quad$ **while** $\alpha \leq \theta$ **do**

13: $\quad\quad\quad\quad (\alpha, \beta) \leftarrow E[j]$

14: $\quad\quad\quad\quad$ **if** $\alpha < \beta$ **then**

15: $\quad\quad\quad\quad\quad$ push 0 onto S $\qquad\qquad$ ▷ *We mark pre-existing arcs with 0*

16: $\quad\quad\quad\quad$ **else**

17: $\quad\quad\quad\quad\quad$ pop S

18: $\quad\quad\quad\quad j \leftarrow j + 1$

19: $\quad\quad\quad\quad$ **if** $\alpha = \theta$ **then**

20: $\quad\quad\quad\quad\quad$ **continue** from line 10 $\qquad$ ▷ *We ignore arcs of lower period*

21: $\quad\quad\quad \theta' \leftarrow \frac{1}{N} \cdot$ PeekTop(S) $\qquad\qquad$ ▷ *Default to 0 if S is empty*

22: $\quad\quad\quad$ **if** $\theta' \neq 0$ **then** $\qquad$ ▷ *We've found a new arc (θ', θ) of period n*

23: $\quad\quad\quad\quad$ push (θ', θ) to E'

24: $\quad\quad\quad\quad$ push (θ, θ') to E'

25: $\quad\quad\quad\quad$ pop S

26: $\quad\quad\quad$ **else**

27: $\quad\quad\quad\quad$ push k onto S

28: $\quad\quad$ Sort E' by first coordinate

29: $\quad\quad$ Merge E' into E ▷ *E must be sorted at each step of loop 10 to ensure correctness*

30: $\quad\quad A_n \leftarrow \Big((\theta_0, \theta_1) \in E' : \theta_0 < \theta_1\Big)$ ▷ *Newly found arcs, which have period n, filtered to only include the positively oriented copies*

31: $\quad\quad$ push A_n to $\mathcal{L}$

$\quad$ **output** $\mathcal{L}$

Remark A.3.1. The above implementation of Lavaurs' algorithm requires exponential space to store all the arcs, and is infeasible on current hardware beyond periods 25-30. The author is not aware of any way around this, since the non-crossing criterion for new arcs requires that older arcs be kept in memory. It would be very interesting to learn of a way to iterate through arcs of a given period without this exponential space requirement.

APPENDIX B

Parameterizations for Specific Curves

B.1   Parameterizing Cubic $\mathrm{Per}(2, \lambda)$

We are interested in the curve $\mathrm{Per}(2, \lambda)$ consisting of all cubic polynomials whose unique 2-cycle has multiplier λ.

We consider a general monic cubic $f(z) = z^3 + az^2 + bz + c$ and restrict the coefficients so that $f(c) = 0$ and so that $bf'(c) = \lambda$, thus guaranteeing that $(0, c)$ is a 2-cycle of multiplier λ.

The former restriction is equivalent to

$$ac + c^2 + b + 1 = 0. \tag{B.1}$$

Indeed, $f(c) = (ac + c^2 + b + 1)c$, where the solution $c = 0$ may be ignored since 0 is fixed in that case.

The latter restriction is equivalent to

$$(2ac + 3c^2 + b)b - \lambda = 0. \tag{B.2}$$

Solving for b in (B.1) gives $b = -ac - c^2 - 1$. Plugging this into (B.2), we obtain the equation $-a^2c^2 - 3ac^3 - 2c^4 - c^2 - \lambda + 1 = 0$. The corresponding (negated) homogenized polynomial is
$$F(a, c, h) = a^2c^2 + 3ac^3 + 2c^4 + c^2h^2 + (\lambda - 1)h^4.$$

For λ outside $\{0, 1\}$, this defines a singular plane curve C_λ of arithmetic genus 3 and geometric genus 1. We wish to parameterize this curve.

Using a, c, h as homogeneous coordinates, C_λ always contains the points $p_1 = [1 : 0 : 0]$,

$p_2 = [1 : -1 : 0]$ and $p_3 = [2 : -1 : 0]$. While p_1 is a doubly singular point, p_2 and p_3 are regular.

We wish to find a regular function f with a pole of order 2 at, say, p_2, and with no other poles. Letting $D = 2[p_3]$, by Riemann-Roch we have that $l(D) \geq \deg(D) - g + 1 = 2 - 3 + 1 = 0$, so we expect to find a solution.

The regular function

$$P_2(a, c, h) = \frac{c\,(a + 2c)}{h^2}$$

has a pole of order 2 at p_2 and no other poles.

$$P_3(a, c, h) = \frac{2c^2 - (1 - \lambda)h^2 + ac}{h(a + c)}$$

Thus, P_2 and P_3 generate the function field $\mathcal{O}(C_\lambda)$ of our curve. A computation shows that P_2 and P_3 satisfy the relation

$$-P_2^3 - (\lambda - 1)P_2 + P_2^2 + P_3^2 + \lambda - 1 = 0$$

in $\mathcal{O}(C_\lambda)$. Thus, setting $x = P_2 + \frac{1}{3}$ and $y = \frac{P_3}{2}$, we obtain the elliptic curve

$$y^2 = 4x^3 - \frac{4}{3}(4 - 3\lambda)x - \frac{64 - 72\lambda}{27}.$$

The j-invariant is

$$\frac{64(3\lambda - 4)^3}{\lambda^2(\lambda - 1)},$$

which has poles where $\mathrm{Per}(2, \lambda)$ degenerates to a rational curve.

A few other notes:

- Each affine conjugacy class in $\mathrm{Per}(2, \lambda)$ contains two points on C_λ, corresponding to which point in the 2-cycle we mark.

- C_0 is the union of two plane quadrics defined by $ac + c^2 + h^2$ and $ac + 2c^2 - h^2$, which intersect at $[-\frac{3}{\sqrt{2}} : \sqrt{2} : \pm 1]$ and are tangent at the singular point at infinity $[1 : 0 : 0]$. The two finite intersection points correspond to the two (affine conjugate) cubic polynomials for which the critical points swap places.

- C_1 is the union of a plane quadric defined by $a^2 + 3ac + 2c^2 + h^2$ with the double line defined by c^2. The quadric describes the honest Milnor curve $\mathrm{Per}(2, 0)$, while the

double line is actually the curve $\mathrm{Per}(1, -1)$, in which 0 is fixed with multiplier -1.

- For $\lambda \neq 1$, there are no finite points on C_λ with $c = 0$. Since $(0, c)$ is the 2-cycle, C_λ contains no degenerate polynomials in which the 2-cycle is actually a fixed point with multiplier $\pm\sqrt{\lambda}$.

B.2   Parameterizing $\mathrm{Cyc}_4(\mathrm{Per}_3)$

To parameterize maps in Per_3 with a marked 4-cycle, we begin with the coordinates

$$f_c(z) = \frac{z^2 + c^3 - c - 1}{z^2 - c^2}.$$

The map f_c has a critical 3-cycle $\infty \mapsto 1 \mapsto -c$ and free critical point 0. Since the only Möbius transformation fixing three points in $\hat{\mathbb{C}}$ is the identity map, it follows that f_c is conjugate to $f_{c'}$ if and only if $c = c'$.

The dynatomic curve $\mathrm{Dyn}_4(\mathrm{Per}_3)$ may be described as the vanishing locus of the polynomial

$$\varphi_{4,\mathrm{Per}_3}(c, z) = \frac{\nu(f_c^4(z) - z)}{\nu(f_c^2(z) - z)},$$

where ν denotes the numerator of a rational expression. This degree 13 polynomial defines a singular algebraic curve of geometric genus 12.

We may obtain an expression for the marked cycle curve by taking the resultant in z of $\varphi = \varphi_{4,\mathrm{Per}_3}(c, z)$ with $\nu(h(c, z) - t)$, where $h(c, z)$ is a nonconstant rational expression invariant within 4-cycles of f_c, but which takes different values at different 4-cycles for generic c.

Taking[1]

$$h(c, z) = \sum_{0 \le k < 4} f_c^k(z),$$

we obtain

$$\mathrm{Res}_z(\varphi, \nu(h - t)) = (c^4 + 2c^3t + c^2t^2 - ct^3 - 4c^3 + 2c^2t + t^3 + 14c^2 - 6ct - t^2 + 12c - 6t + 9)^4 (c + 1)^{127} (c - 1)^{51}.$$

The spurious solutions $c = \pm 1$ correspond to punctures in Per_3, wherein $f_c(z) \equiv 1$ is not a quadratic rational map (and certainly does not have a 4-cycle). The remaining irreducible

---

[1]The dynamically more natural choice would be the multiplier of the 4-cycle, since it is Möbius invariant. However, the resultant computation is quite expensive, so it is practical to choose a polynomial h of minimal degree.

factor

$$E_0(c, t) = c^4 + 2c^3t + c^2t^2 - ct^3 - 4c^3 + 2c^2t + t^3 + 14c^2 - 6ct - t^2 + 12c - 6t + 9$$

defines an algebraic curve of geometric genus 1 birationally equivalent to the marked cycle curve $\mathrm{Cyc}_4(\mathrm{Per}_3)$.

To parameterize E_0 by points on the plane, we must first convert it to Weierstrass form. We can do this by a sequence of birational changes of variables. The substitution

$$t = x_0c + \sqrt{13}(x_0 - 1) - 4x_0 - 1,$$
$$c = y_0(x_0 + 1) + \sqrt{13} + 4$$

converts E_0 to the form

$$E_1(x_0, y_0) = x_0^2 y_0^2(x - 1) + 3\left(\sqrt{13} + 1\right) x_0^2 y_0 - 2x_0 y_0^2 - \left(2\sqrt{13} + 14\right) x_0 y_0$$
$$- y_0^2 + \left(6\sqrt{13} + 26\right) x_0 - \left(2\sqrt{13} + 10\right) y_0 - 14\sqrt{13} - 50.$$

The blowup

$$x_0 = \frac{x}{y}, \quad y_0 = \frac{y}{z}$$

then converts E_1 to a homogeneous polynomial E_2 of degree 3:

$$E_2(x, y) = x^3 + 3\left(\sqrt{13} + 1\right) x^2 y + \left(6\sqrt{13} + 26\right) xy^2 - x^2 z - \left(2\sqrt{13} + 14\right) xyz$$
$$- \left(14\sqrt{13} + 50\right) y^2 z - 2xz^2 - \left(2\sqrt{13} + 10\right) yz^2 - z^3$$

The projective plane curve C_2 defined by E_2 contains the base point

$$P_0 = \left[\sqrt{13} + 1 : -1 : 2\right].$$

The tangent line L_0 to C_2 at P_0 has defining equation $2y + z = 0$. This line also intersects C_2 at the point
$$P_1 = \left[\sqrt{13} + 3 : -1 : 2\right],$$

where the tangent line L_1 is defined by $x + (\sqrt{13} + 3)y = 0$. Finally, we may choose a toward line L_2 through P_0; for instance, $2x - (\sqrt{13} + 1)z = 0$ suffices.

We then perform the change of variables

$$X = x + \left(\sqrt{13} + 3\right) y,$$
$$Y = 2x - \left(\sqrt{13} + 1\right) z,$$
$$Z = 2y + z,$$

so that $L_0 = V(Z)$, $L_1 = V(X)$, and $L_2 = V(Y)$. The inverse change of variables is given by

$$x = \frac{\left(\sqrt{13} + 3\right) Y - 2\left(\sqrt{13} + 1\right) X}{4} + \left(\sqrt{13} + 4\right) Z,$$
$$y = \frac{2X - Y - \left(\sqrt{13} + 1\right) Z}{4},$$
$$z = \frac{Y + \left(\sqrt{13} + 3\right) Z}{2} - X.$$

In the affine patch $Z = 1$, this gives rise to the equation

$$E_3\left(X, Y\right) = XY^2 - 4X^2 + \left(2\sqrt{13} + 2\right) XY + \left(2\sqrt{13} + 10\right) X - 2Y - \left(2\sqrt{13} + 6\right).$$

The substitution

$$y = \frac{\hat{y} + 1}{x} - \sqrt{13} - 1, \quad x = \hat{x} - \frac{1}{3}$$

then converts our curve to Weierstrass form:

$$E_4\left(u, v\right) = \hat{y}^2 - \left(4\hat{x}^3 - g_2\hat{x} + g_3\right),$$

where $g_2 = -8/3$ and $g_3 = 1/27$. Putting $u = \wp_{g_2, g_3}(s)$ and $v = \wp'_{g_2, g_3}(s)$ gives an explicit formula for the universal covering map $\mathbb{C} \to V(E_4)$, and following the changes of variables, we obtain a parameterization for $\mathrm{Cyc}_4(\mathrm{Per}_3)$.

The elliptic curve E_4 has a j-invariant of $\frac{2^{15}}{19}$ and a conductor of 19. The author is unaware of a relationship between the reduction of genus 1 dynamical moduli spaces and the underlying dynamics.

APPENDIX C

Remarks on Computer Graphics

All images appearing in this thesis were generated using the author's software project Dynamo. The source code for this program is freely available under the GNU General Public License and may be found at [Sto23a]. Interested readers are encouraged to experiment with and modify the software to their needs.

In all images with colored hyperbolic or Fatou components, points within these components are colored with brightness given by the absolute value of the multiplier of the attracting cycle, and with hue depending on the period, according to the following table:

Table C.1: Colors used to represent periodic components

PERIOD MOD 7	COMPONENT COLOR
0	Cyan
1	Blue
2	Purple
3	Magenta
4	Orange
5	Yellow
6	Green

BIBLIOGRAPHY

[AY08]   Magnus Aspenberg and Michael Yampolsky. "Mating Non-Renormalizable Quadratic Polynomials". In: *Communications in Mathematical Physics* 287.1 (Aug. 2008), pp. 1–40. ISSN: 1432-0916. DOI: 10.1007/s00220-008-0598-y.

[BDK91] Paul Blanchard, Robert L. Devaney, and Linda Keen. "The dynamics of complex polynomials and automorphisms of the shift". In: *Inventiones mathematicae* 104.1 (Dec. 1991), pp. 545–580. ISSN: 1432-1297. DOI: 10.1007/bf01245090.

[BG22]   Anna Belova and Igors Gorbovickis. "Critical Points of the Multiplier Map for the Quadratic Family". In: *Experimental Mathematics* 31.1 (2022), pp. 337–345. DOI: 10.1080/10586458.2019.1627682.

[Bou92] Thierry Bousch. "Sur quelques problèmes de dynamique holomorphe". PhD thesis. Université de Paris-Sud, 1992.

[BT11]   Xavier Buff and Lei Tan. "The quadratic dynatomic curves are smooth and irreducible". In: *Frontiers in Complex Dynamics: In Celebration of John Milnor's 80th Birthday* (July 2011).

[Buf+23] Xavier Buff et al. "Factoring Gleason polynomials modulo 2". In: *Journal de théorie des nombres de Bordeaux* 34 (Jan. 2023), pp. 787–812. DOI: 10.5802/jtnb.1228.

[Dav+23] Caroline Davis et al. "A cell decomposition for marked cycle curves". Dec. 2023.

[DH84]   Adrien Douady and John H. Hubbard. *Étude dynamique des polynômes complexes.* Princeton: Princeton University Press, 1984.

[DH85]   Adrien Douady and John Hamal Hubbard. "On the dynamics of polynomial-like mappings". en. In: *Annales scientifiques de l'École Normale Supérieure* Ser. 4, 18.2 (1985), pp. 287–343. DOI: 10.24033/asens.1491.

[Dud11] Dzmitry Dudko. *Matings with laminations.* 2011. eprint: arXiv:1112.4780.

[EL92]   A. Eremenko and M. Yu Lyubich. "Dynamical properties of some classes of entire functions". en. In: *Annales de l'Institut Fourier* 42.4 (1992), pp. 989–1020. DOI: 10.5802/aif.1318.

[FG20]   Tanya Firsova and Igors Gorbovickis. *Accumulation set of critical points of the multipliers in the quadratic family.* 2020. eprint: arXiv:2005.00665.

[Gao16] Yan Gao. "Preperiodic dynatomic curves for $z - z^d + c$". en. In: *Fundamenta Mathematicae* 233 (2016), pp. 37–69. URL: http://dml.mathdoc.fr/item/bwmeta1.element.bwnjournal-article-doi-10_4064-fm91-12-2015.

[Hub16] John H. Hubbard. *Teichmüller Theory Volume 2: Surface Homeomorphisms and Rational Functions*. Matrix Editions, 2016. ISBN: 9781943863006. URL: https://matrixeditions.com/TeichVol2TOC.html.

[Lav89] Pierre Lavaurs. "Systèmes dynamiques holomorphes: explosion de points périodiques paraboliques". PhD thesis. Université de Paris-Sud, 1989.

[Lei90] Tan Lei. "Similarity between the Mandelbrot set and Julia sets". In: *Communications in Mathematical Physics* 134 (Dec. 1990). DOI: 10.1007/BF02098448.

[Lei92] Tan Lei. "Matings of quadratic polynomials". In: *Ergodic Theory and Dynamical Systems* 12.3 (1992), pp. 589–620. DOI: 10.1017/S0143385700006957.

[Luo95] Jiaqi Luo. "Combinatorics and Holomorphic Dynamics: Captures, Matings, Newton's Method". PhD thesis. Cambridge University, 1995.

[McM95] Curtis T. McMullen. *Complex Dynamics and Renormalization (AM-135), Volume 135*. Princeton: Princeton University Press, 1995. ISBN: 9781400882557. DOI: doi:10.1515/9781400882557.

[Mil00] John Milnor. "Periodic orbits, externals rays and the Mandelbrot set: an expository account". en. In: *Géométrie complexe et systèmes dynamiques - Colloque en l'honneur d'Adrien Douady Orsay, 1995*. Ed. by Flexor Marguerite, Sentenac Pierrette, and Yoccoz Jean-Christophe. Astérisque 261. Société mathématique de France, 2000. URL: http://www.numdam.org/item/AST_2000__261__277_0/.

[Mil06] J Milnor. *Dynamics in one complex variable. (AM-160)*. en. 3rd ed. Annals of Mathematics Studies. Princeton, NJ: Princeton University Press, Jan. 2006.

[Mil93] John Milnor. "Geometry and dynamics of quadratic rational maps, with an appendix by the author and Tan Lei". In: *Experimental Mathematics* 2.1 (1993), pp. 37–83.

[MSS83] R. Mañé, P. Sad, and D. Sullivan. "On the dynamics of rational maps". en. In: *Annales scientifiques de l'École Normale Supérieure* Ser. 4, 16.2 (1983), pp. 193–217. DOI: 10.24033/asens.1446.

[MT88] John Milnor and William Thurston. "On iterated maps of the interval". In: *Lecture Notes in Mathematics*. Springer Berlin Heidelberg, 1988, pp. 465–563. ISBN: 9783540459460. DOI: 10.1007/bfb0082847. URL: http://dx.doi.org/10.1007/BFb0082847.

[Ree90] M. Rees. "Components of degree two hyperbolic rational maps". In: *Inventiones Mathematicae* 100.1 (Dec. 1990), pp. 357–382. ISSN: 1432-1297. DOI: 10.1007/bf01231191. URL: http://dx.doi.org/10.1007/BF01231191.

[Sch94]   Dierk Schleicher. "Internal addresses in the Mandelbrot set and irreducibility of polynomials". PhD thesis. Stony Brook University, 1994.

[Seg79]   Graeme Segal. "The topology of spaces of rational functions". In: *Acta Mathematica* 143 (1979), pp. 39–72. DOI: 10.1007/BF02392088.

[Sto23a]   Danny Stoll. *Dynamo, a tool for studying complex dynamics.* https://github.com/DannyStoll1/dynamo. Version 1.0. Nov. 2023.

[Sto23b]   Danny Stoll. *Dynatomic cell structure implementation.* https://github.com/DannyStoll1/marked-cycles. Version 0.3.0. Oct. 2023.

[Tim08]   Vladlen Timorin. *The external boundary of* $\mathcal{M}_2$. Sept. 2008. DOI: 10.1090/fic/053/11. URL: http://dx.doi.org/10.1090/fic/053/11.

[TY96]   Lei Tan and Yin Yongcheng. "Local connectivity of the Julia set for geometrically finite rational maps". In: *Science in China. Series A* 39 (Jan. 1996).

[Wit88]   Ben Scott Wittner. *On the bifurcation loci of rational maps of degree two.* Thesis (Ph.D.)–Cornell University. ProQuest LLC, Ann Arbor, MI, 1988, p. 238.